

THE *DROSOPHILA* HOMOLOGUES OF THE HUMAN *ATRX*
GENE UNDERLYING THE *ATRX* MENTAL RETARDATION
SYNDROME HAVE INDEPENDENT FUNCTIONS AT
CHROMATIN



Addie Kolybaba-Stewart

Ludwig-Maximilians-Universität München

München 2016

THE *DROSOPHILA* HOMOLOGUES OF THE HUMAN *ATRX*
GENE UNDERLYING THE *ATRX* MENTAL RETARDATION
SYNDROME HAVE INDEPENDENT FUNCTIONS AT
CHROMATIN

Dissertation

an der Fakultät für Biologie
der Ludwig-Maximilians-Universität München

vorgelegt von

Addie Kolybaba-Stewart

München, den 04.07.2016

Erstgutacher: Dr. Anne-Kathrin Classen

Zweitgutachter: Prof. Dr. Nicolas Gompel

Tag der Abgabe: 04.07.2016

Tag der mündlichen Prüfung: 06.12.2016

Declaration

Eidesstattliche Versicherung

Hiermit erkläre ich an Eides statt, dass ich die vorliegende Arbeit selbstständig und ohne unerlaubte Hilfe von Dritten angefertigt habe.

München, den 04.07.2016

.....

Addie Kolybaba-Stewart

Erklärung

Hiermit erkläre ich, dass die Dissertation weder als Ganzes, noch in Teilen an einem anderen Ort einer Prüfungskommission vorgelegt wurde. Ich habe weder an einem anderen Ort eine Promotion angestrebt, noch angemeldet oder versucht eine Doktorprüfung abzulegen.

München, den 04.07.2016

.....

Addie Kolybaba-Stewart

Master's Thesis Supervision

Two master's thesis projects were supervised and successfully defended that contributed to the scientific knowledge in this thesis. Relevant data sets are acknowledged in the text and in figures.

Analysis of tissue level expression and subcellular localization of *Drosophila* dADD1
and XNP

Kathrin Bergel, 2014

and

Molecular Investigation of the *Drosophila* Polycomb Group Protein Posterior sex
combs

Inke Lena Hänsch, 2015

Contributions

Contributions from those that assisted in generating specific sets of data are credited in the figure legends and are also mentioned in Aim of this study.

Manuscript preparation

A manuscript is currently in preparation from the data presented in this thesis.

Acknowledgements

Where to begin. There are so many people who have helped, supported and stood by me on my way to this accomplishment. Yes, it is my name on the cover but this is an achievement that would not have been possible without all of my amazing mentors, friends and family.

First and foremost, I want to thank Anne. You are so much more than a supervisor to me, you are a superwoman who I really look up to and strive to be more like every day. Your passion for science, combined with your compassion for those around you kept me motivated these last few years especially when we hit obstacles, over and over and over again. I cannot thank you enough for the unending support you showed me both scientifically and personally, allowing me to pursue many crazy ideas (student council, open house day, career advancement opportunities...) and for your unwavering support of my goals and aspirations

To my scientific advisors. Many of the experiments in this thesis would not have been possible without you. Andi, Ignasi and Catherine thank you so much for sharing your expertise, time and for answering the slew of emails. To my TAC members, Axel and Heinrich. Thank you for the great scientific discussion and for posing the questions that are necessary but sometimes hard to hear. Of course also thank you to my defense committee for taking the time to read through and evaluate my thesis. I know this is not an easy job!

My Munich lab family Christina, Marco, Ramya, Andrea, Isabelle, Vanessa, Ryan, Tom, Rosie, Kathrin, Lena, Nik, Ian and Renate. Where to begin. You guys

made me excited to go to work every morning knowing I would have your smiles, jokes and support there waiting for me. Thanks for also always letting me talk you into signing up to help me bring many of my ideas to life. For all of the wonderful (and sometimes heated) discussions, the Friday beers, the never ending supply of cakes and candy, vacations, dinners, brunches the list of things is never ending, you guys are an amazing group of friends! To my Vancouver lab family, Shabby. I am always in awe of you at how you can maintain such positivity in the face of so many obstacles. Your continued and unlimited supply of optimism inspired me to face many of my own obstacles with confidence and enthusiasm.

Niels. Thanks for planting the nutty idea that I should do my PhD in Germany. This experience has shown me how crazy, strong and brave I can be, especially with you there by my side. Thanks for dealing with all the nerdy science talk and for being genuinely interested in what I do, although it may not always be the easiest to understand. We have come a long way since our swimming days and I look forward to what the future holds.

To my family. There is not enough space here to express the gratitude for all of the years of enduring support. Thanks for always believing in me and supporting me through thick and thin, both athletically and academically. I know there have been many sacrifices to let me live my dreams and I am eternally grateful for them. You always told me that I could do anything I set my mind to and here I am, completing one of my long term goals, in big part because of you.

Table of contents

<u>Declaration</u>	<u>1</u>
<u>Acknowledgements</u>	<u>3</u>
<u>Table of contents</u>	<u>5</u>
<u>List of figures</u>	<u>11</u>
<u>List of tables</u>	<u>13</u>
<u>Summary</u>	<u>14</u>
<u>Zusammenfassung</u>	<u>17</u>
<u>1 Introduction</u>	<u>20</u>
1.1 Chromatin compact: the basics	20
1.2 Alpha-thalassemia mental retardation syndrome	22
1.2.1 ATRX syndrome	22
1.2.2 Chromatin function of ATRX	22
1.2.3 The ATRX ADD domain: a unique histone recognition domain	23
1.2.4 SNF2 domain	24
1.3 Conservation in <i>Drosophila melanogaster</i>	24

2	<u>Aim of this study</u>	<u>28</u>
3	<u>Results</u>	<u>30</u>
3.1	Biochemical characterization of dADD1	30
3.1.1	dADD1-PA is a 250kD protein	30
3.2	Relationship between dADD1 and XNP	34
3.2.1	dADD1 and XNP are expressed in both neurons and glia	37
3.2.2	dADD1 but not XNP is enriched in the oocyte germinal vesicle	39
3.2.3	dADD1 and XNP show distinct chromatin localization patterns at nurse cell chromatin	40
3.2.4	dADD1 and XNP are recruited independently to chromatin	44
3.3	Biochemical and genetic interaction between dADD1 and XNP	46
3.3.1	dADD1 and XNP do not directly interact but both interact with HP1a and HP1b	46
3.3.1	dADD1 and XNP interact genetically	48
3.4	Other interaction partners of dADD1 and XNP	51
3.4.1	dADD1 interacts with chromatin proteins Bonus, Eggless and Mod(mdg4)	51
3.4.2	Overexpression of Bonus in egg chamber follicle cells recruits dADD1 and HP1b to euchromatically localized Bonus foci	52
3.4.3	Pull downs of dADD1 and XNP identify a number of new interaction partners	55
3.5	Effect of loss or overexpression of dADD1 and XNP on chromatin	59
3.5.1	Loss of dADD1 or XNP does not affect localization of HP1a, HP1b or H3.3 to chromatin	59
3.5.2	Overexpression of dADD1 increases cellular H3K9me3 and H3.3 levels	61
3.5.3	Overexpression of dADD1 but not XNP increases incorporation of HP1a, H3.3 and H3K9me3 into heterochromatin	63

3.5.4	Overexpression of dADD1 in follicle cells recruits euchromatic proteins Bonus and HP1b into heterochromatin	66
3.5.5	Loss of dADD1 and XNP results in impaired resolution of double-strand DNA breaks	68
3.5.6	dADD1 and XNP regulate transposon sequences	71
4	<u>Discussion</u>	74
4.1	dADD1 and XNP do not directly interact but function in similar pathways	74
4.1.1	dADD1 and XNP do not physically interact	74
4.1.2	dADD1 and XNP show unique localization patterns at chromatin	75
4.1.3	Chromatin recruitment of dADD1 and XNP is independent of one another	76
4.1.4	Mutations in dADD1 and XNP give rise to similar mutant phenotypes	78
4.1.5	dADD1 and XNP interact genetically	79
4.2	Role of dADD1 and XNP at chromatin	80
4.2.1	Involvement in stress responsive chromatin regulation	80
4.2.2	dADD1 and XNP associate with a number of known telomere associated proteins	81
4.2.3	Loss of dADD1 or XNP does not affect localization of HP1a, HP1b or H3.3 to chromatin	82
4.2.4	dADD1 increases levels of HP1a, H3.3, H3K9me3, HP1b and Bonus at heterochromatin	83
4.3	Model	85
5	<u>Conclusion</u>	89
6	<u>Materials and Methods</u>	91
6.1	General cell culture	91
6.1.1	Counting cells	91
6.1.2	Freezing insect cell lines	91

Table of Contents

6.2 S2 cell culture	91
6.2.1 Culturing conditions	91
6.2.2 Transfection	92
6.2.3 Stable cell line generation	92
6.2.4 RNAi	92
6.2.5 Whole cell lysis	93
6.2.6 Salt nuclear extraction	93
6.2.7 Triton nuclear extraction	93
6.3 HELA Kyoto cell culture	94
6.3.1 Culturing conditions	94
6.3.2 Transfection	94
6.4 Protein expression, purification and detection	95
6.4.1 S2 cell protein expression	95
6.4.2 Ovary, brain and imaginal disc protein extraction	95
6.4.3 Immunoprecipitation	95
6.4.4 Measuring protein concentration	96
6.4.5 Western blotting	96
6.5 Fly Husbandry	97
6.6 Immunofluorescence	97
6.6.1 Imaginal discs	97
6.6.2 Adult Brains	98
6.6.3 Larval Brains	98
6.6.4 Ovaries	98
6.6.5 S2 Cells	99
6.6.6 HELA Kyoto Cells	99
6.7 Nucleic acid techniques	100
6.7.1 Plasmid purification	100
6.7.2 Gateway cloning	100

6.7.3	Rolling circle PCR	101
6.7.4	gDNA extraction	101
6.7.5	RNA extraction	102
6.7.5.1	<i>TRIzol RNA extraction</i>	102
6.7.5.2	<i>Turbo DNase treatment</i>	102
6.7.6	cDNA preparation	102
6.7.7	RT-qPCR	103
6.7.8	dsRNA	103
6.8	Materials	104
6.8.1	Fly stocks	104
6.8.2	Cell Lines	104
6.8.3	Antibodies	105
6.8.3.1	<i>Primary Antibodies</i>	105
6.8.3.2	<i>Secondary Antibodies</i>	105
6.8.4	Plasmids	106
6.8.4.1	<i>Backbone Plasmids</i>	106
6.8.4.2	<i>cDNA Plasmids</i>	106
6.8.4.3	<i>Gateway Destination Plasmids</i>	106
6.8.4.4	<i>Injection Plasmids</i>	106
6.8.4.5	<i>Gateway Entry Plasmids</i>	107
6.8.4.6	<i>Expression Plasmids</i>	108
6.8.5	Primers	110
6.8.5.1	<i>Cloning Primers</i>	110
6.8.5.2	<i>CRISPR Primers</i>	112
6.8.5.3	<i>RNAi Primers</i>	113
6.8.5.4	<i>RT-qPCR Primers</i>	113
6.8.6	Reagents and buffers	113
6.8.6.1	<i>Kits</i>	113
6.8.6.2	<i>Reagents</i>	114
6.8.6.3	<i>Buffers</i>	116
6.8.7	Equipment	117

Table of Contents

6.8.7.1	<i>Microscope Equipment</i>	117
6.8.7.2	<i>Consumables</i>	118
6.8.7.3	<i>Software</i>	120
<u>Abbreviations</u>		<u>121</u>
<u>References</u>		<u>123</u>
<u>7</u>	<u>Supplementary Materials</u>	<u>129</u>
<u>Curriculum Vitae</u>		<u>135</u>

List of figures

Figure 1: Model of ATRX function at heterochromatin.....	23
Figure 2: Alignment of Drosophila dADD1 and XNP isoforms with human ATRX.	25
Figure 3: Amino acid sequence alignment of the ADD domain of dADD1/ATRX and the SNF2 domain of XNP/ATRX shows a high degree of conservation.....	26
Figure 4: The long isoform of dADD1 is much larger than predicted and is the dominantly expressed isoform in ovaries.....	31
Figure 5: Increased molecular weight of the long dADD1 isoform is not the result of dimerization, O-linked N-acetylglucosamination or Poly-ADP ribosylation. dADD1 may be ubiquitinated but the RING domain containing protein Bonus is not the primary ubiquitin ligase of dADD1.....	33
Figure 6: XNP ⁴⁰³ and XNP ⁴⁰⁶ mutants are null mutants as staining with XNP antibody does not detect XNP in either mutant.....	35
Figure 7: Confirmation of dADD1-8F11 antibody, dADD1 _{endoGFP} fly line and dADD1 ² homozygous fly line.	36
Figure 8: dADD1 and XNP are present in neurons and glia of the adult brain. Loss of these proteins results in learning and memory defects in adults.	38
Figure 9: dADD1 is selectively enriched in the oocyte germinal vesicle.....	40
Figure 10: Schematic of egg chamber morphology from stage 6 to stage 10.	41
Figure 11: dADD1, H3.3 and H3K9me3 co-localize with HP1a GFP at heterochromatin, while XNP, HP1b and Bonus show uniform staining across nurse cell chromatin.	43
Figure 12: dADD1 is recruited to H3K9me3 rich regions in HELA Kyoto cells.	44
Figure 13: Loss of dADD1 or XNP does not affect the chromatin localization of the other protein.	45

List of figures

Figure 14: Overexpression of dADD1 or XNP does not increase the chromatin recruitment of the other.....	46
Figure 15: dADD1 and XNP do not directly interact but both interact with HP1a and HP1b.	48
Figure 16: Combination mutations of dADD1 and XNP show increased incidence of melanotic tumors as well as decreased pupal survival.....	50
Figure 17: dADD1 interacts with chromatin proteins Egless, Mod(mdg4) and Bonus.	52
Figure 18: Overexpression of Bonus recruits dADD1 but not XNP to euchromatic Bonus foci.....	53
Figure 19: Overexpression of Bonus recruits HP1b but not HP1a to euchromatic Bonus foci.	54
Figure 20: Neither H3K9me3 or H3.3 is enriched at euchromatic Bonus foci.	55
Figure 21: Localization of HP1b and HP1a to chromatin is independent of the presence of dADD1 and XNP.	60
Figure 22: Western blot of whole cell ovary lysates reveals decreased H3K9me3 in homozygous dADD1 ² mutant ovaries.....	61
Figure 23: Overexpression of dADD1 in S2 cells increases cellular levels of H3K9me3 and H3.3.	62
Figure 24: Overexpression of dADD1 in somatic ovary follicle cells increases incorporation of HP1a, H3.3 and H3K9me3 to heterochromatin.	64
Figure 25: HP1a and H3.3 are not recruited to XNP rich chromatin in overexpressing cells.	65
Figure 26: Overexpression of dADD1 recruits euchromatic proteins Bonus and HP1b to heterochromatin.	67
Figure 27: Overexpression of XNP does not increase recruitment of HP1b to XNP rich chromatin.	68
Figure 28: Homozygous XNP ⁴⁰³ and dADD1 ² mutants show similar γ -H2Av stainings under normal growth conditions.	70
Figure 29: Hydroxyurea treatment of adult females leads to increased γ -H2Av accumulation in XNP ⁴⁰³ and dADD1 ² mutant ovaries.....	71
Figure 30: Loss of dADD1 or XNP results in increased transcription of transposons.....	72
Figure 31: Model of dADD1 and XNP chromatin associated functions.....	86

List of tables

Table 1: Top 10 dADD1 specific interactors	56
Table 2: Top 10 XNP specific interactors	57
Table 3: Gene ontology scores of shared dADD1 and XNP interactors	58
Table 4: dADD1 specific interactors with \log_2 iBAQ (dADD1/S2 control) greater than 3 and P-Value less than 0.06.....	129
Table 5: XNP specific interactors with \log_2 iBAQ (XNP/S2 control) greater than 3 and P-Value less than 0.06.....	131
Table 6: Shared interactors of dADD1 and XNP with \log_2 greater than 3 and P-Value less than 0.06 listed in alphabetical order.	134

Summary

Establishment and maintenance of chromatin integrity is very important for proper organism development. Chromatin structure is highly regulated and controlled by the dynamic interplay of many chromatin-associated and chromatin-remodeling proteins. While uncontrolled alterations to chromatin structure can have catastrophic consequences for an organism, a certain degree of plasticity is necessary to enable adaptation to environmental changes. Using *Drosophila melanogaster* as a model system we undertook two projects investigating the importance of both epigenetic stability as well as plasticity.

Once thought to be only stably inherited, epigenetic modifications are now recognized to be dynamically modulated allowing for chromatin remodeling in response to changes in extracellular environments. The mechanism by which extracellular signals, specifically in response to tissue stress, are transmitted to chromatin to facilitate remodeling are still unknown, however, many studies have implicated stress-mediated phosphorylation of chromatin proteins in this process.

We identified 73 chromatin-associated proteins that have a greater than two-fold increase or decrease in phosphorylation in response to stress signaling. From these proteins we aimed to specifically investigate the effect that stress-induced phosphorylation of the Polycomb group protein Posterior sex combs (Psc) has on its ability to maintain compacted chromatin at target genes. Psc is an essential component of the Polycomb Repressive Complex 1 (PRC1) and regulates cell cycle, differentiation and tissue growth. Intriguingly, we identified stress-induced

phosphorylation sites at threonine 724 and serine 727 are that are located in a domain of Psc essential for nucleosome binding and compaction. While we could characterize these phosphorylation sites, technical limitations prevented determination of the effect that phosphorylation of these sites has on the ability of Psc to compact nucleosomes *in vitro* and *in vivo*.

While plasticity is necessary for adaptation that enables cellular survival to stress signaling, misregulation or mutations in chromatin-associated proteins can also lead to dramatic biological consequences. For example, mutations within the mammalian chromatin associated protein alpha-thalassemia mental retardation syndrome X-linked (ATRX) causes learning and memory defects and has been implicated in a number of cancers. ATRX contains two important chromatin-associated domains, an N-terminal ATRX-DNMT3-DNMT3L (ADD) domain that binds to specific histone tail modifications and a C-terminal SNF2 nucleosome remodeling domain.

A BLAST of the *Drosophila melanogaster* genome for the ADD and SNF2 domains of ATRX yields two proteins, XNP and dADD1. XNP contains the SNF2 remodeler domain while dADD1 contains the chromatin-binding ADD domain. Little is known about the function of these two proteins and the relationship between them in *Drosophila*. Through localization experiments, biochemical characterization, phenotypic analysis and behavioral assays we determined that these two proteins do not directly interact, however, they do function in similar pathways and share a number of common interaction partners. Furthermore, mutations in these proteins show a number of phenotypes similar to mutations in ATRX such as learning and memory defects and impaired transposon silencing.

These two projects address the balance between epigenetic plasticity and stability. While plasticity is necessary for stress mediated repair, stability is essential for maintaining chromatin integrity. Together these projects highlight the complexity of epigenetic regulation and the necessity to further investigate both dynamic as well as static chromatin regulation. While I undertook two projects during my thesis, I

S u m m a r y

present here the work only from the characterization of dADD1 and XNP which investigated the importance of stable epigenetic inheritance.

Zusammenfassung

Aufbau und Erhalt der Integrität von Chromatin ist essentiell für die Entwicklung eines Organismus. Die Struktur von Chromatin wird durch das dynamische Zusammenspiel vieler chromatin-assoziiierter und chromatin-remodellierender Proteine reguliert. Während unkontrollierte Veränderungen an der Chromatinstruktur katastrophale Folgen für den Organismus haben können, ist andererseits ein gewisses Maß an Plastizität notwendig, um die Anpassung an veränderte Umweltbedingungen zu ermöglichen. Mit Hilfe des Modelorganismus *Drosophila melanogaster* untersuchten wir im Zuge zweier Projekte die Bedeutung von epigenetischer Stabilität als auch Plastizität.

Epigenetische Modifikationen galten lange Zeit als stabile Marker spezifischer Chromatinzustände. Mitterweile ist jedoch bekannt, dass ihre dynamische Regulierung Veränderungen an der Chromatinstruktur und damit die Reaktion auf wechselnder Umweltbedingungen ermöglicht. Die Mechanismen, welche extrazelluläre Signale, wie zum Beispiel Gewebestress, auf Chromatin übertragen sind noch weitestgehend unbekannt, jedoch wurde in mehreren Studien die stress-vermittelte Phosphorylierungen von chromatin-assoziierten Proteinen mit dieser Funktion in Verbindung gebracht.

Im Zuge meiner Forschung, habe ich 73 chromatin-assoziierte Proteine, die eine mehr als zweifache Zunahme oder Abnahme der Phosphorylierung als Antwort auf Stresssignale aufweisen, identifiziert. Aus dieser Gruppe von Proteinen wollten wir die Auswirkungen stressinduzierter Phosphorylierung anhand des

Polycombgruppenproteins Posterior Sex Combs (Psc) analysieren und untersuchten spezifisch die Fähigkeit von Psc, Chromatin an Zielgenen zu kompaktieren. Psc ist ein wesentlicher Bestandteil des Polycomb Repressor Komplex 1 (PRC1) und reguliert den Zellzyklus, Gewebewachstum und Differenzierung. Wir haben festgestellt, dass sich die stress-induzierten Phosphorylierungen an Serin 724 und Threonin 727 in einer Domäne von Psc befinden, welche essentiell für die Bindung und Kompaktierung von Nukleosomen ist. Während wir einzelne Aspekte dieser Phosphorylierungsstellen charakterisieren konnten, verhinderten technische Einschränkungen eine tiefgreifende funktionelle Analyse dieser Phosphorylierung *in vitro* und *in vivo*.

Während Plastizität für eine dynamische Anpassung an Stresssignale und somit für das zelluläre Überleben notwendig ist, können Deregulation oder Mutationen in chromatin-assoziierten Proteinen dramatische Konsequenzen haben. Zum Beispiel führen Mutationen innerhalb des chromatin-assoziierten Proteins *Alpha-thalassemia mental retardation syndrome X-linked (ATRX)* zu Lern- und Gedächtnisstörungen und wurden mit einer Reihe von Krebserkrankungen in Verbindung gebracht. ATRX enthält zwei wichtige chromatin-assoziierte Domänen, eine N-terminale ATRX-DNMT3-DNMT3L (ADD) Domäne, die spezifische Histonmodifikationen bindet und eine C-terminale SNF2 Nukleosomremodellierungsdomäne.

Eine BLAST Analyse des *Drosophila melanogaster* Genoms der ADD und SNF2 Domänen von ATRX identifizierte zwei Proteine, XNP und dADD1. XNP enthält die SNF2-remodeler Domäne, während dADD1 die chromatin-bindende ADD-Domäne enthält. Über die Funktion und die Beziehung dieser beiden Proteine in *Drosophila* ist wenig bekannt. Durch Immunlokalisierungsexperimente, biochemische Charakterisierung, phänotypische Analysen und Verhaltenstests stellten wir fest, dass beide Proteine nicht direkt miteinander interagieren, aber einige zelluläre Funktionen, sowie eine Reihe von gemeinsamen Interaktionspartnern teilen. Mutationen in diesen beiden Proteinen führen zu Phänotypen, welche denen von ATRX ähneln, wie zum Beispiel Lern- und Gedächtnisstörungen, sowie Beeinträchtigungen in der DNA-Reparatur und der Transposon-Stillegung.

Beide der oben beschriebenen Studien befassen sich mit der Balance zwischen epigenetischer Plastizität und Stabilität. Während Plastizität für stressinduzierte Geweberegeneration notwendig ist, ist Stabilität im Gegenzug für den Erhalt der Chromatinintegrität unerlässlich. Zusammenfassend widerspiegeln beide Projekte die Komplexität der epigenetischen Regulation und zeigen auf, wie wichtig es ist weiterhin dynamische als auch statische Mechanismen der Chromatinregulation zu untersuchen. Obwohl ich im Rahmen meiner Doktorarbeit an zwei Projekten gearbeitet habe, stelle ich hier nur den Teil Charakterisierung von dADD1 und XNP, welche die Wichtigkeit von stabiler epigenetischer Vererbung untersucht, vor.

1 Introduction

1.1 Chromatin compact: the basics

DNA is one of the most basic building blocks of life, providing the blue prints on how to build some of the simplest single celled organisms, such as bacteria, to more complex multicellular organisms such as humans. The smallest known genome of only 531 000 base pairs and 473 genes, belongs to an artificially generated *Mycoplasma mycoides* bacterial strain JCVI-syn3.0, that contains only the DNA and genes essential to provide life [1]. In comparison the human genome contains over 3 billion base pairs and contains enough DNA in a single cell to stretch to a length of around 1.8 meters [2]. While exact gene numbers are not known, a 2013 estimate from an analysis of RefSeq data suggest that the human genome contains around 26 000 genes [3]. In order to store so much genetic information in the small space of a very tiny nucleus, some organisms evolved DNA packaging systems.

The most fundamental packaging block for DNA is the histone. Histones are conglomerates of four basic protein subunits, which include histone 3 (H3), histone 4 (H4), histone 2A (H2A) and Histone 2B (H2B). Each histone contains two copies of the four core histone proteins, generating the so called histone octamer (reviewed in [4]). As histones are slightly positively charged they provide the perfect environment around which the DNA can wrap, with 147 bases of DNA being able to fit around a single histone octamer [5].

DNA repeatedly wraps around histones, with variable lengths of linker DNA between each histone (reviewed in [4]). These DNA wrapped histones are called nucleosomes and long strings of nucleosomes are referred to as chromatin, which can be further compacted. Usually, chromatin that is actively transcribed remains loosely packaged while silenced chromatin is highly condensed and is often inaccessible to transcriptional machinery. In general, loosely packaged, actively transcribed chromatin is referred to as euchromatin, while highly compacted, silenced chromatin is referred to as heterochromatin.

Proteins that are involved in the regulation of chromatin structure are referred to as epigenetic regulators. These proteins have diverse functions at chromatin and may be involved in the maintenance or conversion of chromatin between active and inactive states. While many epigenetic regulators were first classified to play a role in either activation or inactivation of chromatin, more and more evidence is pointing towards these proteins having diverse, and sometimes opposing roles, at chromatin. For example, Heterochromatin Protein 1 a (HP1a), which will be discussed below, was classically defined as a chromatin silencing protein that is important for the formation of very compacted and silenced heterochromatin. However, more recently HP1a has been also shown to be important for gene expression (reviewed in [6]).

The determination of active and inactive chromatin regions can be regulated by the addition of post translational modifications (PTM) to histone tails. These PTMs can include phosphorylation, methylation or acetylation, among other modifications, and collectively are referred to as the histone code (reviewed in [7]). This histone code is established by so called writer proteins that add the PTMs to histones. These PTMs are then recognized by so called reader proteins that bind the modified histone tails and can recruit other factors that help establish, maintain and regulate chromatin structure. These histone marks can also be removed by eraser proteins enabling the introduction of different histone PTMs by writer proteins, facilitating the conversion of chromatin between active and inactive states (reviewed in [8, 9]).

Proper regulation of chromatin is essential for the health of an organism, with many diseases developing as a result of epigenetic misregulation. For example, many different cancer types are the result of misregulation or mutations in epigenetic regulators (reviewed in [10, 11]). However, many other disease types such as neurodegenerative disorders, autoimmune disorders and cardiovascular disease can also be caused by aberrant epigenetic regulation highlighting the importance of epigenetic regulation in human health and disease (reviewed in [12]).

1.2 Alpha-thalassemia mental retardation syndrome

1.2.1 ATRX syndrome

Alpha-thalassemia mental retardation syndrome (ATRX) is a human X-linked disorder that causes mild to severe intellectual impairment in males and is caused by mutations within the *ATRX* gene. Hemizygous males display a number of symptoms such as alpha-thalassemia, altered facial features and genital abnormalities. Typically, carrier females are healthy but may display subtle signs of alpha-thalassemia, with the majority of carrier females showing skewed X-inactivation, where disease carrying chromosomes are preferentially inactivated [13, 14]. Increased frequency of mutations within *ATRX* have also been observed in a number of different cancer types including non-familial pancreatic neuroendocrine tumors, gliomas, sarcomas and carcinomas [15-21]. Interestingly, patients with *ATRX* syndrome do not show an increased prevalence of cancer.

1.2.2 Chromatin function of ATRX

Functionally *ATRX* is very important in the regulation of chromatin as loss or mutations of *ATRX* results in mitotic and meiotic defects, as well as alternative lengthening of telomeres [14, 22-24]. *ATRX* contains a C-terminal SNF2 chromatin remodelling domain and an N-terminal *ATRX*-*DNMT3*-*DNMT3L* (*ADD*) domain. The *ADD* domain of *ATRX* is unique in that it combinatorially recognizes and binds tri-methylated histone 3 lysine 9 (*H3K9me3*) and un-methylated histone 3 lysine 4 (*H3K4me0*) [25-27]. Together, *HP1 α* , the Human homologue of *Drosophila* *HP1a*, and the *ATRX* *ADD* domain recruit *ATRX* to pericentric heterochromatin [26].

ATRX has a number of functions and has been implicated in the formation and maintenance of heterochromatin at pericentric heterochromatin, telomeres and retrotransposons [28, 29]. In addition ATRX, along with its interaction partner Death-domain associated protein (DAXX), incorporates the histone variant H3.3 into ribosomal repeat sequences, telomeres and pericentric heterochromatin which is important for maintenance of silencing at these regions [30-32]. ATRX is also important for proper DNA damage response, where ATRX knock-out cells are more sensitive to hydroxyurea-induced replication stress [33]. Overall ATRX is very important for maintenance of genomic stability, and it is unsurprising that mutations within ATRX result in disease. Interestingly, 80% of the mapped ATRX Syndrome causing mutations within ATRX are located within either the ADD domain or the SNF2 domain, demonstrating the importance of chromatin regulation for human health and disease [13].

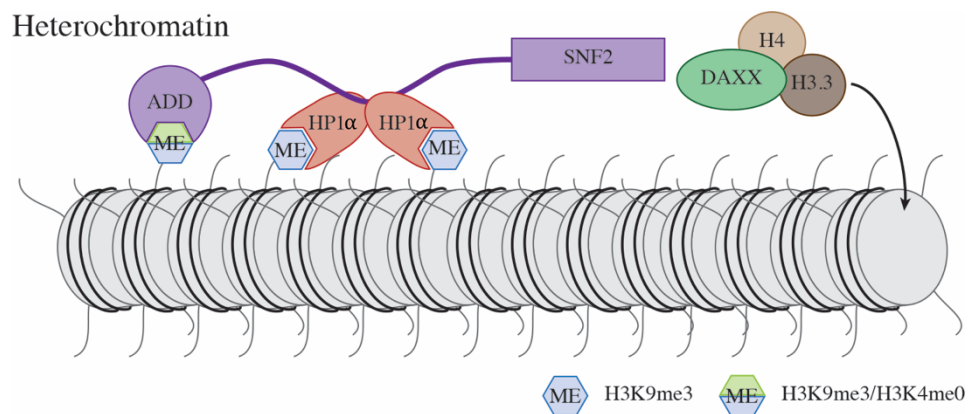


Figure 1: Model of ATRX function at heterochromatin.

ATRX is recruited to heterochromatin through the ADD domain binding to H3K9me3/H3K4me0 histones as well as the interaction between HP1 α . Here, ATRX works in cooperation with DAXX to replace H3 with histone 3 variant H3.3. Adapted from Eustermann et. al, 2011.

1.2.3 The ATRX ADD domain: a unique histone recognition domain

Located at the N-terminal region of ATRX between amino acids 169-262 is the specialized H3 tail binding domain, known as the ADD domain. In addition to ATRX the ADD domain in humans is also found in the DNA methyltransferase (DNMT) proteins DNMT3A and DNMT3B as well as the related but catalytically

inactive DNMT3L protein [34]. The ADD domain is composed of a singular GATA-like finger domain followed by an imperfect Plant homeodomain (PHD), which together bind three zinc ions, resulting in the formation of a globular domain [25]. This globular domain forms a pocket that binds very specifically to H3 tails that are H3K4me0, since methylation of H3K4 decreases ADD domain binding affinity to H3 tails [35, 36]. While the ADD domain of the DNMT proteins recognizes only the absence of H3K4 methylation, the ADD domain of ATRX is unique in its combined ability to recognize H3K9me3 together with H3K4me0, binding most efficiently to histones containing this combination of marks [25-27]. The amino acids important for recognition of H3K9me3 and H3K4me0 in the ATRX ADD domain are highlighted in Figure 3.

1.2.4 SNF2 domain

The SNF2 domain is an ATP-dependent chromatin remodeling domain that is capable of nucleosome sliding and re-positioning [37]. The SNF2 family can be divided into 24 distinct subfamilies, with many proteins being involved in transcriptional regulation, chromatin unwinding, DNA repair and DNA recombination [38, 39]. The SNF2 domain of ATRX is considered a Rad54-like domain based on the spacing between helicase domains [38]. Further analysis of this domain revealed that the SNF2 domain of ATRX is capable of nucleosome repositioning and that this repositioning is dependent on the presence of ATP [40]. Interestingly, a number of mapped disease causing mutations within the ATRX SNF2 domain interfere with nucleosome repositioning, suggesting that the nucleosome remodeling function of ATRX is essential for proper organism development [41].

1.3 Conservation in *Drosophila melanogaster*

A Basic Local Alignment Search Tool (BLAST) search of the *Drosophila* genome against the ATRX ADD domain and SNF2 domain returns two results, dADD1 and XNP. However, unlike Human ATRX which contains both the ADD

and SNF2 domain in a single protein, these domains are split between the two proteins in *Drosophila* with dADD1 containing the N-terminal ADD domain and XNP containing the SNF2 domain (Schematic alignment Figure 2). These domains are highly conserved with the ADD domain of dADD1 showing a 36% sequence conservation (37/102 amino acids) and a 52% score of sequence identity to the Human sequence (Figure 3). The SNF2 domain of XNP shows a 52% sequence conservation (172/326 amino acids) and a 70% score of sequence identity in comparison to the Human sequence (Figure 3). A phylogenetic analysis of ATRX homologues suggested that dADD1 and XNP became two independent proteins as the result of a gene split in insects [42].

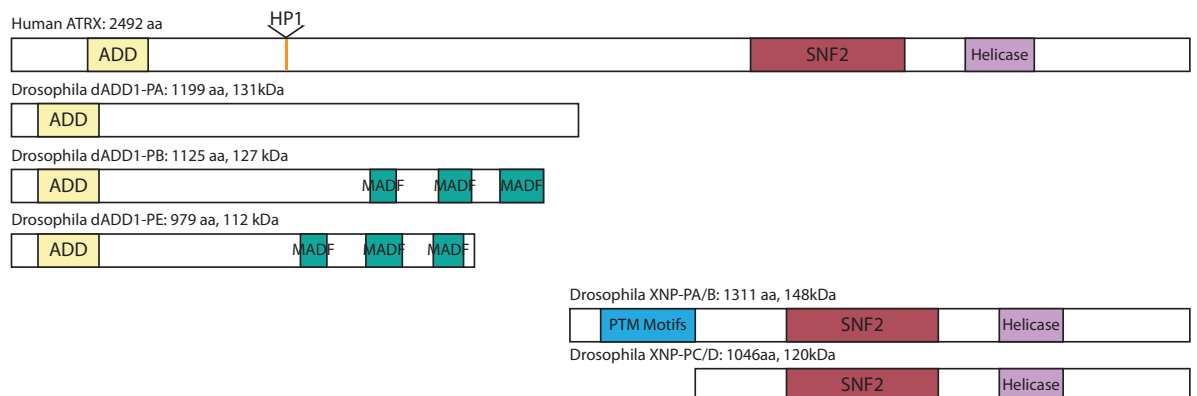


Figure 2: Alignment of *Drosophila* dADD1 and XNP isoforms with human ATRX.

A BLAST search of the *Drosophila* genome for the ADD and SNF2 domains of human ATRX returns two proteins dADD1 which contains the ADD domain and XNP containing the SNF2 domain. Representative alignment of all annotated isoforms of dADD1 and XNP compared to human ATRX, including the additional protein domains such as a MADF DNA binding motif in dADD1-PB and PE and a motif targeted for posttranslational modifications in the long isoforms of XNP.

Introduction



- * Disease causing mutations
 - * Involved in H3K9me3 recognition
 - * Involved in H3K4me0 recognition
- Full Conservation
 Partial Conservation

Figure 3: Amino acid sequence alignment of the ADD domain of dADD1/ATRX and the SNF2 domain of XNP/ATRX shows a high degree of conservation.

Amino acid sequence alignments of the human and *Drosophila* ADD and SNF2 domains. These domains show a high degree of amino acid conservation, especially between the amino acids necessary for H3K9me3 recognition in the ADD domain and within mapped disease causing mutations.

Interestingly, the majority of the mapped disease causing mutations within ATRX show either full or partial conservation within *Drosophila*, suggesting these amino acids are important for chromatin domain function in multiple species (Figure 3, red stars). This conservation is also very apparent within the amino acids of the ADD domain that are necessary for H3K9me3 recognition, with 8/10 of these amino acids showing full or partial conservation (Figure 3, purple stars). However, the conservation between the dADD1 and ATRX ADD domain is not as strong between the amino acids involved in H3K4me0 recognition, with only 1/4 amino acids being partially conserved (Figure 3, blue stars).

2 Aim of this study

Cellular loss of ATRX function results in mitotic and meiotic defects, altered DNA damage response and impaired transposon silencing. ATRX contains two important chromatin associated domains, an N-terminal ATRX-DNMT3-DNMT3L (ADD) domain and a C-terminal SNF2 chromatin remodeler domain. The ADD domain together with the HP1a interacting domain, is important for the recruitment of ATRX to heterochromatin and mediate the chromatin regulatory function of ATRX. The majority of mapped disease causing mutations fall within either the ADD or SNF2 domain, highlighting the importance of proper chromatin architecture for human health and development.

Since mutations in ATRX cause ATRX syndrome and have been linked to different cancer types, we sought to understand if *Drosophila* could be used as a model system to further investigate the the molecular mechanisms of ATRX. To do so we aimed to undertake an analysis of the *Drosophila* ATRX homologues dADD1 and XNP to determine if these proteins show function conservation to ATRX. Through localization experiments, biochemical characterization, phenotypic analysis and behavioral assays this project aimed to better understand the cellular and organismal functions of these two proteins and to investigate the relationship between them.

To analyze functional conservation with human ATRX, we sought to test *dADD1* and *XNP* mutants for known ATRX mutant phenotypes including defects in learning and memory, double-strand DNA repair response and transposon

silencing. In addition, we sought to characterize the interaction between dADD1 and XNP and to identify new interaction partners of both proteins through co-immunoprecipitation and mass spectrometry, as well as immunolocalization experiments. The identification of new interaction partners was expected to provide new leads into which biological processes not only XNP and dADD1 but also human ATRX proteins may be involved in.

Many people worked on this project and contributed ideas, methods, lab space and time at the bench. Those directly involved in this project include: Dr. Anne-Kathrin Classen, Dr. Axel Imhof, Dr. Andreas Thomae, Dr. Ignasi Forne, Dr. Annette Schenck, Dr. Michaela Fenckova, Isabelle Grass, Kathrin Bergel, Nikolai Hörmann, Ian Will, Marco La Fortezza and Sarah Schäfer. For those who helped perform the experiments their names appear in the figure legends.

3 Results

3.1 Biochemical characterization of dADD1

3.1.1 dADD1-PA is a 250kD protein

At the beginning of this project dADD1 was an uncharacterized and unnamed protein known to us by its CG identifier CG8290. As little was known about this protein we first began to investigate the biochemical characteristics of dADD1, using tools established by Dr. Andreas Thoma. These reagents included a cloned construct of the long isoform of dADD1-PA and a stable cell line expressing C-terminally Flag/HA-tagged dADD1-PA under the control of an inducible pMT promoter and an antibody raised against an N-terminal sequence common to all isoforms. On western blots of stable cell extracts overexpressing the long isoform dADD1-PA, the dADD1 antibody detects a band that is 250 kD in length, which is consistent with the molecular weight protein identified using an HA antibody (Figure 4 B). This molecular weight was much larger than the predicted weight of dADD1-PA of 130 kD (Figure 4 A).

To confirm this molecular weight increase we tested brain and ovary cell lysate extracts from a dADD1-BioTAP line as well as ovary cell lysates from a dADD1 GFP trap line (dADD1_{endoGFP}). The dADD1-BioTAP fly line contains a gDNA bacmid clone inserted onto the third chromosome with a C-terminal protein A tag that only tags the long isoform of dADD1 (Figure 4 A, arrow BioTAP). The dADD1_{endoGFP} was generated through random insertion of a MiMIC construct

containing GFP-Streptavidin-Flag (GFP-ST-F) tags as well as acceptor and donor splice sites, inserted into the endogenous *dADD1* locus at a sequence common to all isoforms, and should therefore be spliced into all isoforms (Figure 4 A, arrow MiMIC GFP-ST-F). In both the *dADD1*-BioTAP and the *dADD1*_{endoGFP} a high molecular weight protein around 250 kD was observed, consistent with our observation from stable cell lines expressing the long isoform of *dADD1*, indicating that the long isoform of *dADD1* is actually a 250kD protein (Figure 4 C and D).

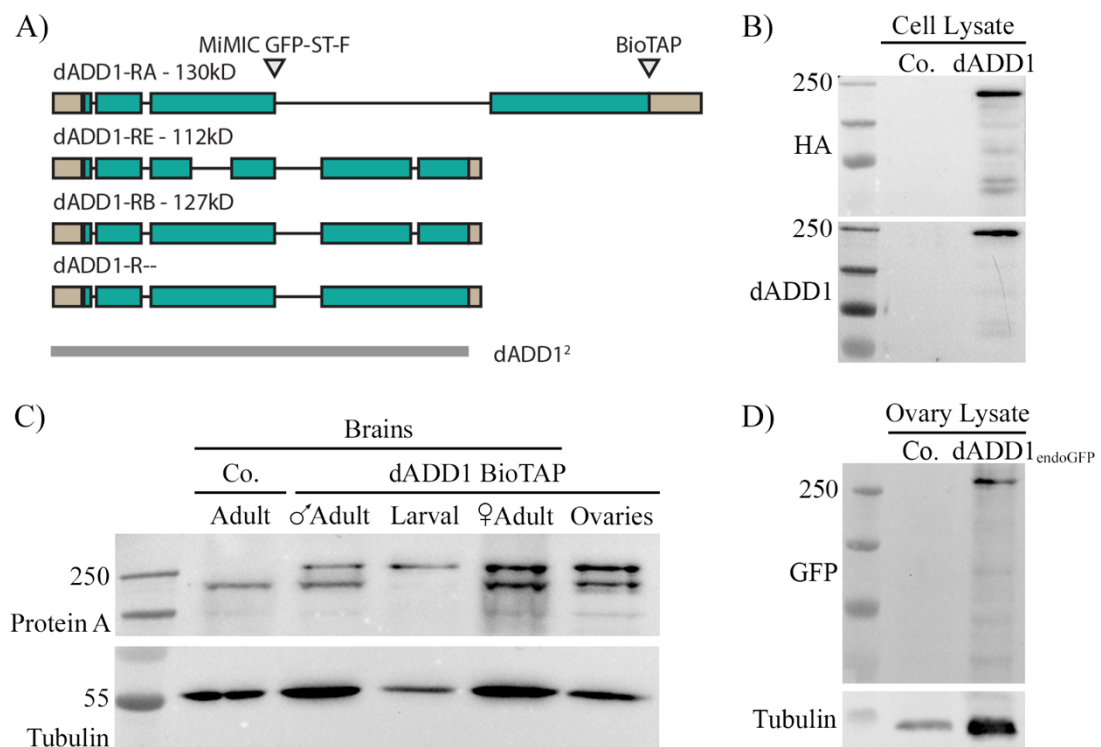


Figure 4: The long isoform of *dADD1* is much larger than predicted and is the dominantly expressed isoform in ovaries.

dADD1-PA is much larger than predicted. A) There are three Flybase annotated isoforms of *dADD1*, and a fourth isoform identified by Lopez-Falcon et.al, 2014, that is similar to *dADD1*-RB but retains the fifth intron. Arrows indicate tag insertion of MiMIC cassette (MiMIC GFP-ST-F) into all isoforms of *dADD1* and BioTAP insertion that tags only the long isoform with a biotin and Protein A tag. Genomic deletion of P-element excision mutant *dADD1*² is indicated by grey box, outlining approximate length and location of the deletion. B) Overexpression of the long isoform of *dADD1*-PA in stable S2DRSC cells. Construct contains a dual C-Terminal Flag/HA tag and is detected by both an HA antibody as well as a *dADD1* specific antibody. The *dADD1*-PA-Flag/HA construct runs around 250kD, much larger than the 130kD predicted weight. Control are wild type S2DRSC cells. C) BioTAP tagged *dADD1*-PA is expressed in ovaries, larval brains as well as female and male adult brains. The BioTAP *dADD1*-PA protein has a molecular weight of about 250kD. Control flies are *w*¹¹¹⁸ D) *dADD1* MiMIC construct (*dADD1*_{endoGFP}) is expressed in ovaries. GFP antibody detects a very strong band at over 250kD but also lower molecular weight bands that correspond to the other isoforms of *dADD1* plus the additional MiMIC tag. The long isoform of *dADD1* appears to be the most dominantly expressed isoform in ovaries. Control are ovaries from HP1a GFP flies. Western blot in C performed by Ian Will and western blot in D performed by Sarah Schäfer.

Results

The expression of dADD1 in different tissue was tested using the dADD1-BioTAP line and revealed that dADD1-PA is expressed in both female and male adult brains, in larval brains and in ovaries. Analysis of the dADD1_{endoGFP} line also revealed that, at least in ovaries, this high molecular weight dADD1-PA isoform is the most dominantly expressed isoform, although smaller molecular weight bands corresponding to the other isoforms are also present. These results are in contrast to previous publications that suggest dADD1 isoforms are equally expressed and run at their predicted molecular weights [42].

To understand why dADD1-PA has a molecular weight almost double the predicted weight we tested whether the long isoform was a dimer by boiling stable cell lysates in high concentrations of β -mercapotethanol (BME) for up to 5 hours. BME is a reducing agent that disrupts di-sulphide bonds between cysteine residues, dissolving tertiary and quaternary protein structures. Boiling cell lysates in 10% BME resulted in no change in the molecular weight of dADD1-PA when compared to normal western blot boiling conditions with 1% BME for 5 minutes (Figure 5 A). The same results were obtained when samples were boiled in 10% DTT, another reducing agent similar to BME re-confirming that dADD1-PA does not form a dimer (data not shown).

Since the molecular weight increase was not caused by protein dimerization, we then tested if dADD1-PA contained PTMs that added to the total weight of the protein. We tested for the addition of Ubiquitin, O-linked N-acetylglucosamine (O-GlcNAc) and Poly-(ADP Ribose) (PAR). Classically defined as a PTM that marks proteins for proteosomal degradation, ubiquitin is now known to function in a number of different cellular processes such as cell signaling and transcriptional regulation. A single ubiquitin protein weighs 8.5 kD with ubiquitin being added to proteins either as a single molecule or as a poly-ubiquitin chain, where multiple ubiquitin proteins are covalently linked [43]. O-GlcNAc is a sugar molecule that is added to serine and threonine residues of proteins by the enzyme O-linked N-acetylglucosaminyl transferase or OGT. Addition of O-GlcNAc to a protein has many different biological functions and is known to be involved in transcriptional regulation as well as regulation of protein-protein interactions [44]. PAR is another

protein PTM that is mainly triggered by DNA damage responses and can help to initiate programmed cell death. Many nuclear proteins have been shown to be PAR modified including many DNA associated proteins including histones [45].

By western blot dADD1 appears to be ubiquitinated but contains no O-GlcNAc or PAR modifications (Figure 5 B). Since a known interaction partner of dADD1 contains a RING E3 ubiquitin ligase domain we tested if this protein, called Bonus, was the ubiquitin ligase of dADD1. To do so we knocked down Bonus in dADD1 stable cells and compared ubiquitination levels of dADD1 after Bonus knockdown (Figure 5 C). After RNAi knockdown Bonus was not detectable in the cell lysate, indicating that the knockdown was efficient (Figure 5 C, +RNAi Bonus). However, we observed no decrease in total ubiquitination of dADD1 between the control and the Bonus RNAi samples indicating that Bonus is not the primary ubiquitin ligase of dADD1. Pull downs of dADD1 were also tested for ubiquitinated peptides by MS, but no ubiquitin modified peptides were identified (data not shown). It is therefore difficult to definitively conclude that dADD1 is ubiquitinated, and more work should be done to determine if ubiquitination does indeed contribute to the increased molecular weight of dADD1-PA.

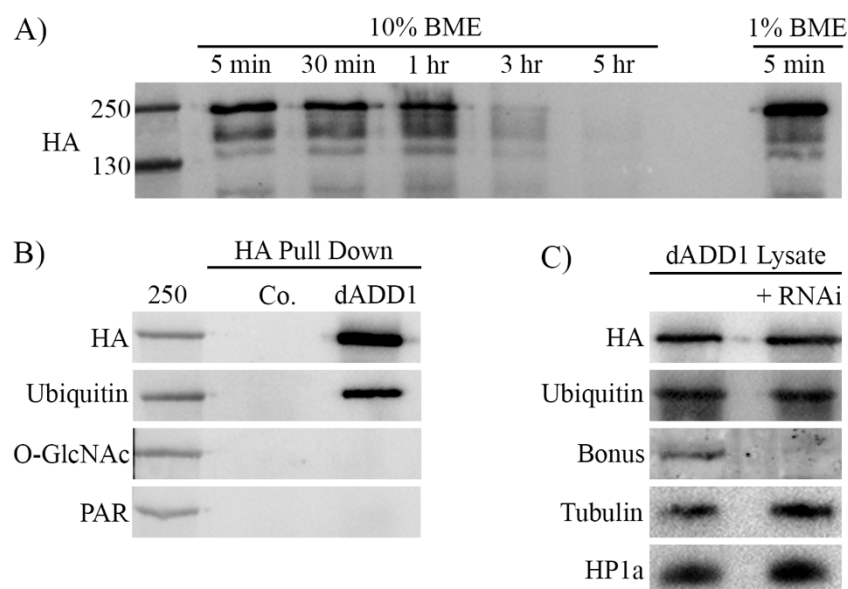


Figure 5: Increased molecular weight of the long dADD1 isoform is not the result of dimerization, O-linked N-acetylglucosamination or Poly-ADP ribosylation. dADD1 may be ubiquitinated but the RING domain containing protein Bonus is not the primary ubiquitin ligase of dADD1.

Results

Experiments were performed in a stable S2 cell line expressing the long dADD1 isoform. A) dADD1 does not form a dimer. Boiling of stable cell lysates in 10% BME for up to 5 hours does not decrease the molecular weight of the protein when compared to the normal western blot preparation conditions of 1% BME for 5 minutes. B) dADD1 is ubiquitinated. Pull downs of dADD1 from stable cells show that dADD1 is ubiquitinated but is not O-GlcNAc or PAR modified. Control sample of HA pull downs from S2DRSC cells. C) Bonus is not the primary ubiquitin ligase of dADD1. Knock down of *bonus*, a known interaction partner of dADD1 that contains a E3 ubiquitin ligase RING domain, does not decrease ubiquitination of dADD1. *bonus* is efficiently knocked down by RNAi, but RNAi treated samples show no decrease in total cellular dADD1, tubulin or HP1a levels.

3.2 Relationship between dADD1 and XNP

A phylogenetic analysis of ATRX homologues suggested that dADD1 and XNP became two independent proteins as the result of a gene split in insects [42]. Since dADD1 and XNP are the *Drosophila* homologues of mammalian ATRX we sought to determine whether these proteins function together or in similar pathways. To do so we looked at tissue level and subcellular localization, biochemical interactions and molecular phenotypes caused by loss or overexpression of these proteins.

Previously published reagents for XNP were kindly provided by the lab of Dr. Kami Ahmad. These included an antibody against all isoforms of XNP as well as two deletion mutant alleles for XNP, *XNP⁴⁰³* and *XNP⁴⁰⁶* [46]. These XNP mutants were generated by P-element excision which resulted in the loss of a large genomic fragment from the 5' end of XNP, removing the start codon and the majority of the first exon from all isoforms (Figure 6 A). We tested the XNP antibody for specificity by staining *XNP⁴⁰³* and *XNP⁴⁰⁶* mutant ovaries with the XNP antibody (Figure 6). We observed a complete loss of XNP staining in the nucleus of homozygous mutant ovaries, verifying antibody specificity and also that the *XNP⁴⁰³* and *XNP⁴⁰⁶* alleles are homozygous null alleles.

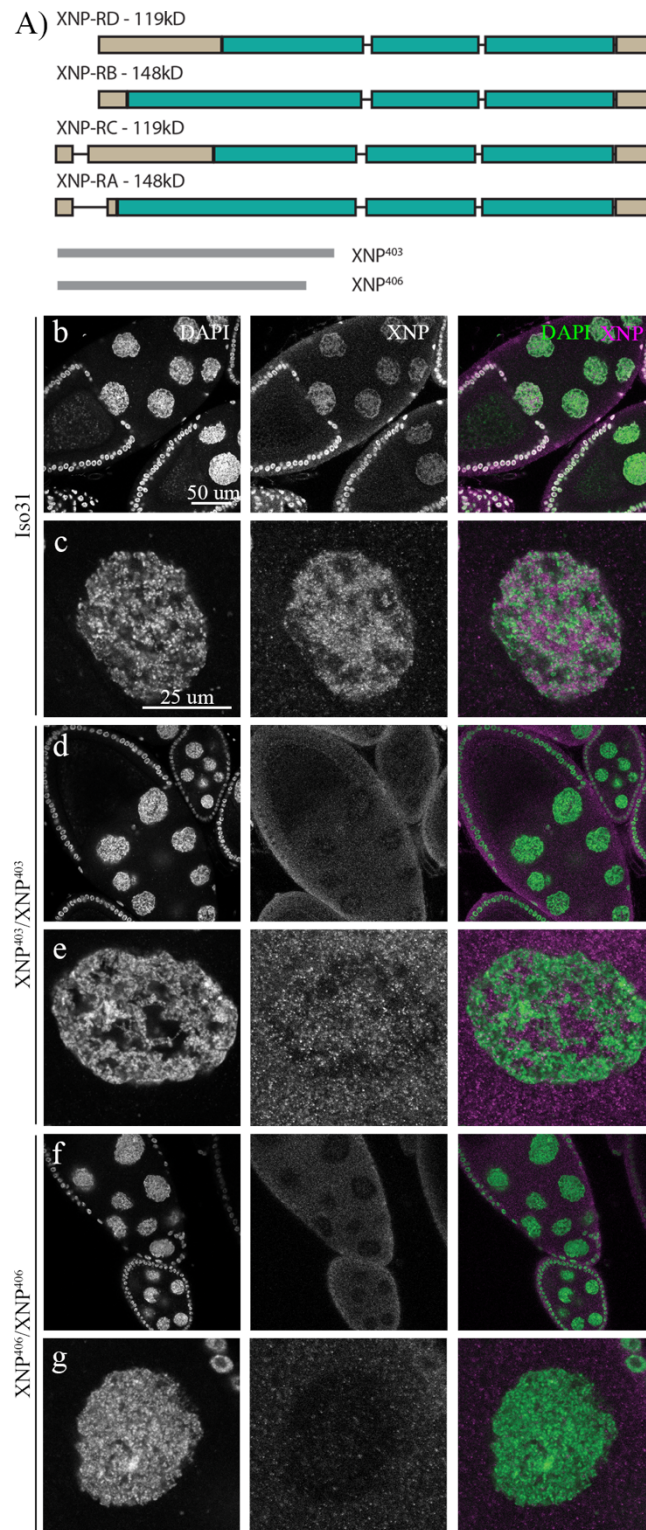


Figure 6: XNP⁴⁰³ and XNP⁴⁰⁶ mutants are null mutants as staining with XNP antibody does not detect XNP in either mutant.

Results

Testing of XNP mutants and antibodies. A) Gene structure of XNP. XNP has four isoforms with XNP-RA/B and XNP-RD/C sharing the same coding sequence but different 5' and 3' UTR's. Genomic deletions from two p-element excision mutants, *XNP⁴⁰³* and *XNP⁴⁰⁶*, are outlined by the grey box indicating approximate size and location of the deletions. b-g) Antibody stainings of XNP in Iso31 control and homozygous *XNP⁴⁰³* and *XNP⁴⁰⁶* mutant ovaries. The XNP antibody signal strongly overlaps with the DNA signal in Iso31 control ovaries. This staining is lost in both the *XNP⁴⁰³* and *XNP⁴⁰⁶* mutant ovaries. Microscopy images produced by Kathrin Bergel.

An excision mutant of *dADD1*, *dADD1²*, was generously provided by the lab of Dr. Mitzi Kuroda, who also provided the BioTAP line discussed in section 3.1.1 *dADD1-PA* is a 250kD protein. The excision mutant contains a genomic deletion of *dADD1* that removes almost the entire coding sequence of *dADD1*-RB and RE while deleting all but the last exon from *dADD1*-RA (Figure 4 A). Antibodies specific to *dADD1* that recognizes an N-terminal epitope common to all *dADD1* isoforms were provided by Dr. Andreas Thoma. From these antibodies a single hybridoma clone, 8F11, proved to be specific to *dADD1* as we observed a complete loss of staining in homozygous *dADD1²* mutant ovaries, and simultaneously observed a significant overlap in staining with *dADD1_{endoGFP}* (Figure 7).

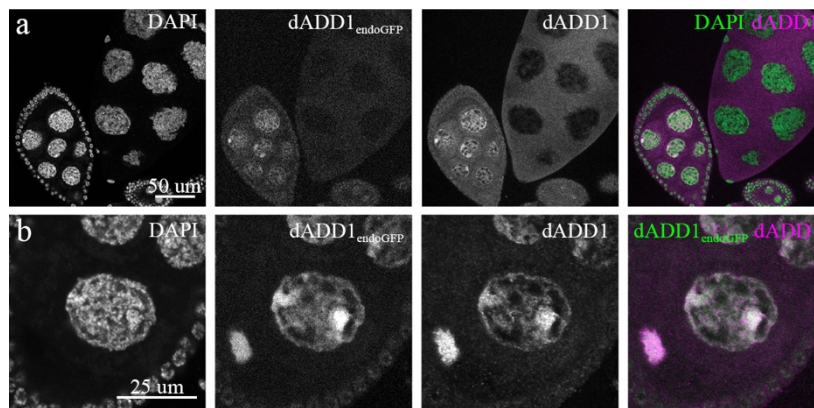


Figure 7: Confirmation of *dADD1*-8F11 antibody, *dADD1_{endoGFP}* fly line and *dADD1²* homozygous fly line.

a) *dADD1_{endoGFP}* and *dADD1²* homozygous mutants stained with DNA dye DAPI and *dADD1*-8F11 (*dADD1*) antibody. Homozygous *dADD1²* ovaries show complete lack of staining with *dADD1* antibody. *dADD1_{endoGFP}* localization overlaps with DAPI bright AT rich DNA regions representing heterochromatin. b) *dADD1*-8F11 antibody and *dADD1_{endoGFP}* show significant overlap at chromatin, with a strong enrichment at heterochromatin and a diffuse staining over euchromatin. Stainings performed by Nikolai Hörmann

These tools, and others, were used to help dissect the relationship between dADD1 and XNP in the following sections.

3.2.1 dADD1 and XNP are expressed in both neurons and glia

Both dADD1 and XNP are highly expressed in embryonic and larval central nervous system as well as in neurons and glia in adult brains [47, 48] (Figure 8 a and b). Since loss of ATRX in humans causes intellectual impairment, we sought to determine if *Drosophila* could be used as a model to elucidate the mechanisms that underlie learning disabilities in human ATRX patients. To do so we employed a well-established assay for studying learning and memory defects in *Drosophila* that measures habituation to a light-off stimulus that induces startle-jump responses [49].

Previously characterized mutants for both dADD1 (*dADD1²*) and XNP (*XNP⁴⁰³* and *XNP⁴⁰⁶*) were isogenized over 7 generations to an Iso31 background and tested in habituation assays. Since habituation assays rely on the measurement of startle-jump response to repetitive light-off stimulus, flies need to be tested for fitness as reduced fitness can cause false positives in this assay when the lack of startle response results from flies being physically unable to jump. We first tested homozygous *dADD1²* and heterozygous *dADD1²*, *XNP⁴⁰³* and *XNP⁴⁰⁶* mutants for fitness. Homozygous *XNP* mutants were not tested for fitness or habituation as *XNP* homozygous mutant lines could not be maintained and too few progeny eclosed from balanced crosses.

Fitness was tested by repeatedly subjecting the flies to a prolonged light off stimulus that should cause a continued startle response in wild type flies. Of all the mutants tested none of them showed a significant decrease in their fitness in comparison to the wild type (Figure 8 C). Although it appears the *dADD1²* homozygous mutants have a slightly decreased fitness, this change is not significant and has a P-Value 0.25. As the heterozygous *XNP⁴⁰³* and *XNP⁴⁰⁶* flies as well as *dADD1²* heterozygous mutants did not display a reduced fitness, *dADD1* homozygous as well as *dADD1* and *XNP* heterozygous mutant lines were further tested in habituation assays to test how long it takes for flies to learn to stop jumping in response to a light-off stimulus.

Results

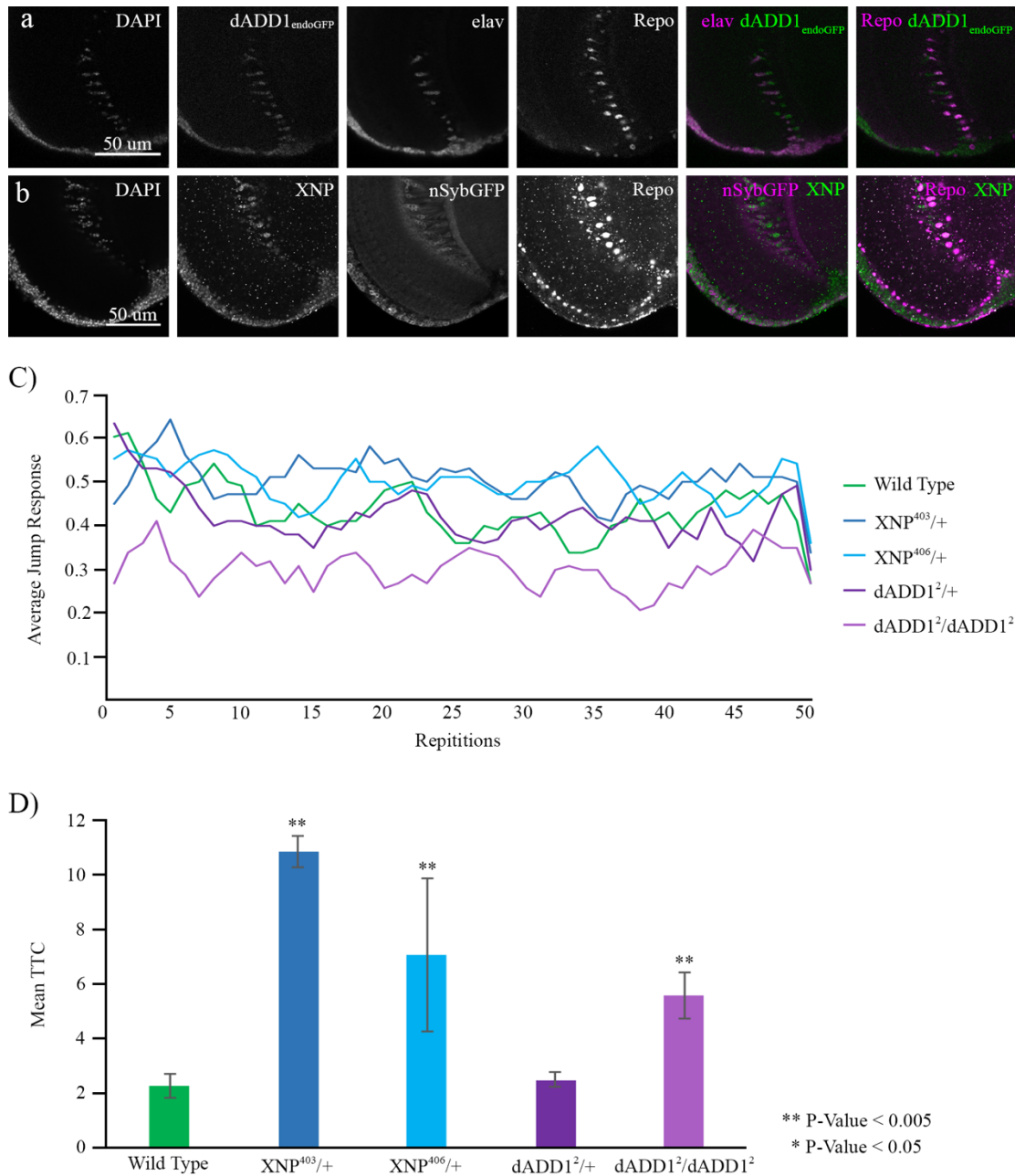


Figure 8: *dADD1* and *XNP* are present in neurons and glia of the adult brain. Loss of these proteins results in learning and memory defects in adults.

dADD1 and *XNP* are found within neurons and glia and are important for brain function. a) Staining of adult *dADD1_{endoGFP}* brains with a neuronal marker (*elav*) and glial marker (*Repo*) shows that *dADD1* is present in both neurons and in glia of the adult brain. b) Adult brain staining of brains expressing a neuronal marker *nSyb GFP* stained for *XNP* and *Repo* to mark glia. *XNP* is found in both neurons and in glia of the adult brain. c) Fitness assays of heterozygous *XNP⁴⁰³* and *XNP⁴⁰⁶* mutants as well as *dADD1²* heterozygous and homozygous mutants. Flies were subjected to repetitive light off stimulus that induces continued startle response in wild type (*w¹¹¹⁸*) flies. Calculated P-Values for mutants are all above 0.05 indicating mutant fitness is not significantly different than the wild type. d) Habituation assay measuring how quickly wild type (*w¹¹¹⁸*) and mutant flies learn to not startle in response to light off stimulus. Heterozygous *XNP* mutants as well as *dADD1* homozygous mutants show a slowed learning response as indicated by an increase in the mean TTC. P-Values denote significance in comparison to wild type response. Brain stainings were performed by Nikolai Hörmann. Fitness and habituation assays were performed by collaborators at the Radboud University Nijmegen Medical Center in the lab of Dr. Annette Schenck.

Startle response to a light-off stimulus was tested 50 times using a 15 millisecond light-off pulse followed by 1 second of light-on. The light-off pulses are frequent enough that eventually wild type flies stop jumping as they learn that the stimulus poses no threat. Flies met the criteria of being habituated when they did not startle for 5 consecutive light-off pulses and the number of light pulses needed to reach the criteria for habituation were counted as the trials to criteria (TTC). The *XNP* heterozygous mutants as well as the *dADD1* homozygous mutants displayed a slowed habituation response in the habituation assays, indicated by an increase in mean TTC, while the *dADD1* heterozygotes showed a speed of habituation comparable to wild type flies (Figure 8 D). This indicated that a loss of dADD1 or XNP causes learning and memory defects in flies, similar to mutations of ATRX in humans.

3.2.2 dADD1 but not XNP is enriched in the oocyte germinal vesicle

modENCODE RNA-Seq data showed that, in addition to the larval central nervous system, both dADD1 and XNP are highly expressed in ovaries [47]. Using the XNP and dADD1 antibodies we stained ovaries of fattened, mated females to determine if dADD1 and XNP proteins are present in egg chambers, and in which cells of the developing egg chamber they localize.

Drosophila ovaries contain both germline and somatic tissue. The germline is composed of both nurse cells and a single oocyte, that are encapsulated by somatic follicle cells. In late stage egg chambers, the oocyte is the largest cell and contains the oocyte nucleus contained in a structure called the germinal vesicle. Through antibody stainings we determined that both XNP and dADD1 are present in the germline nurse cells as well as the germinal vesicle (Figure 9). While XNP was also present in the somatic follicle cells, the dADD1 antibody did not detect any signal in these cells. However, we were able to detect low levels of dADD1 in the follicle cells of dADD1^{endoGFP} ovaries (Figure 7).

Interestingly we observed a striking difference in the enrichment of dADD1 and XNP in the germinal vesicle. While the intensity of the XNP signal is similar between the germinal vesicle, nurse cells and follicle cells, the intensity of the

Results

staining of dADD1 in the germinal vesicle is significantly higher than the staining of nurse cell chromatin. This indicates that dADD1 may be selectively enriched into the germinal vesicle, suggesting that dADD1 may be important for chromatin establishment during the first embryonic cellular divisions.

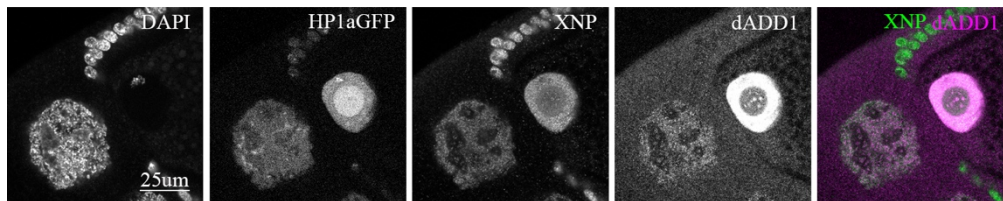


Figure 9: dADD1 is selectively enriched in the oocyte germinal vesicle.

Staining of both XNP and dADD1 using protein specific antibodies in HP1a GFP ovaries. HP1a GFP, XNP and dADD1 localize to nurse cell chromatin and all are pre-packaged into the oocyte germinal vesicle, with dADD1 being selectively enriched. HP1a GFP and XNP but not dADD1 show staining in the somatic follicle cells surrounding the oocyte. Stainings performed by Kathrin Bergel.

During the first mitotic cellular divisions following fertilization, the zygotic genome is inactive and is not actively transcribing genes. In *Drosophila* there are two waves of zygotic genome activation, the first occurring at mitotic cycle 8 and the second at mitotic cycle 14, however, until this point the zygote must rely on maternally deposited mRNAs and proteins to establish the early chromatin landscape [50]. dADD1 and XNP homozygous mutants are viable, indicating that these proteins are not essential, but may assist in the establishment of early embryonic chromatin. Their non-essential role in this process may be conceptually similar to the observed role that ATRX plays in transposon silencing, where transposons in homozygous ATRX mutant cells are silenced, but at a much slower rate than in wild type cells [29].

3.2.3 dADD1 and XNP show distinct chromatin localization patterns at nurse cell chromatin

To study the chromatin localization of dADD1 and XNP we chose to look at the polytenized chromatin of egg chamber cells. When a developing egg leaves the stem cell niche of the germarium, the cells divide until the egg chamber contains around 800 follicle cells, 15 nurse cells and a single oocyte containing the germinal

vesicle (see schematic in Figure 10). At this point, around stage 6, the cells stop dividing and both somatic follicle cells as well as germline nurse cells begin to endoreplicate, causing polytenization of egg chamber chromatin. The highly replicated genome enables simple visualization of chromatin protein localization.

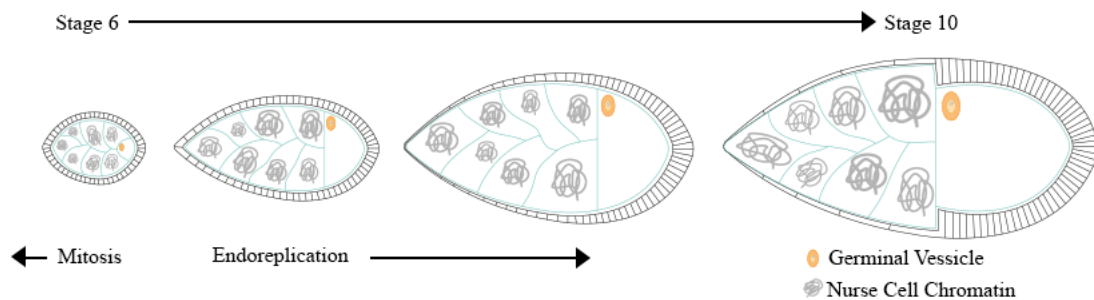


Figure 10: Schematic of egg chamber morphology from stage 6 to stage 10.

Drosophila egg chambers contain both somatic tissue as well as germline tissue. The somatic follicle cells surround the germline cells which consist of nurse cells and the oocyte. Within the oocyte is the germinal vesicle where the maternally contributed DNA is stored. Until stage 6 cells undergo cell division until the egg chamber contains approximately 800 follicle cells, 15 nurse cells and a single oocyte. At this point both the somatic follicle cells as well as the nurse cells begin to endoreplicate causing chromatin polytenization. The majority of images in this thesis are from egg chambers between stages 6-10.

Using this system, we visualized the subnuclear localization patterns of dADD1 and XNP by looking at co-localization in flies also expressing a GFP tagged HP1a construct. HP1a is enriched at heterochromatin and is commonly used as a heterochromatin marker. For simplicity of discussion in this thesis, I refer to any region enriched with HP1a or associated marks (H3K9me3 and H3.3, discussed in the next paragraphs) as heterochromatin and all other chromatin regions as euchromatin. We found that XNP uniformly distributed across nurse cell chromatin and showed no enrichment at heterochromatin or euchromatin (Figure 11 b). dADD1 showed a widespread distribution across euchromatin similar to XNP, but additionally displayed a strong enrichment at heterochromatin, as determined by co-localization with HP1a GFP (Figure 11 a).

We additionally looked at co-localization with other chromatin proteins and components known to be associated with dADD1 or XNP (See section 3.4 Other interaction partners of dADD1 and XNP). These included histone variant H3.3,

Results

histone modification H3K9me3, HP1b and Bonus. H3.3 is a known interactor of mammalian ATRX, with ATRX and interaction partner DAXX incorporating H3.3 into telomeres and transcribed heterochromatin repeat sequences [30, 31]. In mammalian systems H3.3 has been shown to be incorporated into both euchromatin and heterochromatin and is associated with both actively transcribing as well as silenced chromatin [32, 51, 52]. Furthermore, it has been suggested that XNP is one of two proteins in *Drosophila* capable of replication-independent nucleosome replacement of H3.3 [53]. Stainings of nurse cell chromatin show that H3.3 is present in euchromatin, but also shows enrichment at heterochromatin as determined by strong co-localization with HP1a (Figure 11 c). This indicates, that at least in *Drosophila*, H3.3 is enriched at heterochromatin, and in further experiments chromatin regions enriched for H3.3 were superficially classified as heterochromatin.

The histone modification H3K9me3, which is bound by the chromo-domain of HP1a and by the ADD-domain of dADD1 and ATRX, unsurprisingly showed very specific staining at heterochromatin. H3K9me3 significantly overlaps with HP1a and in further experiments was also used as a marker for heterochromatin (Figure 11 d).

HP1b is a heterochromatin protein 1 family member that has been implicated in transcriptional activation of euchromatic genes [54]. As reported previously, we found in nurse cell chromatin stainings that HP1b appears to occupy chromatin domains distinct from HP1a, primarily staining euchromatic regions and showing little enrichment at heterochromatin [55] (Figure 11 e). Localization of the dADD1 interaction partner Bonus was also tested, with Bonus showing a uniform staining across euchromatin, and in many instances was excluded from HP1a rich heterochromatin.

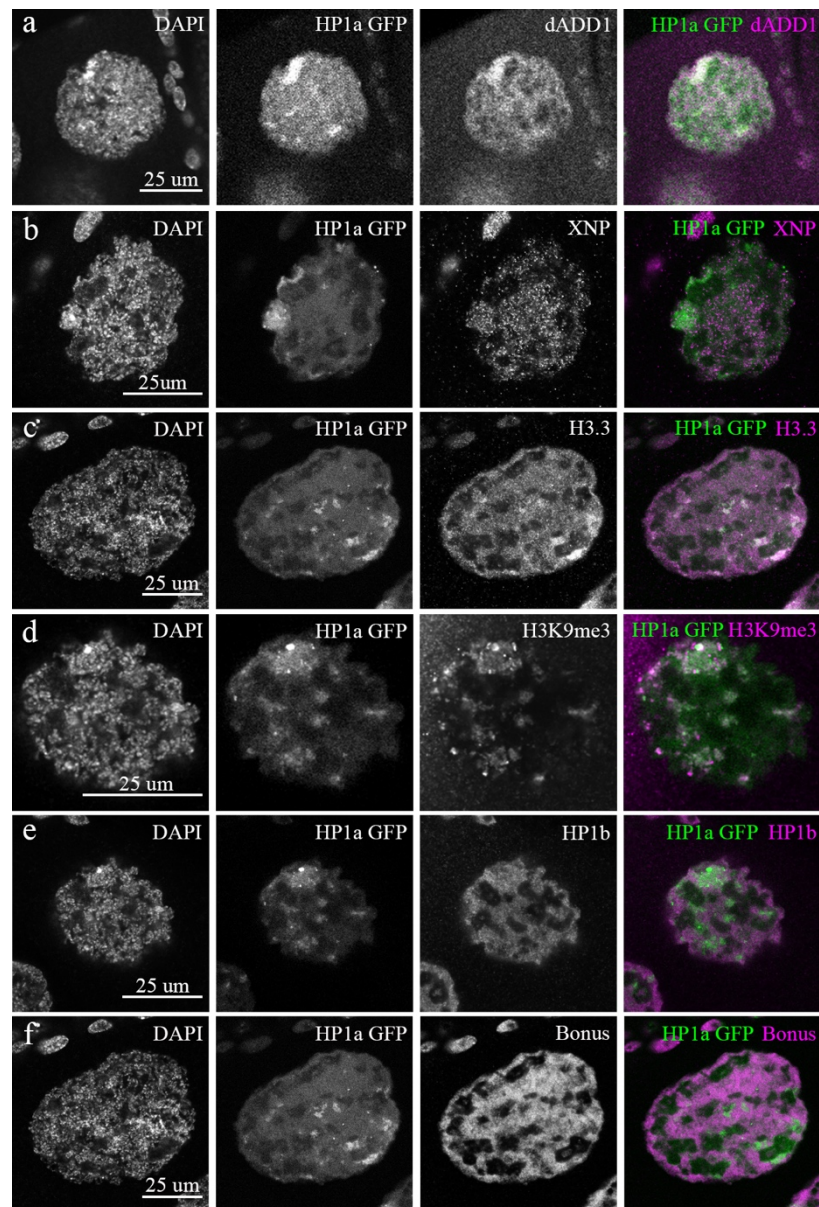


Figure 11: dADD1, H3.3 and H3K9me3 co-localize with HP1a GFP at heterochromatin, while XNP, HP1b and Bonus show uniform staining across nurse cell chromatin.

Localization of dADD1, XNP, H3.3, H3K9me3, HP1b and Bonus to nurse cell chromatin compared to localization of HP1a GFP. a) dADD1, stained with the dADD1 antibody, shows significant overlap with HP1a GFP, showing enrichment at heterochromatin, and a diffuse staining over euchromatin. b) XNP shows no enrichment at heterochromatin, but displays a uniform staining across nurse cell chromatin. c) Histone variant H3.3 shows strong co-localization and enrichment with HP1a GFP at heterochromatin, but also stains euchromatin. d) Histone 3 modification H3K9me3 shows significant co-localization with HP1a GFP at heterochromatin. e) HP1b displays a uniform staining across chromatin, and appears to occupy distinct chromatin regions from HP1a GFP. f) Bonus, a known dADD1 interactor, localizes to euchromatin and occupies distinct chromatin regions from HP1a GFP.

We observed similar localization patterns of dADD1 and XNP to chromatin in HELA Kyoto cells where dADD1 but not XNP is highly enriched at H3K9me3-rich chromatin (Figure 12 a and b). The localization of dADD1 to H3K9me3-rich regions

Results

in HELA cells supports previous *in vitro* data showing the ADD domain has a conserved H3K9me3 binding function, and suggests that binding of the ADD domain to H3K9me3 may recruit dADD1 to chromatin [56]. Expression of XNP in HELA cells results in nuclear localization and a relatively uniform staining across chromatin, although some chromatin regions showed increased XNP localization. A few of these XNP domains overlapped with H3K9me3 rich chromatin domains but the enrichment was significantly reduced in comparison to dADD1. Unfortunately, co-transfection experiments of dADD1 and XNP in HELA cells were unsuccessful, and through these experiments we could not determine if dADD1 is capable of recruiting XNP chromatin.

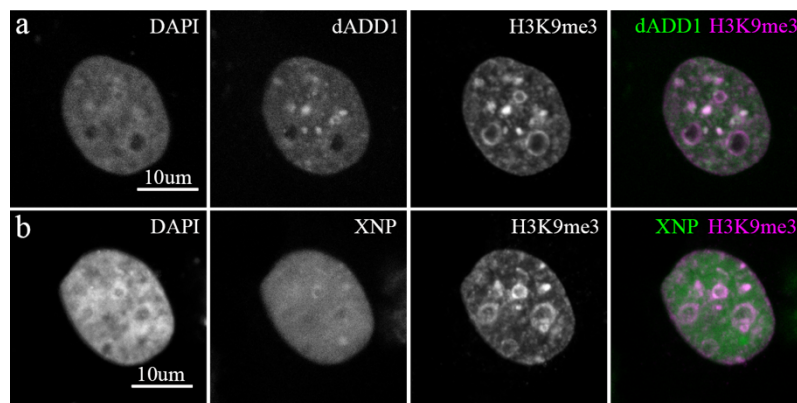


Figure 12: *dADD1* is recruited to H3K9me3 rich regions in HELA Kyoto cells.

Overexpression of dADD1-GFP and XNP-GFP constructs in human cancer cell derived HELA Kyoto cells. a) dADD1-GFP shows nuclear localization and strongly co-localizes with H3K9me3 rich chromatin in HELA cells. b) XNP-GFP localizes to the nucleus, and shows a relatively uniform staining across chromatin. There is some enrichment of XNP to specific chromatin regions, with few of these enriched regions co-localizing with H3K9me3 rich chromatin.

3.2.4 dADD1 and XNP are recruited independently to chromatin

To better understand if the localization of dADD1 and XNP to chromatin was dependent on the presence of the other protein we stained homozygous *dADD1*² and *XNP*⁴⁰³ egg chambers with dADD1 and XNP antibodies. Wild type control ovaries in the majority of the imaging experiments contained a ubiquitously expressed RFP tagged shotgun (shg) construct labeled shgRFP. Shg encodes fly E-cadherin, which localizes to cell-cell contacts and enables easy identification of wild type control

ovaries. Interestingly, localization of either dADD1 or XNP protein did not change in the corresponding mutants when compared to localization in control ovaries, indicating that dADD1 and XNP are recruited to chromatin independently of one another (Figure 13).

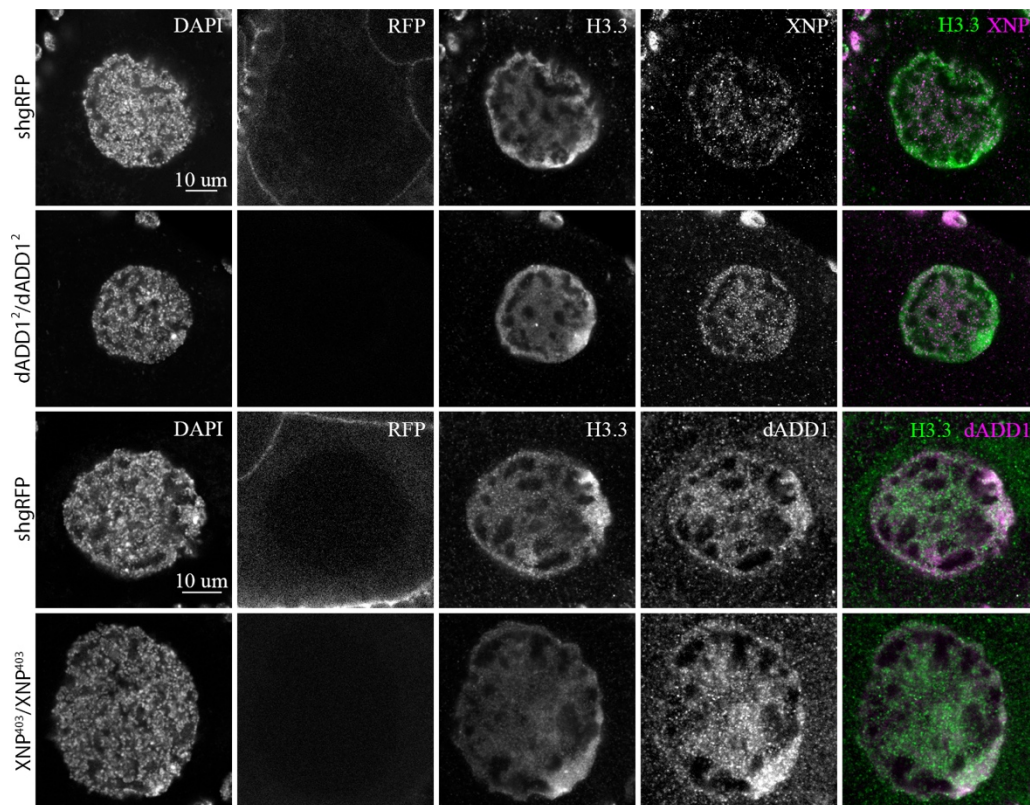


Figure 13: Loss of dADD1 or XNP does not affect the chromatin localization of the other protein.

Staining of dADD1 and XNP in *dADD1*² and *XNP*⁴⁰³ homozygous mutants. XNP shows a normal nurse cell chromatin staining in *dADD1*² homozygous mutants when compared to shgRFP controls. dADD1 shows normal staining in *XNP*⁴⁰³ homozygous mutants when compared to shgRFP controls, with enrichment at heterochromatin. H3.3 deposition at heterochromatin is unchanged by loss of either dADD1 or XNP.

Similarly, overexpression of dADD1 in somatic follicle cells of the egg chamber did not increase the recruitment of XNP to heterochromatin, but did increase the localization of other associated proteins at heterochromatin (Figure 14 a and b, Discussed in sections 3.5.3 and 3.5.4). Furthermore, overexpression of XNP in follicle cells did not increase the incorporation of dADD1 into euchromatin or heterochromatin (Figure 14 c and d). Taken together, loss and overexpression data

Results

indicates that dADD1 and XNP are recruited independently to chromatin, and do not rely on the presence of the other protein for chromatin localization.

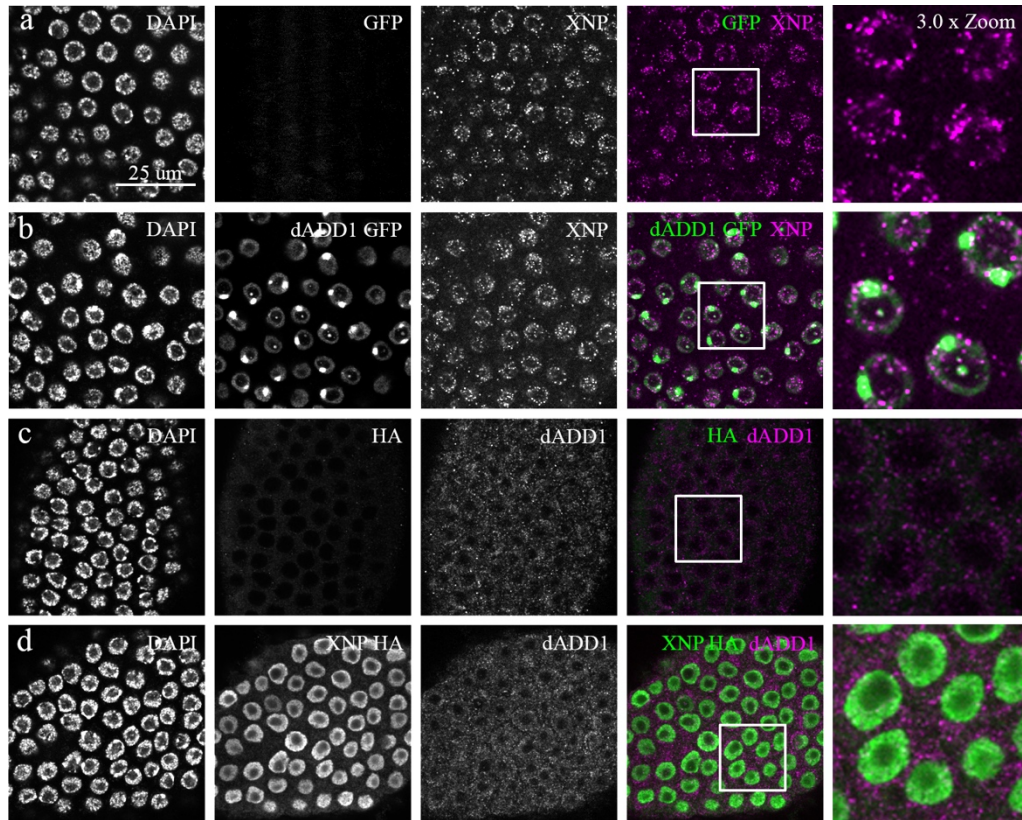


Figure 14: Overexpression of dADD1 or XNP does not increase the chromatin recruitment of the other.

dADD1 and XNP do not recruit one another to chromatin. a) XNP shows a uniform staining across follicle cell chromatin in control shgRFP ovaries b) A dADD1-GFP construct that is specifically expressed in egg chamber follicle cells using the TJGLA4 driver is recruited to heterochromatin but XNP is not recruited to dADD1-GFP rich heterochromatin. Note localization of the dADD1-GFP construct to the nucleolus. c) Endogenous dADD1 antibody does not detect dADD1 in follicle cells of shgRFP control ovaries. d) Overexpression of an XNP-HA construct specifically in egg chamber follicle cells using the TJGAL4 driver results in a general recruitment of XNP-HA to follicle cell chromatin. dADD1 recruitment to chromatin is not increased in XNP-HA overexpressing cells.

3.3 Biochemical and genetic interaction between dADD1 and XNP

3.3.1 dADD1 and XNP do not directly interact but both interact with HP1a and HP1b

Both dADD1 and XNP were previously identified to interact with HP1a [46, 56]. Since both proteins share this common interaction partner, but do not rely on the

presence of the other protein for chromatin recruitment we decided to further investigate the nature of the relationship between these two proteins.

Previous reports indicated that all dADD1 isoforms are capable of interacting with the long isoforms of XNP, although these interactions were based on the detection of a molecular weight band in *in vitro* binding assays that was much smaller than dADD1-PA [42]. We therefore co-transfected dADD1-PA Flag/HA tagged stable cells with a Myc tagged long isoform of XNP-PA/B and pulled down either dADD1 or XNP using Flag and Myc antibodies, respectively. Eluate samples from dADD1 pull downs showed no evidence of an interaction with XNP (Figure 15 A, α -Flag IP Elu. Myc). Conversely, dADD1 was detected in the eluate samples from XNP pull downs, however, dADD1 is also present in the bead-binding control sample indicating that dADD1 binds independently to the beads (Figure 15 A, compare Bead Only and α -Myc IP Elu. HA). As a positive control, endogenous HP1a was detected in both dADD1 and XNP pull downs (Figure 15 A, α -Flag IP Elu. and α -Myc IP Elu. HP1a).

To confirm these results we performed pull downs from cells overexpressing either dADD1-PA or XNP-PA/B and performed MS to determine if the long isoforms of either protein interacted with endogenous dADD1 or XNP. Again we did not detect any interaction between dADD1 or XNP, but see both proteins interacting with HP1a and HP1b (Figure 15 B). Unfortunately, we were unable to re-confirm the interaction between dADD1 and HP1b by targeted Co-IP analysis due to the inability of the HP1b antibody to detect an epitope on western blot and the lack of an HP1b cDNA clone for analysis of tagged constructs. Although we were not able to detect a direct interaction between dADD1 and XNP, the presence of common interaction partners indicates that although these proteins do not directly work together, they may act in common pathways and may share many interaction partners.

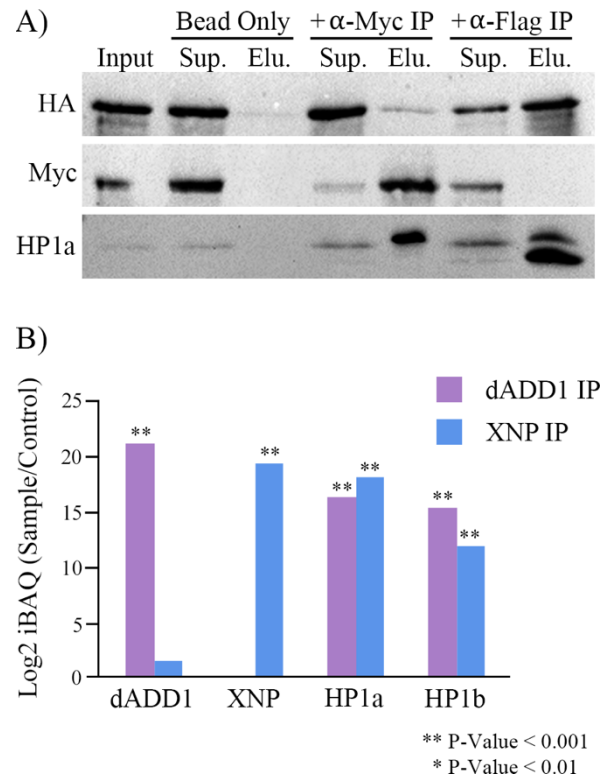


Figure 15: dADD1 and XNP do not directly interact but both interact with HP1a and HP1b.

Western blot and Mass Spec data detect no interaction between dADD1 and XNP but both interact with HP1a and HP1b. A) Co-transfection of dADD1-Flag/HA tagged stable cell line with XNP-Myc tagged construct. Pull down of dADD1 (+α-Flag IP) contains no XNP-Myc in the eluate. Pull down of XNP (+α-Myc IP) shows a band corresponding to dADD1-Flag/HA in the eluate, however, a band corresponding to dADD1-Flag/HA is also present in the bead only IP control. Both proteins pull down HP1a B) Flag pull downs of Flag tagged dADD1-PA (dADD1 IP) or XNP-PA/B (XNP IP) from S2 cells followed by MS. Pull down of dADD1 or XNP does not detect significant amounts of the corresponding proteins by MS. dADD1 IP and XNP IP are significantly enriched for HP1a and HP1b. Bars represent the Log₂ iBAQ dADD1 IP or XNP IP/Control IP. Control IP of was a Flag IP on untransfected cell lysates. P-Values represent the enrichment of each peptide in a single IP sample compared to the control IP. MS pull downs and protein preparation performed by Dr. Andreas Thomae and MS peptide identification by Dr. Ignasi Forne.

3.3.1 dADD1 and XNP interact genetically

Habituation assays demonstrated that loss of either dADD1 or XNP results in learning and memory phenotypes giving merit to the idea that these proteins may interact in similar pathways. We thus investigated if these proteins genetically interact. To do so we generated mutants from isogenized stocks that contained combinations of *dADD1*² and *XNP*⁴⁰³ or *XNP*⁴⁰⁶ mutations.

Homozygous XNP mutants display only one visible phenotype when compared to the Iso31 controls. Approximately 25% of homozygous *XNP*⁴⁰³ and 50% of *XNP*⁴⁰⁶ mutants develop melanotic tumors in the abdomen (Figure 16 A).

Melanotic tumors are non-cancerous lesions formed by the fly immune system encapsulating self-cells resulting in the formation of a black tumorous mass [57]. Although the exact cause of melanotic tumor formation is not known, it has been linked to deregulation of stress responses and apoptosis pathways [58]. Interestingly, addition of a single copy of the *dADD1*² allele into either homozygous XNP mutant background resulted in an increase in melanotic tumor incidence as well as an increase in size of the melanotic mass (Figure 16 B).

*dADD1*² homozygous mutants display no visible phenotypes, and the addition of a single copy of either *XNP*⁴⁰³ or *XNP*⁴⁰⁶ mutant allele caused no changes in wing or eye shape, size or patterning, bristle patterning, thorax closure or melanotic tumor formation (data not shown). However, the addition of one mutant copy of XNP to homozygous *dADD1*² flies resulted in increased organismal lethality during pupal stages. All tested mutants show comparable rates of lethality at larval stages, indicating that a similar percentage of larvae successfully pupariate, but many of the double mutants do not eclose and die in the pupal casing.

Results

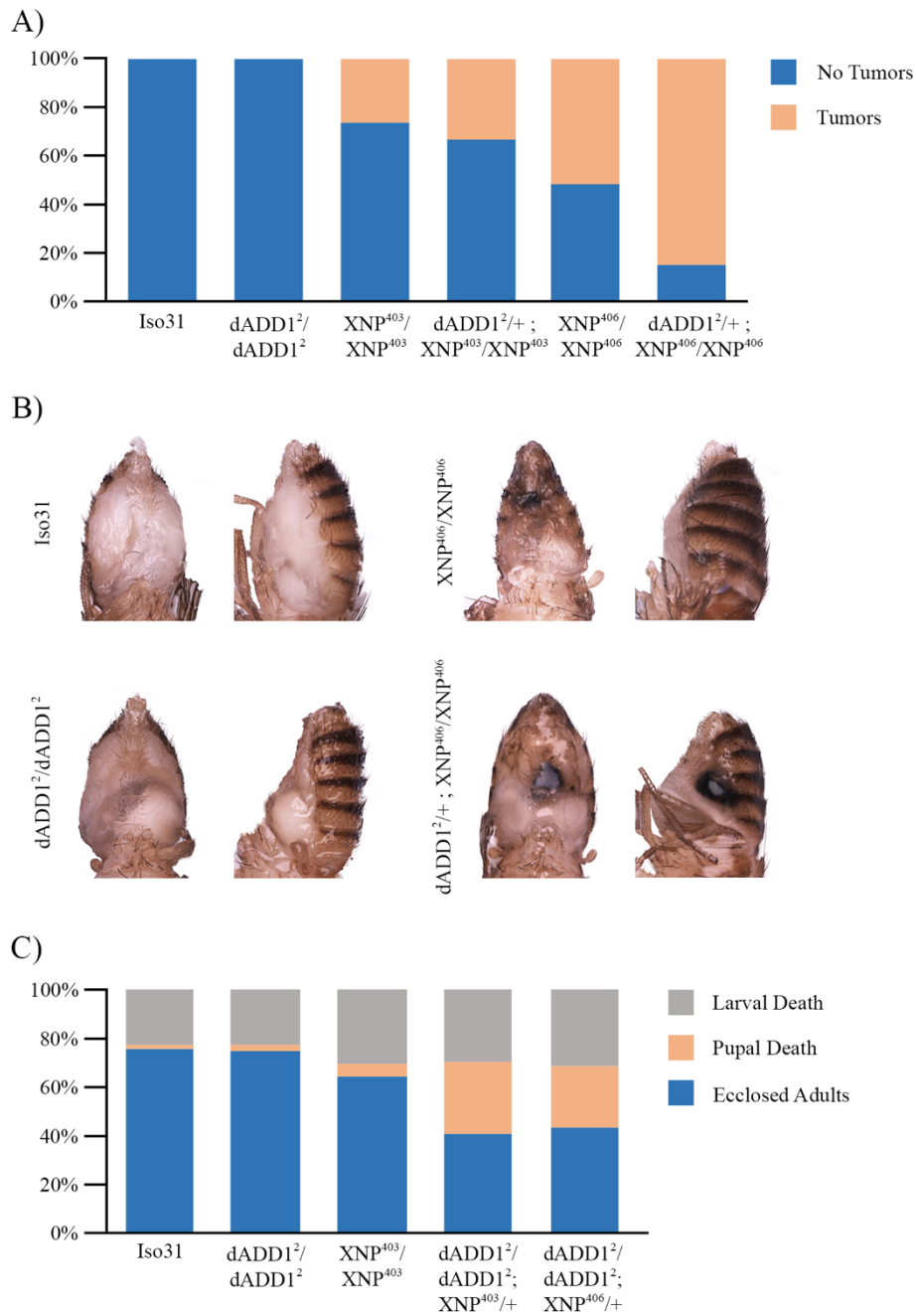


Figure 16: Combination mutations of *dADD1* and *XNP* show increased incidence of melanotic tumors as well as decreased pupal survival.

Quantification of mutant phenotypes of *dADD1* and *XNP* combination mutants. A) Addition of a single copy of *dADD1*² mutant allele increases melanotic tumor incidence in homozygous *XNP* adult flies. Both control Iso31 and *dADD1*² homozygous mutants do not form melanotic tumors. *XNP* homozygous mutants do form melanotic tumors, but the rate of melanotic tumors increases with the addition of a single copy of *dADD1*². B) Melanotic tumors in the abdomen of adult females. Iso31 and *dADD1* flies show no melanotic tumors while *XNP* mutants show small melanotic masses in the abdomen. The size of these masses increases in the double mutants. Flies chosen were representative of the specified genotype. Each genotype contains images of two different adult females. C) Addition of a single copy of either *XNP*⁴⁰³ or *XNP*⁴⁰⁶ to homozygous *dADD1* mutants results in increased pupal lethality. Rates of pupariation are similar between control Iso31 and mutant lines, but fewer adults ecdyse in the double mutant context.

While our data does not support the previous report of a direct protein-protein interaction between dADD1 and XNP, the exacerbation of mutant phenotypes in genetic combination strongly suggests that these proteins do indeed work in common pathways. Although the mechanisms that result in increased melanotic tumor incidence or increased pupal lethality are difficult to elucidate, we interpret these results to indicate that dADD1 and XNP both function in pathways important for development and also resistance to stress.

3.4 Other interaction partners of dADD1 and XNP

3.4.1 dADD1 interacts with chromatin proteins Bonus, Eggless and Mod(mdg4)

A previous study identified a number of interaction partners of dADD1, which included the chromatin proteins Eggless, Bonus and Mod(mdg4) [56]. Eggless, also known as SetDB1, is one of two *Drosophila* H3K9 methyltransferases that implements H3K9me3 marks onto histone tails. This protein is important for recruitment of HP1a to chromosome 4, as Eggless mutants show a loss of HP1a staining at chromosome 4 in salivary polytene chromosome squashes [59]. Bonus is another chromatin associated protein that has been implicated in both positive and negative regulation of chromatin [60]. In brains, Bonus associates with the transcription factor Fruitless, a protein important for male specific neuronal development. In males, Bonus recruits Histone deacetylase 1 to chromatin at Fruitless target genes causing formation of male typical neurons, while in females Bonus recruits HP1a to these same genes resulting in the development of female typical neurons [61]. Mod(mdg4) is an insulator protein that works together with the highly conserved insulator protein CTCF and regulates proper expression of the bithorax complex in *Drosophila* [62].

Pull downs of dADD1 from stable dADD1-PA-FLAG/HA expressing cells co-transfected with Myc-tagged Eggless, Mod(mdg4) and Bonus re-confirmed the interaction between these proteins and dADD1 (Figure 17 A). The interaction between dADD1 and endogenous Mod(mdg4) and Bonus was furthermore detected

Results

in MS analysis of dADD1 pull downs from S2 cells. However, this experiment did not detect any peptides corresponding to Eggless in dADD1 pull downs (Figure 17 B). Lack of Eggless in the dADD1 pull downs could be the result of IP conditions, which in the MS experiment was performed by Dr. Andreas Thomae and involved a very different extraction protocol. MS analysis of pull down fractions interacting with XNP, which were also performed by Dr. Andreas Thomae, showed that XNP interacts with the dADD1 interaction partner Mod(mdg4) (Figure 15 B, Figure 17 B). Further analysis of the MS pull down data for dADD1 and XNP is discussed in 3.4.3 *Pull downs of dADD1 and XNP identify a number of new interaction partners.*

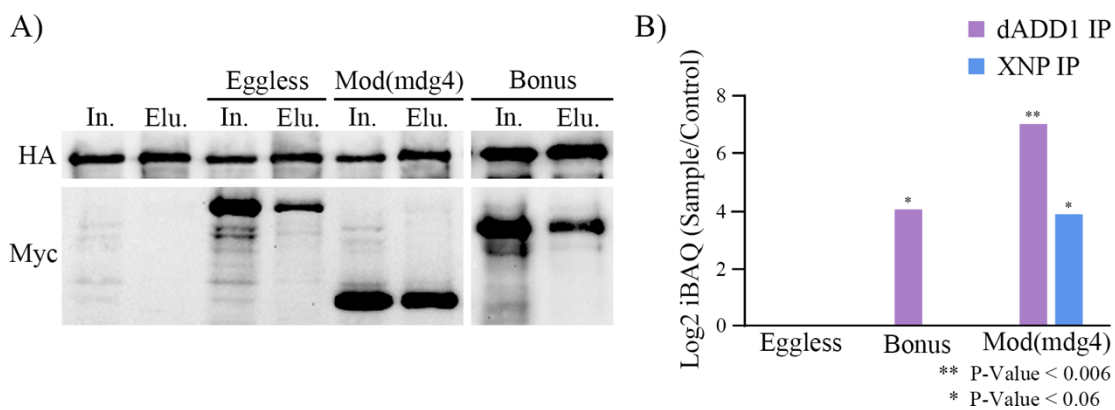


Figure 17: dADD1 interacts with chromatin proteins Eggless, Mod(mdg4) and Bonus.

A) Pull downs of Flag/HA tagged dADD1-PA from S2 stable cells co-transfected with Myc tagged Eggless, Mod(mdg4) and Bonus. Eluate samples from dADD1 pull downs contain Eggless, Mod(mdg4) and Bonus proteins. B) Flag pull downs of Flag tagged dADD1-PA (dADD1 IP) or XNP-PA/B (XNP IP) from S2 cells followed by MS. Peptides for both Bonus and Mod(mdg4) were identified in the dADD1 IP, while only Mod(mdg4) peptides were identified in the XNP IP. Peptides corresponding to Eggless were not identified in either IP. Bars represent the Log₂ iBAQ dADD1 IP or XNP IP/Control IP. Control IP of was a Flag IP on untransfected cell lysates. P-Values represent the enrichment of each peptide in a single IP sample compared to the control IP. MS pull downs and protein preparation performed by Dr. Andreas Thomae and MS peptide identification by Dr. Ignasi Forne.

3.4.2 Overexpression of Bonus in egg chamber follicle cells recruits dADD1 and HP1b to euchromatically localized Bonus foci

In addition to its interaction with heterochromatin associated proteins HP1a and Eggless, we wanted to further elucidate the significance of the interaction of dADD1 with Bonus. Bonus is the only *Drosophila* homologue of the mammalian TIF1 family proteins that are important for many transcriptional and chromatin regulatory processes and are also known to phosphorylate HP1 proteins [60, 63, 64].

In nurse cells Bonus is normally uniformly distributed across euchromatin and shows a chromatin localization pattern similar to HP1b (Figure 11, e and f).

Overexpression of Bonus in egg chamber somatic follicle cells using a TJGal4 driver results in the formation of punctate, euchromatically localized Bonus foci. These foci overlap with DAPI stained DNA regions, indicating that these foci are not just protein aggregates, but may represent clustering of euchromatic domains enriched with Bonus. Interestingly, both dADD1 and HP1b are recruited to Bonus foci while XNP, HP1a, H3.3 and H3K9me3 show no enrichment (Figure 18, Figure 19 and Figure 20). The specific recruitment of both dADD1 and HP1b to Bonus foci, gives merit to the idea that dADD1 can also be recruited into euchromatin and forms a euchromatin-specific complex with Bonus and HP1b.

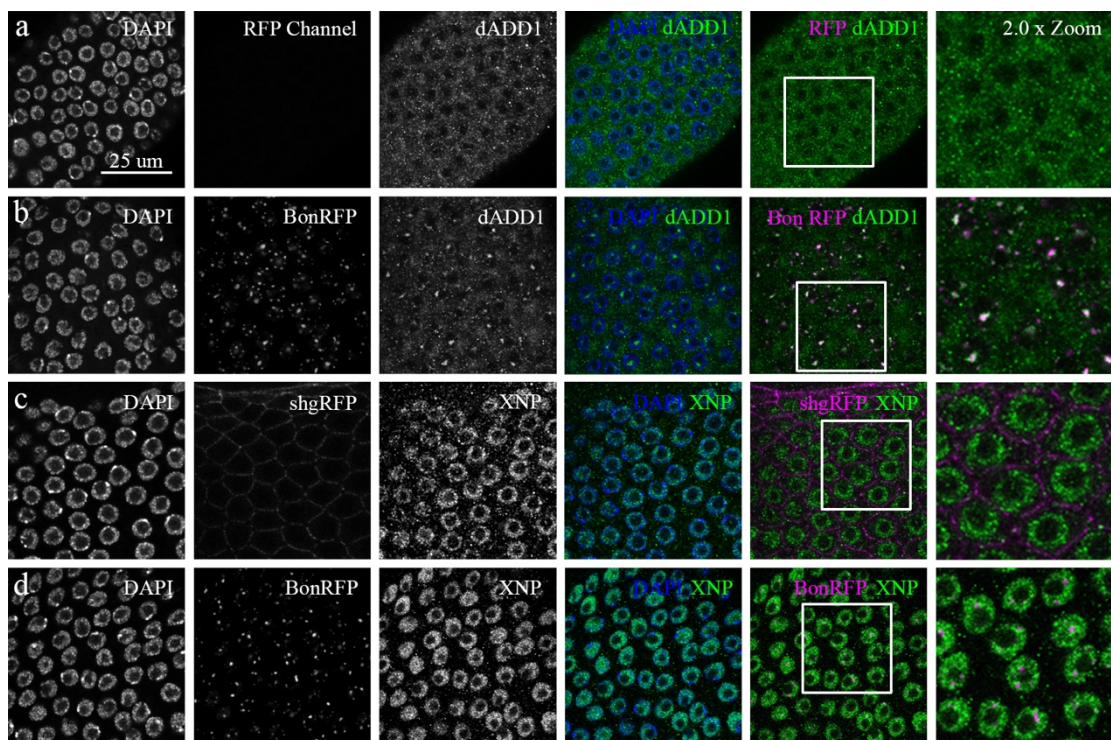


Figure 18: Overexpression of Bonus recruits dADD1 but not XNP to euchromatic Bonus foci.

Control and Bonus-RFP (BonRFP) overexpressing ovaries were fixed and stained together with each antibody to ensure comparable staining conditions. Follicle cell expression of Bonus was driven using a TJGAL4 driver a-b) Staining of dADD1^{endoGFP} control ovaries together with ovaries overexpressing BonRFP in ovary follicle cells stained with the dADD1 antibody. dADD1 and Bonus co-localize at euchromatin in BonRFP overexpressing follicle cells. d) Staining of shgRFP control ovaries and BonRFP overexpressing ovaries with the XNP antibody. XNP staining is unchanged in control and BonRFP follicle cells.

Results

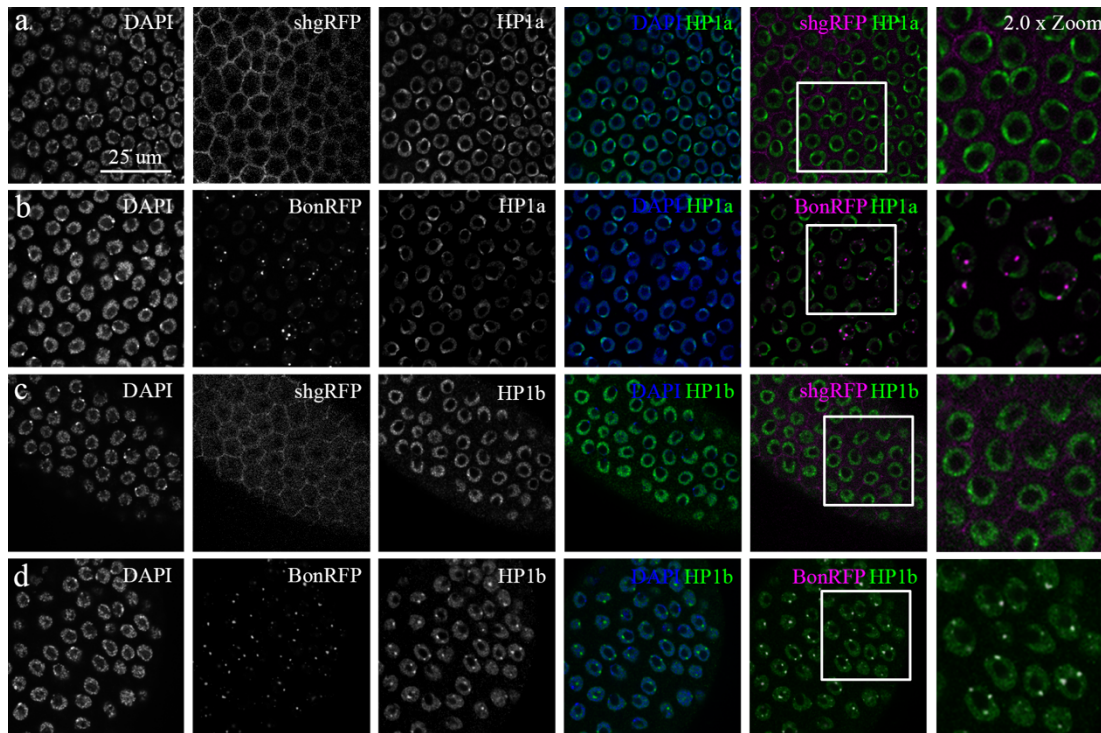


Figure 19: Overexpression of Bonus recruits HP1b but not HP1a to euchromatic Bonus foci.

Control and Bonus-RFP (BonRFP) overexpressing ovaries were fixed and stained together with each antibody to ensure comparable staining conditions. Expression of Bonus in follicle cells was driven with a TJGAL4 driver. a-b) Staining of shgRFP control ovaries together with ovaries overexpressing BonRFP in the ovary follicle cells with an HP1a antibody. HP1a chromatin localization is unchanged in BonRFP follicle cells in comparison to shgRFP controls. c-d) Staining of shgRFP control ovaries and BonRFP overexpressing ovaries with an HP1b antibody. HP1b co-localizes with BonRFP at follicle cell euchromatin.

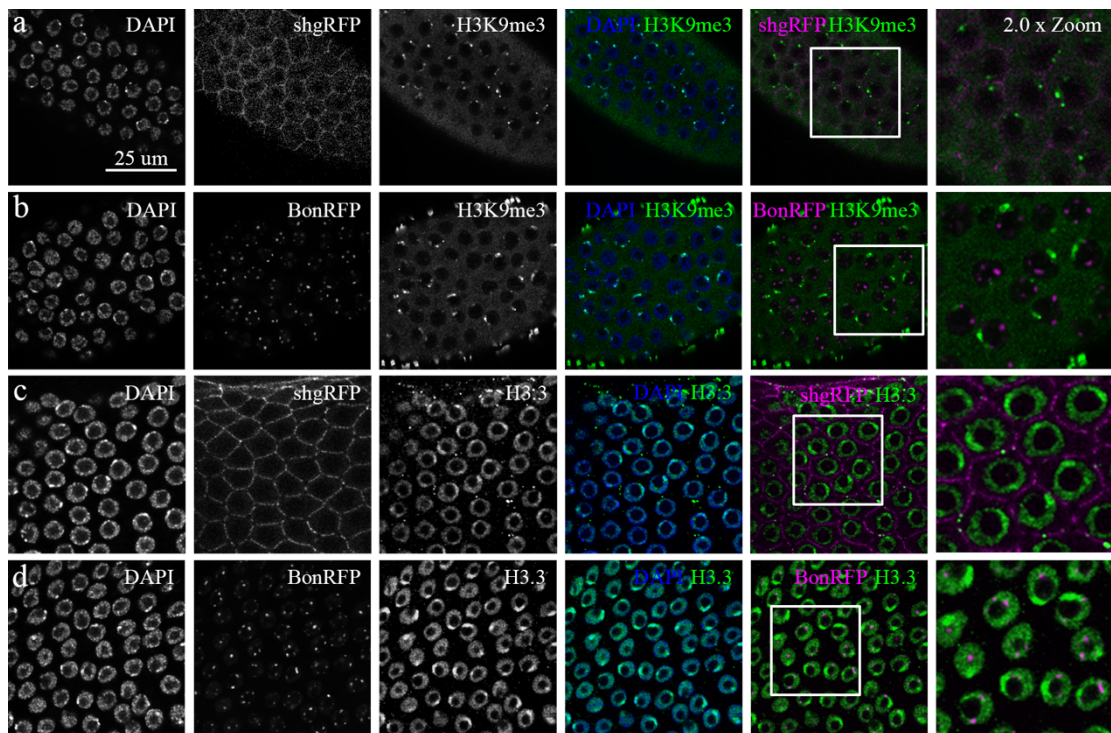


Figure 20: Neither H3K9me3 or H3.3 is enriched at euchromatic Bonus foci.

Control and Bonus-RFP (BonRFP) overexpressing ovaries were fixed and stained together with each antibody to ensure comparable staining conditions. Bonus was expressed using the follicle specific cell driver TJGAL4. a-d) Staining of shgRFP control ovaries together with ovaries overexpressing BonRFP in the ovary follicle cells with either an H3K9me3 or H3.3 antibody. Neither H3K9me3 or H3.3 are enriched at euchromatic Bonus foci at follicle cell chromatin.

3.4.3 Pull downs of dADD1 and XNP identify a number of new interaction partners

To identify new interaction partners of dADD1 and XNP we performed an MS analysis on pull downs of tagged dADD1-PA or XNP-PA/B from S2 cells. An interactome of dADD1-PA was recently published by the lab of Dr. Mitzi Kuroda, but no interactome has been published for XNP [56]. While XNP has been described to interact with HP1a and H3.3, additional interaction partners have yet to be identified.

As discussed above, we re-identified a number of previously identified interactors of dADD1 through this MS approach including HP1a, HP1b, Mod(mdg4) and Bonus, confirming the validity of our data (Figure 15 and Figure 17). To further analyze the data a cut off value of \log_2 3 fold iBAQ dADD1/S2 Control and a maximum P-Value of 0.06 was used to denote a significant protein interaction. While typically a P-Value of 0.01 or 0.05 are taken to denote significance we lowered our

Results

cut off to 0.06 bases on the P-Value of Bonus, a known interactor of dADD1, which was 0.0505.

From the dADD1 pull downs we identified a total of 54 proteins that interacted specifically with dADD1 and did not interact with XNP (Full list in Supplementary Materials Table 4). The top 10 interacting proteins of dADD1 are listed in Table 1. These proteins were enriched for proteins involved in cell cycle progression and mitosis such as Cyclin dependent kinase 5 (cdc5) and Chromator (Chro). Additionally, several chromatin and DNA binding proteins that specifically interacted with dADD1, are also known to interact with each other, suggesting dADD1 is involved in higher order protein complex formation. For example, the protein proliferation disrupter (Prod), which had the highest \log_2 fold enrichment of all dADD1 specific interactors, also interacts with the dADD1 specific interaction partner Chro. Prod also interacts with Germ line transcription factor 1 (Gnf1) and putzig (Pzg), proteins that were significant interactors of both dADD1 and XNP in our MS data sets. Interestingly, in addition to its role in mitosis and cell proliferation, prod is a telomeric associated protein that functions as a repressor of the telomeric transposon HeT-A, and both Chro and Pzg co-localize with prod at telomeres [65, 66].

Table 1: Top 10 dADD1 specific interactors

List of the top 10 proteins that interact with only dADD1. FB ID numbers are the Flybase gene identification number give to all proteins listed on Flybase, an online *Drosophila* resource.

Gene Name	FB ID	Log ₂ dADD1/Control	P-Value
prod	FBgn0014269	12.02	1.53E-03
Hsp60	FBgn0015245	11.37	6.06E-11
Eb1	FBgn0027066	11.19	1.07E-07
Chro	FBgn0044324	10.74	6.74E-04
Vps29	FBgn0031310	10.33	6.91E-10
CG15107	FBgn0041702	9.59	4.88E-04
RpL21	FBgn0032987	9.32	2.75E-11
Hsc70-5	FBgn0001220	8.80	5.51E-07
ncd	FBgn0002924	8.52	5.40E-03
deltaCOP	FBgn0028969	8.09	2.15E-03

Using the same cut off parameters used to determine significant protein interactions for dADD1 we identified 99 proteins that interact specifically with XNP (Full list in Supplementary Materials Table 5). The top 10 interacting proteins of XNP are listed in Table 2. Similar to dADD1 these proteins were enriched for protein involved in mitosis and included a number of chromatin associated and DNA binding proteins. XNP associates with a number of protein involved in DNA repair processes including the nucleotide excision repair proteins PCNA and Rad23, as well as DNA double-strand break repair protein Irbp, that is also involved in telomere maintenance. Many proteins that specifically associate with XNP are also involved in both positive and negative transcriptional regulation, such as Mta1-like, Mbf1, Mlf, MEP-1, Mi-2 and Bin1.

Table 2: Top 10 XNP specific interactors

List of the top 10 proteins that interact with XNP only. FB ID numbers are the Flybase gene identification number give to all proteins listed on Flybase, an online *Drosophila* resource.

Gene Name	FB ID	Log₂ XNP/Control	P-Value
clu	FBgn0034087	14.70	8.95E-12
RpL11	FBgn0013325	12.29	2.63E-03
Su(var)2-10	FBgn0003612	11.95	4.97E-12
CG43736	FBgn0263993	11.91	7.06E-12
CG9253-RA	FBgn0032919	11.39	1.10E-08
tsr	FBgn0011726	10.86	3.49E-03
CHIP	FBgn0027052	10.64	5.67E-08
NHP2	FBgn0029148	10.26	8.31E-09
CG8036	FBgn0037607	9.93	4.92E-04
Nop60B	FBgn0259937	9.66	3.94E-03

Further analysis identified 100 shared protein interaction partners of both dADD1 and XNP that have a log₂ greater than 3 and a P-Value less than 0.06 (Full list in Supplementary Materials Table 6). Shared interaction partners are heavily enriched for chromatin-associated proteins and have GO term enrichment for chromatin-related processes, such as chromatin organization, modification and remodeling as well as heterochromatin assembly and organization. Further analysis suggests that both data sets are enriched for heterochromatic components previously

Results

found to be enriched at telomeric sequences [67]. Table 3 includes a list of GO scores for shared protein interactors of dADD1 and XNP.

Table 3: Gene ontology scores of shared dADD1 and XNP interactors

GO term	P-Value	Matches
Mitotic cell cycle	2.96E-14	34
Spindle organization	9.52E-12	22
Chromatin organization	1.26E-05	20
Chromosome organization	3.50E-05	23
Cellular response to stress	1.56E-04	22
Regulation of chromatin assembly or disassembly	3.42E-04	5
DNA conformation change	9.02E-04	11
Regulation of chromatin organization	2.90E-03	8
Cellular response to DNA damage stimulus	5.70E-03	14
DNA replication	2.14E-02	8
Chromatin modification	2.48E-02	12
Gene expression	3.15E-02	41
Heterochromatin assembly	3.32E-02	4
DNA packaging	3.47E-02	9
Heterochromatin organization	3.74E-02	5
Chromatin remodeling	3.44E-02	8

In addition to interactors HP1a, HP1b and Mod(mdg4), some of the newly identified proteins shared between dADD1 and XNP are involved in regulation of chromatin include dre4, Chromatin assembly factor 1-p55 subunit (Caf1-55), Structure specific recognition protein (Ssrp) and Insulator binding factor 1 (Ibf1). We also see both dADD1 and XNP interacting with a number of heatshock proteins including Hsp83, the *Drosophila* homologue of Hsp90, which has been implicated in negative regulation of transcription by stabilization of paused polymerases [68].

Both dADD1 and XNP also significantly interact with the H2A variant H2Av and H4. While H4 is a member of the canonical histone octamer, H2Av is a H2A variant that replaces H2A in nucleosomes. H2Av has been implicated in DNA damage response, where phosphorylation of H2Av tails is important in the recognition and repair of double-strand DNA breaks [69]. Peptides corresponding to H3.3 as well as H2B were also found within the MS data set, all with log₂ values

greater than 3, however, all had P-Values greater than the 0.06 cutoff set to specify significant interactions. The identification of histones as well as histone variants in our MS data set could suggest that similar to ATRX, dADD1 and XNP may play a role in shuttling and replacement of histones.

3.5 Effect of loss or overexpression of dADD1 and XNP on chromatin

3.5.1 Loss of dADD1 or XNP does not affect localization of HP1a, HP1b or H3.3 to chromatin

Since both dADD1 and XNP have been shown to interact with chromatin proteins HP1a and HP1b we decided to investigate the effect that loss of either dADD1 or XNP had on localization of HP1a and HP1b to chromatin. Complete loss of either protein did not affect the chromatin localization of HP1a to heterochromatin, nor did loss affect the localization of HP1b to euchromatin (Figure 21). This demonstrates that neither dADD1 or XNP is necessary for chromatin recruitment of either HP1a or HP1b. Similar results were obtained for H3.3, where homozygous *dADD1*² and homozygous *XNP*⁴⁰³ mutants show similar H3.3 chromatin deposition as control shgRFP flies (Figure 13).

Results

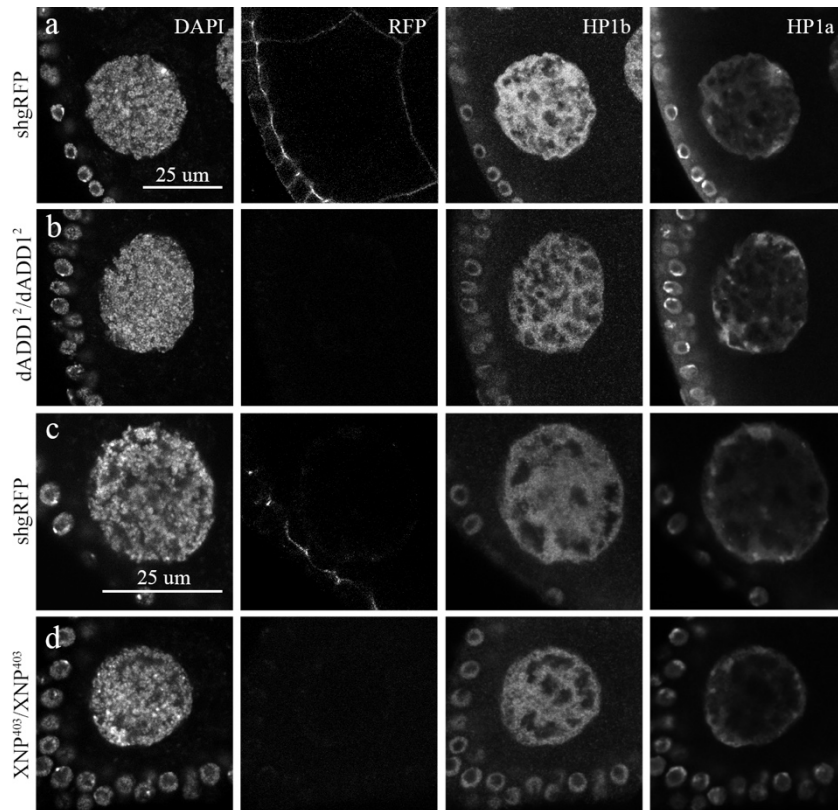


Figure 21: Localization of HP1b and HP1a to chromatin is independent of the presence of dADD1 and XNP.

Loss of dADD1 or XNP does not affect the localization of either HP1a or HP1b to nurse cell and follicle cell chromatin. shgRFP controls as well as mutants were fixed and stained together to maintain consistency as well as were mounted on the same slide and imaged using the same imaging settings. a-b) *dADD1*² homozygous mutants show normal HP1a and HP1b localization patterns at chromatin in comparison to shgRFP control egg chambers. c-d) HP1a and HP1b are recruited normally to *XNP*⁴⁰³ homozygous mutant chromatin in follicle cells and nurse cells.

The results for H3.3 and HP1a were re-confirmed through western blot of ovary cell lysates of homozygous *dADD1*² and homozygous *XNP*⁴⁰³ mutant flies (Figure 22). Total protein levels of H3.3 and HP1a are unchanged in mutants compared to control Iso31 stock. Levels of HP1b could not be analysed as the HP1b antibody was unable to detect HP1b on western blot. We also tested both dADD1 and XNP mutants for H3K9me3 levels and found that the homozygous *dADD1*² mutants but not the *XNP*⁴⁰³ mutants show a slight decrease in the total cellular levels of H3K9me3. However, quantifications of H3K9me3 levels in ovary follicle cells did not detect any difference in H3K9me3 levels between *dADD1*² homozygous mutants and shgRFP control ovaries (data not shown). The decrease in H3K9me3 may be the result of a reduction in the recruitment of the dADD1 interaction partner Eggless, an

H3K9 methyltransferase, to chromatin due to the loss of dADD1. This suggests that dADD1 may be important in maintenance and regulation of cellular H3K9me3, potentially through the recruitment of Eggless.

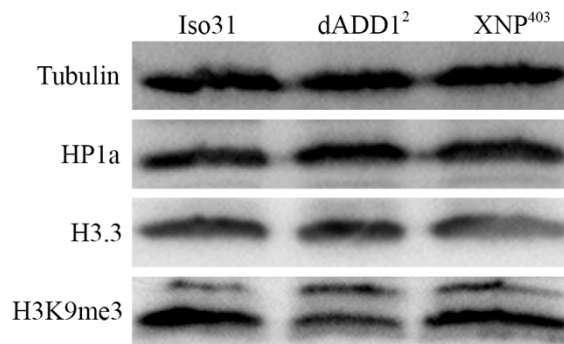


Figure 22: Western blot of whole cell ovary lysates reveals decreased H3K9me3 in homozygous *dADD1*² mutant ovaries.

Whole cell lysates of ovaries from control Iso31 ovaries as well as homozygous *dADD1*² and *XNP*⁴⁰³ ovaries. Ovaries were dissected from females fattened on yeast paste for two days. Total protein levels were standardized before running on western blot. Tubulin was used as a loading control. Both HP1a and H3.3 levels remain unchanged in mutant ovaries compared to Iso31 control. H3K9me3 levels are decreased in the *dADD1*² homozygous mutants but not in the *XNP*⁴⁰³ homozygous mutants in comparison to control Iso31. The lower molecular weight band in the H3K9me3 sample corresponds to the predicted weight of histone 3.

3.5.2 Overexpression of dADD1 increases cellular H3K9me3 and H3.3 levels

Chromatin immunoprecipitation (ChIP) profiles of dADD1 showed a significant enrichment of dADD1 at heterochromatin sequences and dADD1 associates with a number of heterochromatin components such as HP1a and H3K9me3 [56]. We thus tested the effect that overexpression of dADD1 has on total levels of heterochromatin-enriched components HP1a, H3.3 and H3K9me3 by western blot. Total cell lysates of dADD1-PA expressing stable cells revealed that overexpression of dADD1 increased total levels of cellular H3.3 and H3K9me3, but HP1a levels remained unchanged (Figure 23).

Results

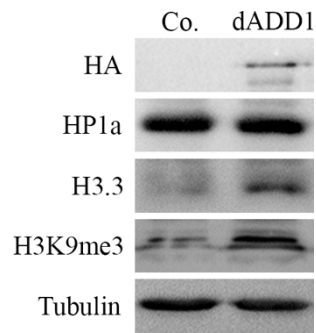


Figure 23: Overexpression of *dADD1* in S2 cells increases cellular levels of H3K9me3 and H3.3.

Whole cell lysates of either control or *dADD1* stable cell lines overexpressing *dADD1*-Flag/HA. Protein concentrations were standardized before running on western blot and total protein levels are comparable based on similar tubulin intensities in both samples. H3.3 and H3K9me3 levels increased in *dADD1* overexpressing cells while HP1a remains unchanged.

Together with the data from homozygous *dADD1*² ovary cell lysates it appears that *dADD1* plays a role in regulating cellular H3.3 and H3K9me3 levels. The function on H3K9me3 levels may be the result of the interaction of *dADD1* with the H3K9 methyltransferase *Eggless*. *Eggless* is one of three H3K9 methyltransferases in *Drosophila*, the others being *Su(var)3-9* and *G9a*, however, only *Eggless* and *Su(var)3-9* implement H3K9me3 marks at HP1a bound heterochromatin [59]. It is possible that the interaction of *Eggless* with *dADD1* recruits *Eggless* to chromatin facilitating tri-methylation of H3K9.

How overexpression of *dADD1* leads to increased H3.3 is less clear, as *dADD1* has not been shown to interact with either XNP or HIRA, the two *Drosophila* proteins responsible for replication independent deposition of H3.3 [53]. However, H3.3 did show up in our MS data set as an interactor of *dADD1* and XNP, having significant log₂ vales of of 9.5 and 8.5 respectively, but with P-values of 0.1 which was above our chosen P-Value cut off of 0.06. It is possible that H3.3 shows up in the MS data set due to the interaction of *dADD1* and XNP with H3.3-rich heterochromatin, which is also pulled down with these proteins during immunoprecipitation. Or it is possible that *dADD1* binds directly to H3.3 through its ADD-domain binding to tri-methylated lysine 9 on histone H3.3. In any case the relationship between *dADD1* and H3.3 needs to be further investigated.

3.5.3 Overexpression of dADD1 but not XNP increases incorporation of HP1a, H3.3 and H3K9me3 into heterochromatin

To better understand the role that dADD1 and XNP play at heterochromatin we overexpressed dADD1 and XNP in ovary follicle cells and performed a co-localization analysis with identified interacting chromatin components. To perform these experiments, we first generated a fly line that expressed a C-terminal GFP tagged dADD1-PA construct under the control of a UAS promoter. Overexpression of XNP was achieved using a fly line containing an inducible XNP-HA construct, again under the control of a UAS promoter, that had been previously generated by the lab of Dr. Marc Muskavitch.

Expression of both constructs was driven specifically in the egg chamber follicle cells using a TJGAL4 driver. Overexpression of dADD1-GFP resulted in significant enrichment of dADD1-GFP at heterochromatin, with a small amount of dADD1 localizing to euchromatic regions. In contrast, overexpression of XNP resulted in enrichment of XNP at euchromatin and general exclusion from heterochromatin. As discussed in 3.2.4 *dADD1 and XNP are recruited independently to chromatin*, overexpression of dADD1 or XNP did not result in increased recruitment of the other protein to chromatin suggesting these proteins are recruited independently (Figure 14).

We then tested the ability of dADD1 to recruit or increase heterochromatin associated factors HP1a, H3.3 and H3K9me3 at heterochromatin or the ability of XNP to increase general incorporation of HP1a and H3.3. Similar to nurse cell chromatin in Figure 11, HP1a, H3.3 and H3K9me3 enriched at follicle cell heterochromatin in wild type ovaries (Figure 24 a, c and e and Figure 25 a and c). Overexpression of dADD1 increased enrichment of all of these heterochromatin proteins and histone methylation mark at heterochromatin (Figure 24 b, d and f). However, HP1a and H3.3 were not enriched in XNP-rich chromatin in XNP-overexpressing cells, with both HP1a and H3.3 showing comparable stainings at XNP-HA follicle cell chromatin and shgRFP control chromatin (Figure 25). Enrichment of HP1a, H3.3 and H3K9me3 at heterochromatin in dADD1-overexpressing cells is specific to these factors since we did not observe XNP

Results

enrichment at heterochromatin in dADD1 overexpressing cells. Furthermore, this enrichment is not an artifact of overexpression as we observe no change in these chromatin factors in XNP overexpressing follicle cells.

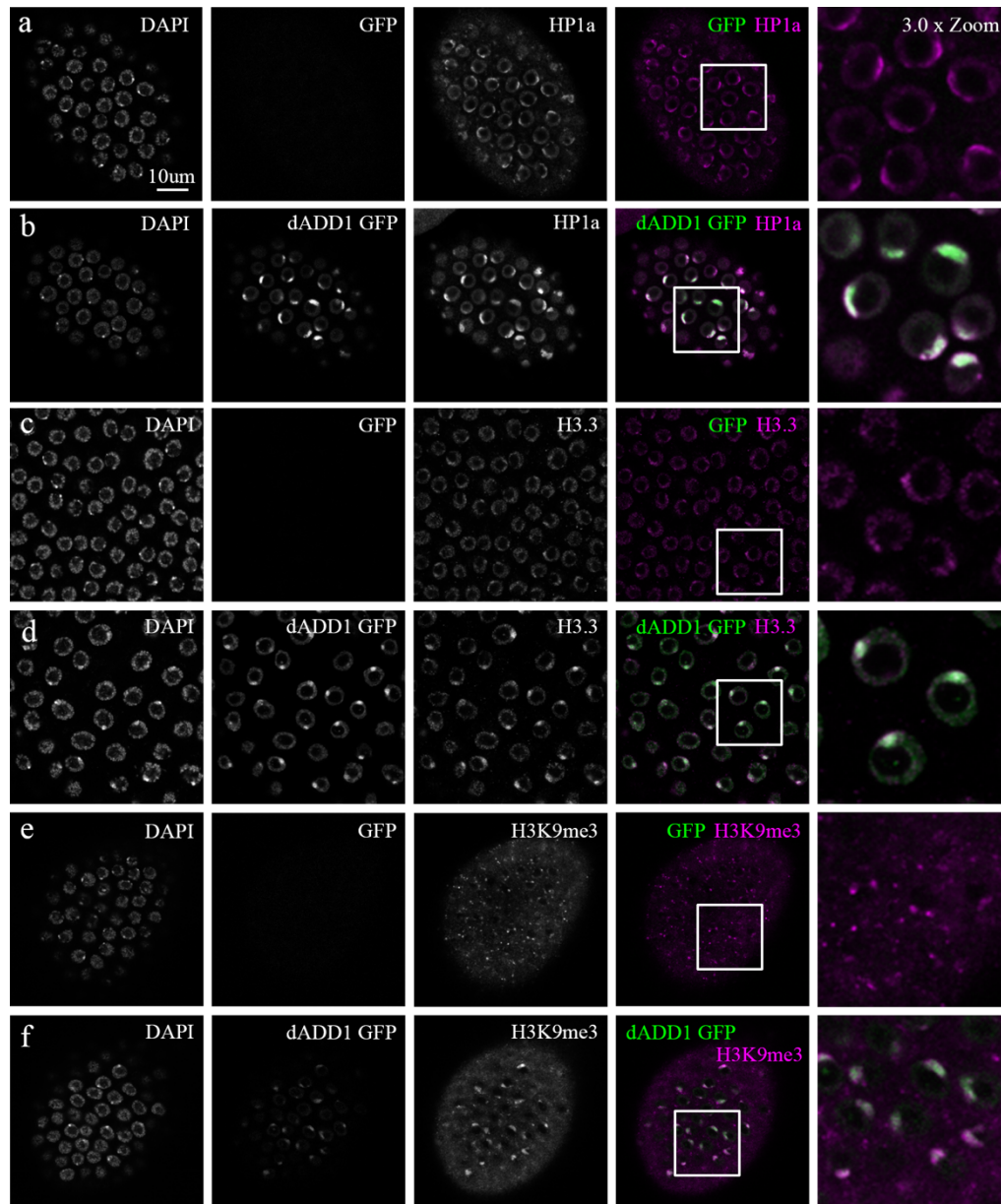


Figure 24: Overexpression of dADD1 in somatic ovary follicle cells increases incorporation of HP1a, H3.3 and H3K9me3 to heterochromatin.

dADD1-GFP was overexpressed specifically in the egg chamber follicle cells using a TJGAL4 driver. Overexpression of dADD1-GFP results in accumulation of dADD1-GFP primarily at heterochromatin. shgRFP ovaries were used as a control and were stained, fixed and imaged together with the dADD1-GFP ovaries to maintain consistency. a) HP1a localizes to follicle cell heterochromatin in shgRFP control ovaries. b) Overexpression of dADD1-GFP results in increased HP1a at heterochromatin in comparison to ovaries in a. c) H3.3 localizes to heterochromatin in ovary follicle cells in shgRFP control ovaries. d) H3.3 levels are increased at heterochromatin in ovary follicle cells overexpressing dADD1-GFP in

comparison to H3.3 in control shgRFP follicle cells in c. e) H3K9me3 shows enrichment at follicle cell heterochromatin in shgRFP control ovaries. f) Overexpression of dADD1-GFP in egg chamber follicle cells results in an increased deposition of H3K9me3 at dADD1-GFP rich heterochromatin in follicle cells in comparison to e.

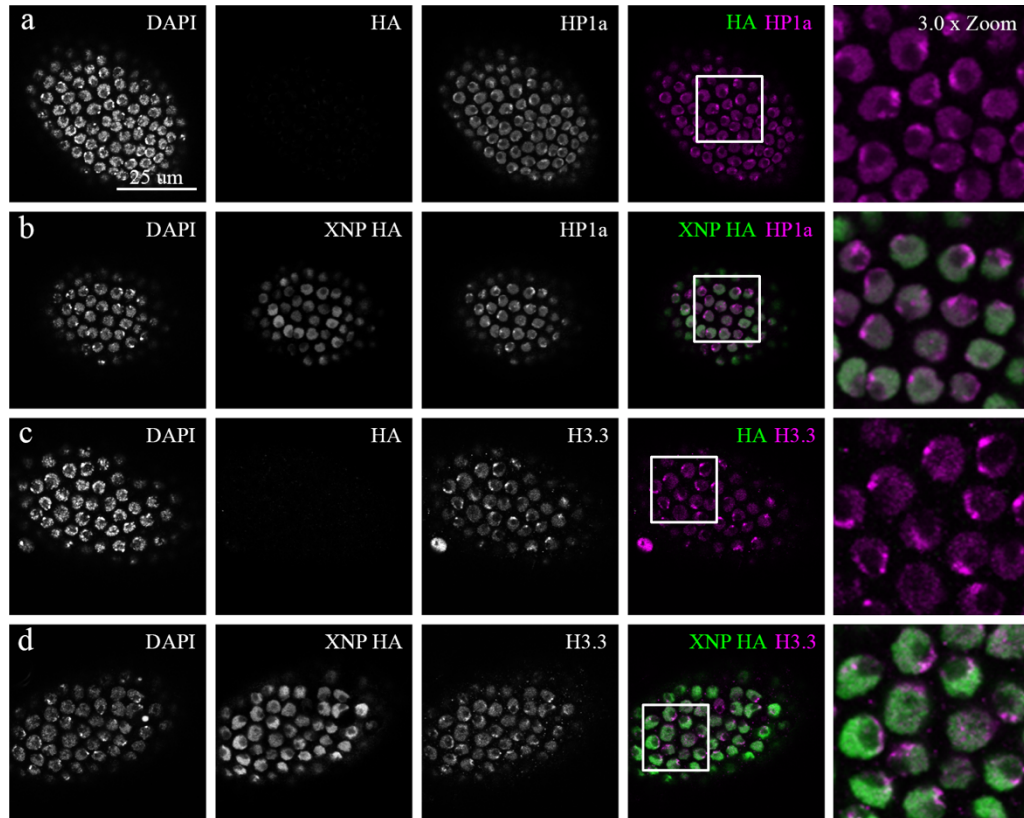


Figure 25: HP1a and H3.3 are not recruited to XNP rich chromatin in overexpressing cells.

Overexpression of XNP-HA was specifically driven in egg chamber follicle cells using the TJGAL4 driver. For consistency and comparability of images shgRFP control ovaries were fixed, stained and imaged together with XNP-HA overexpressing ovaries. a) HP1a is enriched at heterochromatin in control shgRFP follicle cells. b) Overexpression of XNP-HA in ovary follicle cells does not change the localization pattern, or increase chromatin associated HP1a. c) In control shgRFP egg chamber follicle cells H3.3 is enriched at heterochromatin. d) Overexpression of XNP-HA in egg chamber follicle cells does not alter the localization of H3.3 to chromatin.

The data on dADD1 overexpression together with the nurse cell chromatin localization of HP1a, H3.3 and H3K9me3 in *dADD1*² homozygous mutant tissue suggests that dADD1 is sufficient, but not necessary to induce heterochromatin formation through recruitment of heterochromatin factors *in vivo*.

3.5.4 Overexpression of dADD1 in follicle cells recruits euchromatic proteins Bonus and HP1b into heterochromatin

Further experiments were also undertaken to determine what effect overexpression of dADD1 has on its euchromatic interaction partners HP1b and Bonus. In follicle cells both HP1b and Bonus show euchromatic localization and are excluded from heterochromatin (Figure 26 a and c). Overexpression of dADD1-GFP in egg chamber follicle cells results in recruitment of both of these proteins to heterochromatin (Figure 26 b and d). Interestingly, it appears that dADD1 and Bonus are able to recruit one another to chromatin, as overexpression of either protein results in recruitment of the other to chromatin domains enriched for either dADD1 or Bonus (Figure 18 b and Figure 26 b). These dADD1 or Bonus-enriched chromatin domains also contain increased levels of HP1b, indicating that either dADD1 or Bonus or both are capable of recruiting HP1b to chromatin. However, it was shown in Figure 13 that dADD1 is not necessary for the recruitment of HP1b to chromatin, leaving the possibility that Bonus is the protein important for HP1b recruitment to chromatin.

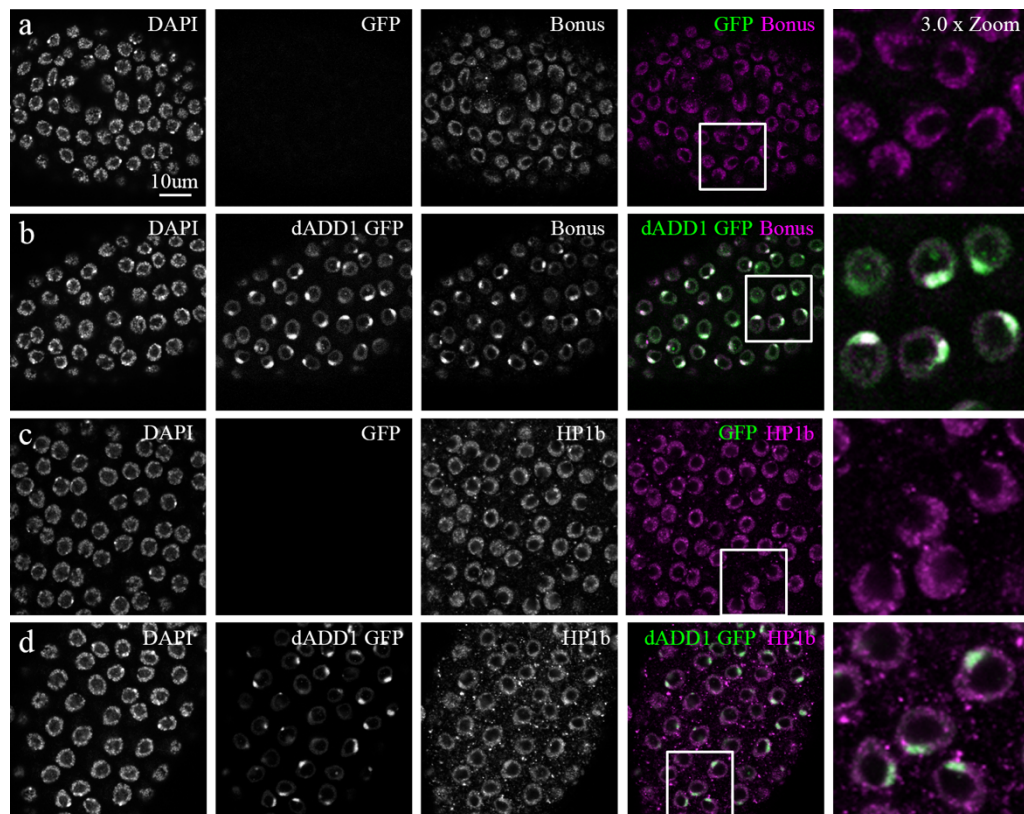


Figure 26: Overexpression of dADD1 recruits euchromatic proteins Bonus and HP1b to heterochromatin.

Overexpression of dADD1-GFP in egg chamber follicle cells using a TJGAL4 driver. Control shgRFP ovaries were fixed, stained and imaged together with the dADD1-GFP overexpressing ovaries. a) Bonus localizes to euchromatin and is excluded from heterochromatin in egg chamber follicle cells in control shgRFP ovaries. b) Overexpression of dADD1-GFP recruits Bonus to heterochromatin. c) HP1b localizes to follicle cell euchromatin and is excluded from heterochromatin in shgRFP control egg chambers. d) Overexpression of dADD1-GFP increases HP1b at follicle cell heterochromatin.

As HP1b was also identified as an interaction partner of XNP we tested next if XNP was capable of recruiting HP1b to chromatin. We again overexpressed XNP-HA in egg chamber follicle cells and stained for HP1b. However, overexpression of XNP did not increase the recruitment of HP1b to XNP-HA rich regions at euchromatin (Figure 27).

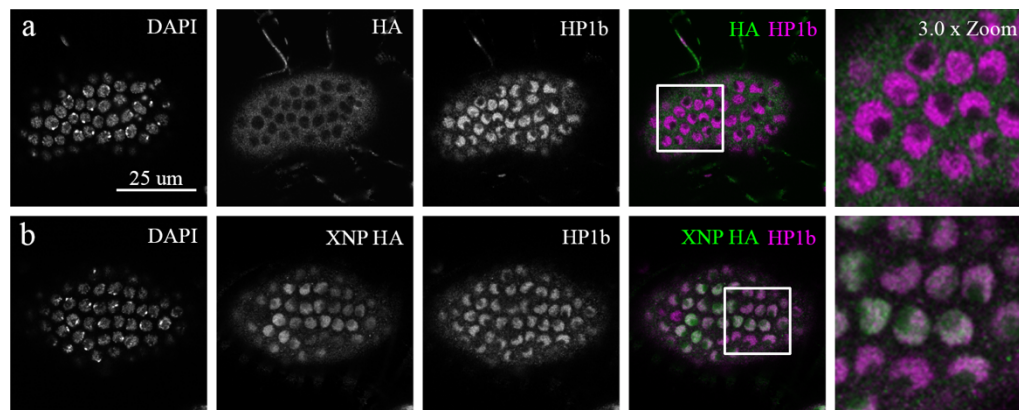


Figure 27: Overexpression of XNP does not increase recruitment of HP1b to XNP rich chromatin.

To ensure consistency and comparability of results control shgRFP and XNP-HA overexpressing ovaries were fixed, stained and imaged together. a) HP1b localizes to euchromatin and is excluded from heterochromatin in control shgRFP follicle cells. b) Overexpression of XNP-HA does not change the recruitment of HP1b to chromatin.

3.5.5 Loss of dADD1 and XNP results in impaired resolution of double-strand DNA breaks

Based on the MS pull down data, both dADD1 and XNP were shown to significantly interact with the Histone variant H2Av. H2Av is a histone variant that replaces H2A in nucleosomes and is typically enriched in heterochromatin [70]. However, H2Av is also incorporated into euchromatic gene coding sequences and transposons [71]. H2Av is also important in response to DNA double-strand breaks, where serine 137 on the H2Av tails near the double-strand break are phosphorylated [69]. In *Drosophila*, phosphorylated H2Av is referred to as γ -H2Av and is used as a marker for double-strand DNA breaks [72]. We furthermore observed that both dADD1 and XNP significantly interacted with the DNA repair Tip60 complex member Pontin, while another complex member Reptin was a significant interactor of dADD1 also identified in the XNP interactor MS data set (\log_2 4.2 and P-Value 0.07). Importantly, the Tip60 complex is important for acetylation of γ -H2Av and for the replacement of γ -H2Av with un-phosphorylated H2Av in response to DNA damage [73].

Analysis of the proteins that interacted with both dADD1 and XNP showed that the shared interactors were enriched for pathways involved in DNA repair. Based on the interaction of dADD1 and XNP with H2Av, as well as with the DNA

repair associated proteins Pontin and Reptin, we tested the ability of *dADD1*² and *XNP*⁴⁰³ homozygous mutants to efficiently repair double-strand DNA breaks. To do so we compared levels of γ -H2Av in nurse cell chromatin in shgRFP control ovaries and homozygous *dADD1*² and *XNP*⁴⁰³ mutants from female flies that were placed on food containing 0.25 μ g/ml hydroxyurea for 4 days. Hydroxyurea induces DNA double-strand breaks by stalling DNA replication machinery through depletion of the dNTP pool, which results in the replication machinery dissociating from replicating DNA [74].

Untreated *XNP*⁴⁰³ mutants show no change in γ -H2Av levels in nurse cell chromatin when compared to shgRFP controls in stage matched egg chambers (Figure 28 a and b). Homozygous *dADD1*² mutants show a slight increase in γ -H2Av at nurse cell chromatin in comparison to stage matched egg chambers of shgRFP control flies, indicating that these mutants have an impaired DNA damage response (Figure 28 c and d). However, both homozygous *XNP*⁴⁰³ and *dADD1*² mutants treated with hydroxyurea show an increased amount of γ -H2Av in nurse cell chromatin when compared to shgRFP control stage matched egg chambers (Figure 29). While the *dADD1*² mutants already show an impaired DNA damage response under normal conditions, the addition of replication stress visibly increases that amount of γ -H2Av at nurse cell chromatin in comparison to the shgRFP controls.

Results

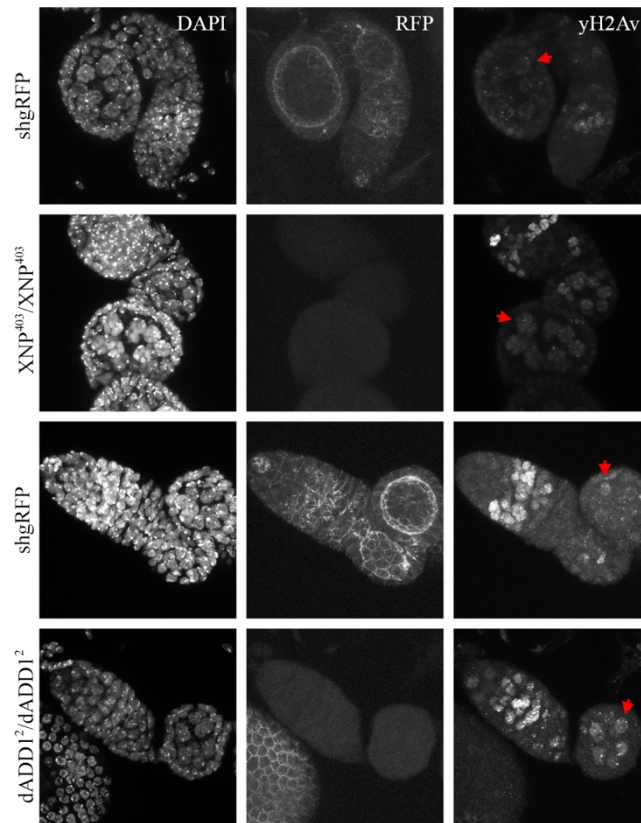


Figure 28: Homozygous XNP^{403} and $dADD1^2$ mutants show similar γ -H2Av stainings under normal growth conditions.

Maximum Z-projections of ovaries from XNP^{403} and $dADD1^2$ mutants compared to shgRFP control ovaries. Mutant and control ovaries were fixed and stained in the same vials and were mounted and imaged on the same slides using identical imaging settings. Comparisons are only possible between mutant and control ovaries from the same slide. The germarium shows a higher level of γ -H2Av staining in both control and mutant ovaries compared to later stage egg chambers. a-b) Comparison of XNP^{403} mutant ovaries to shgRFP control ovaries shows no difference in γ -H2Av in stage matched egg chambers at nurse cell chromatin. c-d) $dADD1^2$ homozygous mutants show a slightly elevated level of γ -H2Av at nurse cell chromatin in comparison to control shgRFP stage matched egg chambers. Arrows denote comparable nurse cell chromatin.

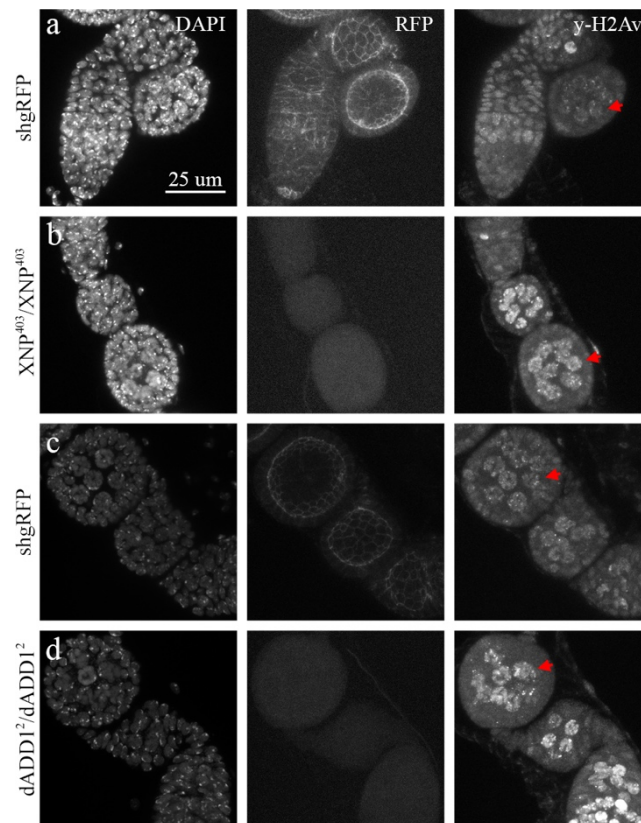


Figure 29: Hydroxyurea treatment of adult females leads to increased γ -H2Av accumulation in XNP^{403} and $dADD1^2$ mutant ovaries.

Maximum Z-projections of ovaries from XNP^{403} and $dADD1^2$ mutants compared to shgRFP control ovaries. Mutant and control ovaries were fixed and stained in the same vials and were mounted and imaged on the same slides using identical imaging settings. Comparisons are only possible between mutant and control ovaries from the same slide. a-b) XNP^{403} mutant ovaries show increased γ -H2Av in comparison to shgRFP control stage matched ovaries in adult female flies treated for 4 days with hydroxyurea. c-d) $dADD1^2$ mutant ovaries display an increase in γ -H2Av in nurse cell chromatin in comparison to shgRFP control stage matched egg chambers. Arrows denote comparable nurse cell chromatin.

These results indicate that dADD1 and XNP mutant cells accumulate γ -H2Av at chromatin containing DNA double-strand breaks, indicating that these proteins are important for DNA repair. This function could be mediated through association of dADD1 and XNP with Tip60 complex members Pontin, Reptin and H2Av. However, further work needs to be done to better understand the mechanism of how dADD1 and XNP function in DNA repair.

3.5.6 dADD1 and XNP regulate transposon sequences

Analysis of dADD1 ChIP data from the lab of Dr. Mitzi Kuroda revealed a number of dADD1 enriched genomic domains correlating with known transposon

Results

sequences. As ATRX had been previously shown to be important for transposon silencing in mammals, we decided to further investigate if dADD1 and XNP also regulate transposon silencing. To this end we compared transcript levels of a number of transposons in ovaries from Iso31 control flies to both *dADD1*² and *XNP*⁴⁰³ homozygous mutants by Real Time (RT)-qPCR.

We specifically tested the expression of four non-LTR transposons (297, roo, mdg3 and 412) and one telomeric transposon (HeT-A) on two independent RNA extractions from female ovaries. Transcription of these transposons was standardized to four different housekeeping genes, actin, tubulin, Rpl13 and Rpl32. All tested transposons were regulated by either dADD1 or XNP and in some cases by both (Figure 30). 297 and HeT-A showed significant increases in transcript levels in XNP homozygous mutants with a 5.8 and 2.6-fold upregulation, respectively, in comparison to Iso31 controls. Homozygous dADD1 mutants showed a significant upregulation of 412, with a 6.5-fold increase in transcript levels in comparison to Iso31 controls. Transcript levels of roo and mdg3 increased in both dADD1 and XNP homozygous mutants by between 4.8 -11.2 fold, in comparison to Iso31 controls.

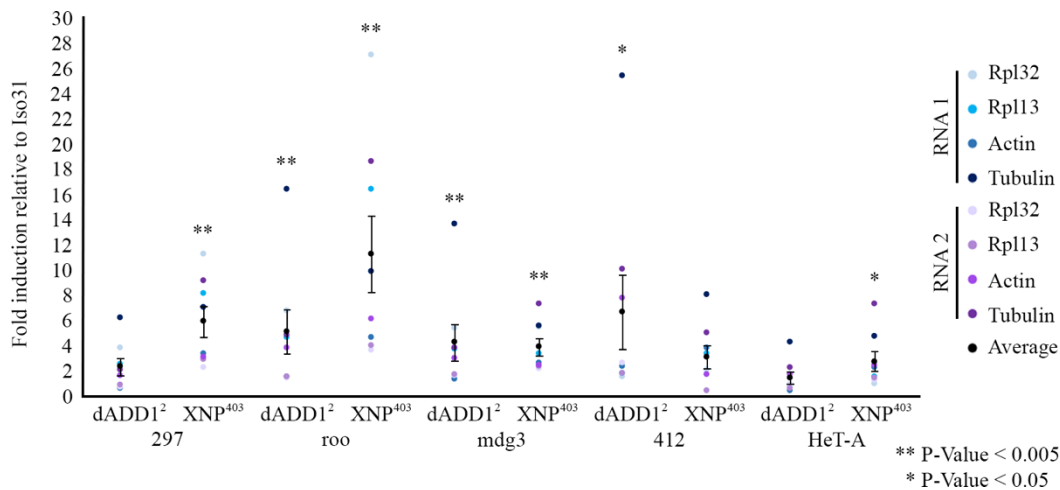


Figure 30: Loss of dADD1 or XNP results in increased transcription of transposons.

RT-qPCR measuring transposon transcription in *dADD1*² or *XNP*⁴⁰³ homozygous mutants standardized to Iso31 control transcript levels. Two independent RNA extracts, each containing ovaries from 10 females, were compared to four housekeeping genes. Both dADD1 and XNP regulate transposons with dADD1 regulating roo, mdg3 and 412 and XNP regulating 297, roo, mdg3 and HeT-A. RT-qPCR performed by Ian Will and Isabell Grass. P-Value calculations performed by Marco La Fortezza.

Combined, these data indicate that dADD1 and XNP have many functions at chromatin and have a multitude of interaction partners mediating these diverse functions. While dADD1 and XNP may not be essential for the deposition of HP1a, HP1b or H3.3 into chromatin, these proteins may play important roles in the replacement of γ -H2Av into H2Av during DNA damage responses. The involvement of these proteins in regulation of transposons suggests that these two proteins are important for maintenance of genomic integrity.

4 Discussion

4.1 dADD1 and XNP do not directly interact but function in similar pathways

4.1.1 dADD1 and XNP do not physically interact

Co-immunoprecipitation experiments in a previous study observed an interaction between dADD1 and XNP, and experiments with truncated proteins in *in vitro* assays suggested that all isoforms of dADD1 interact with the long isoform of XNP [42]. While an interaction between these two proteins may be expected based on sequence conservation with the single mammalian protein ATRX, our experiments could not re-confirm this proposed physical interaction between them.

Specifically, co-expression of the long isoforms of dADD1 and XNP in S2 cells followed by co-immunoprecipitation did not show any interaction between the two proteins. Eluate samples of pull downs of dADD1 did not contain any XNP constructs. While pull downs of XNP showed a slight enrichment for dADD1, this is likely an artifact of dADD1 binding independently to the Protein G sepharose beads as dADD1 was also present in the eluate of the bead binding control. We were also unable to identify an interaction between dADD1 and XNP through MS. The long isoforms of dADD1 and XNP were expressed and pulled down independently from S2 cells and associated proteins for both dADD1 and XNP were identified. In the dADD1 IP no endogenous XNP peptides were detected, and while a few peptides corresponding to dADD1 were present in the XNP samples, they were far below the

\log_2 and P-Values that denoted a significant interaction. As a positive control in both the dADD1 and XNP IPs we identified HP1a, a protein known to interact with both proteins.

One of the reasons for the discrepancy between our work and the previous study is likely to be due to the difference in the observed molecular weight of the long isoform of dADD1 [42]. In the previous paper, identification of dADD1 was based on an anti-dADD1 antibody recognizing a band at the predicted weight of 130 kD of the long isoform, however, we showed here that the long isoform of dADD1 is actually around 250 kD, which is much larger than expected.

4.1.2 dADD1 and XNP show unique localization patterns at chromatin

Chromatin localization of dADD1 and XNP was determined by analyzing immunohistochemical stainings of endogenous proteins in egg chamber nurse cells. Nurse cell chromatin is a fantastic system for investigating chromatin protein localization as the genome is endoreplicated, resulting in polytenized chromatin that enables simple visualization of chromatin domains. While many studies employ the use of larval salivary gland polytene chromosome squashes to visualize chromatin protein localization, endogenous antibodies were unable to identify dADD1 and XNP proteins at chromatin in salivary gland chromosome squashes (data not shown), likely because they are only expressed at low levels [47].

However, we were able to detect dADD1 or XNP at nurse cell chromatin using an antibody raised against a peptide common to all isoforms of dADD1 by Dr. Andreas Thomae, and an antibody developed against a peptide common to all isoforms of XNP by the lab of Dr. Kami Ahmad [46]. Stainings of homozygous *dADD1²*, *XNP⁴⁰³* and *XNP⁴⁰⁶* mutant ovaries confirmed that both antibodies are highly specific as no signal was detected at nurse cell chromatin in these mutants.

We found that dADD1 and XNP showed unique chromatin localization patterns at nurse cell chromatin. In accordance with dADD1 ChIP data from the lab of Dr. Mitzi Kuroda, we observed enrichment of dADD1 at heterochromatin, where dADD1 significantly co-localized with the heterochromatin-associated protein HP1a [56]. However, a population of dADD1 was also present at euchromatin. In contrast,

XNP showed uniform localization to both heterochromatin and euchromatin, but surprisingly showed no enrichment at HP1a-rich chromatin. While these proteins do not show overlapping enrichment, they are both present at euchromatin and heterochromatin in nurse cells, where they may bind and regulate common chromatin elements.

4.1.3 Chromatin recruitment of dADD1 and XNP is independent of one another

ATRX is recruited to chromatin through a combination of the ADD domain binding to H3K9me3 marks on histones as well as through the HP1a-interacting domain binding to HP1a [26]. We observed that dADD1 is enriched at chromatin regions with high levels of H3K9me3 both in nurse cell chromatin and in HELA Kyoto cells suggesting that dADD1 is recruited to heterochromatin, at least in part, through binding of the ADD domain to H3K9me3. dADD1 also contains several putative HP1a binding sites so it is also possible that the interaction between dADD1 and HP1a contributes to the localization of dADD1 to heterochromatin. Identification of the exact HP1a-interacting domain would allow for experiments to be performed that could determine if the interaction between HP1a and dADD1 contributes to the localization of dADD1 to heterochromatin. While a mechanism by which dADD1 is recruited to heterochromatin is suggested by the presence of the ADD-domain, how XNP is recruited to chromatin is still unknown. However, the interaction of XNP with HP1a could offer one explanation of how XNP is recruited to chromatin, but more work needs to be done to identify the HP1a interacting domain within XNP.

While the exact mechanism of chromatin recruitment of these proteins is still open for investigation, we have eliminated the possibility that either dADD1 recruits XNP or that XNP recruits dADD1 to chromatin. Since the SNF2-domain of ATRX is partially dependent on the ADD-domain for chromatin recruitment, we hypothesized that XNP could be recruited to chromatin through interaction with dADD1 or through dADD1-associated proteins. Co-expression experiments of dADD1 and XNP in HELA Kyoto cells to determine if dADD1 could recruit XNP to H3K9me3-rich chromatin regions were unsuccessful. However, we were able to

show that XNP localizes normally to nurse cell chromatin in *dADD1*² homozygous mutant ovaries. Furthermore, XNP was not recruited to dADD1-GFP rich heterochromatin in follicle cells overexpressing dADD1. XNP was the only chromatin factor from six chromatin factors tested that was not enriched at heterochromatin in dADD1-overexpressing cells.

dADD1 is enriched at heterochromatin but also shows localization to euchromatic regions at nurse cell chromatin. The heterochromatic localization of dADD1 is likely dependent on the interaction of the ADD-domain with H3K9me₃, but how dADD1 is recruited to euchromatin was unclear. Since XNP shows a uniform staining across nurse cell chromatin we also tested the possibility that XNP is important for dADD1 recruitment to euchromatin. dADD1 localizes normally to chromatin in *XNP*⁴⁰³ homozygous null mutants indicating the XNP is not necessary for recruitment of dADD1 to chromatin. Additionally, overexpression of XNP-HA in egg chamber follicle cells did not increase recruitment of dADD1 to XNP-HA rich chromatin regions, demonstrating that XNP does not recruit dADD1 to chromatin.

Importantly, however, further testing of known dADD1 interaction partners revealed that Bonus recruits dADD1 to euchromatic Bonus foci in follicle cells overexpressing a Bonus-RFP construct. While Bonus is sufficient to recruit dADD1 to euchromatin, experiments to test the necessity of Bonus for euchromatic dADD1 recruitment were not possible as homozygous *bonus* mutant flies are lethal. In addition, multiple attempts to generate mosaic *bonus* homozygous mutant tissue using the FLP/FRT system, a technique similar to the mammalian CRE/Lox system, in both follicle cells and nurse cells were unsuccessful. Experiments to express a RNAi targeting *bonus* could also be performed to circumvent this limitation. However, significant time would need to be invested to generate a new *bonus* RNAi line that is capable of driving expression in germline nurse cells, as current lines contain UAS promoters that only function in somatic tissue, such as follicle cells, where dADD1 is expressed at levels below the detection limit of our dADD1 antibody.

4.1.4 Mutations in dADD1 and XNP give rise to similar mutant phenotypes

Our biochemical interaction data, as well as chromatin localization data in homozygous dADD1 and XNP mutants and overexpressing follicle cells suggest that dADD1 and XNP do not interact. However, our detailed phenotypic analysis of the mutants revealed that they share common phenotypes. For example, both *dADD1* and *XNP* mutants show learning and memory defects, where mutant flies continued to startle in response to a light off stimulus.

While these learning and memory defects were present in mutants that had a systemic decrease in dADD1 and XNP levels, further experiments investigating the effect of neuron specific loss of either protein should be performed. Preliminary results from RNAi knockdowns of either *XNP* or *dADD1* using a neuron specific elavGAL4 driver showed that knockdown of *XNP* but not *dADD1* in neurons caused learning and memory defects (data not shown). Since RNAi knockdown is rarely 100% efficient, this data supports our mutant data where partial loss of *XNP* is sufficient to induce learning and memory deficits but a complete loss of *dADD1* is needed for the same effect. While this data is promising, preliminary assays to evaluate the efficiency of the RNAi knockdown in brains were not successful and therefore more work needs to be done to validate these results.

Both homozygous *dADD1* and *XNP* mutant flies also showed impaired DNA damage responses as measured by the accumulation of γ -H2Av into nurse cell chromatin. In response to double-strand DNA breaks H2Av histones close to the DNA lesions are phosphorylated. In *Drosophila* these phosphorylated H2Av histones are called γ -H2Av. *dADD1* or *XNP* mutant flies treated with double-strand break inducing hydroxyurea both showed increased γ -H2Av levels when compared to shgRFP wild type control tissues. Interestingly, Pontin, Reptin and H2Av, members of the Tip60 double-strand DNA repair complex, were identified in both dADD1 and XNP MS pulldowns. The Tip60 complex aids in the repair of double-strand DNA breaks by acetylating γ -H2Av and facilitating the replacement of γ -H2Av with unphosphorylated H2Av [73]. Accumulation of γ -H2Av in homozygous *dADD1* or *XNP* mutant tissue may be a result of an impaired DNA damage response, where DNA

lesions are not actually repaired, or because γ -H2Av is not replaced with unphosphorylated H2Av.

Further experiments are needed to determine if the accumulation of γ -H2Av is the result of impaired DNA damage responses, inefficient turnover of γ -H2Av or both. One way to test these possibilities would be to perform Terminal deoxynucleotidyl transferase dUTP Nick-End Labeling (TUNEL) assays on ovaries from hydroxyurea-treated females. TUNEL assays label blunt ends of DNA double-strand DNA breaks and increased TUNEL in homozygous mutants would indicate defective double-strand DNA break repair. However, if the TUNEL staining is similar to that of a wild type control tissue then the accumulation of γ -H2Av is likely the result of defective γ -H2Av/H2Av turnover in *dADD1* or *XNP* mutant tissue.

4.1.5 *dADD1* and *XNP* interact genetically

While we could not identify a direct interaction between *dADD1* and *XNP*, the presence of shared interaction partners such as HP1a as well as the presence of similar phenotypes in the mutants suggested that these proteins may function together in similar biological pathways. To test this, we generated combination mutations of *dADD1* and *XNP* null mutants and analyzed whether melanotic and lethality phenotypes were enhanced. Since homozygous double mutants were lethal, we scored individuals that were homozygous mutant for one gene and heterozygous mutant for the other.

Originally, we observed that between 25-50% of homozygous *XNP* mutant flies developed small melanotic tumors in the abdomen. These melanotic masses are the result of the immune system attacking self-cells and may indicate increased stress within an organism [57, 58]. The addition of a single mutant copy of *dADD1* to homozygous *XNP* mutant genotypes increased both the incidence as well as the severity of melanotic tumors. In these double mutants, melanotic tumor incidence increased to over 30% in the *XNP*⁴⁰³ mutant background and to over 85% in the *XNP*⁴⁰⁶ mutant background. Additionally, the tumors found within these double mutants were much larger than those in the homozygous *XNP* mutant flies alone.

We also quantified the effect that addition of a single mutant copy of *XNP* to *dADD1* homozygous mutant flies had on fitness. While both the *dADD1* homozygous mutant flies as well as the *dADD1* homozygous mutant flies containing one mutant copy of *XNP* showed no visual phenotypes, addition of one mutant copy of *XNP* caused an increase in pupal lethality. While homozygous *dADD1* mutant larvae and double mutant larvae pupariate at similar rates, fewer double mutant adult flies eclosed with many dying in their pupal casing. This exacerbation of mutant phenotypes by addition of one mutant copy of either *dADD1* or *XNP* lends support to the hypothesis that these two proteins function in related pathways.

To further investigate these shared functions, experiments could be performed to analyze γ -H2Av accumulation in double mutant ovaries of hydroxyurea-treated females. Increased levels of γ -H2Av in double mutants in comparison to homozygous single mutants would demonstrate that these two proteins cooperate in DNA double-strand break repair responses. Cooperativity could also be demonstrated by enhancement of transposon silencing defects in double mutants. Unfortunately, experiments to test if learning and memory defects are exacerbated in *dADD1* and *XNP* double mutant flies are not possible as double mutant flies showed a significant decrease in fitness that resulted in false negative scores in habituation assays (data not shown).

4.2 Role of dADD1 and XNP at chromatin

4.2.1 Involvement in stress responsive chromatin regulation

Shared interaction partners of dADD1 and XNP that we identified through MS were enriched for proteins involved in both cellular response to stress and cellular response to DNA damage. Interestingly, in the unbiased analysis of the phosphoproteome screen we performed to look at dynamic regulation of chromatin in response to stress signaling, we identified stress responsive phosphorylation sites in both dADD1 and XNP (data not shown). In response to reactive oxygen species stress, dADD1 becomes phosphorylated, while XNP is de-phosphorylated.

Interestingly, we also observed that interaction partners HP1a, HP1b and Mod(mdg4) become de-phosphorylated in response to ROS stress. The influence that these phosphorylation sites have on the chromatin regulatory function of these proteins is still unknown. However, in the case of dADD1 and XNP, stress responsive alterations in phosphorylation status may play a role in regulating DNA damage responses.

4.2.2 dADD1 and XNP associate with a number of known telomere associated proteins

Analysis of dADD1 or XNP interaction partners showed a significant enrichment of proteins with chromatin-related functions. In addition, this analysis identified 100 proteins that significantly interacted with both dADD1 and XNP. These included the previously identified shared interaction partner HP1a as well as HP1b and Mod(mdg4), proteins known to interact with dADD1. Our list of shared interaction partners was also enriched for proteins identified in an MS analysis for telomere-associated proteins, which identified both XNP and dADD1 as proteins that bind telomere-associated sequences [67].

ATRX is a protein known to be important for maintenance of telomeres, as many tumors harboring ATRX mutations show alternative lengthening of telomeres [75]. We observed that XNP, but not dADD1, regulates transcription of telomere associated transposon HeT-A. While dADD1 homozygous mutant tissues showed no significant change in HeT-A transcription, experiments looking at telomere length indicated that loss of dADD1 but not XNP, slightly increased telomere length (data not shown). Telomere length was measured by RT-qPCR of HeT-A gDNA sequences in homozygous *dADD1* and *XNP* mutant flies, that had been maintained in a homozygous state for over 10 generations. Genomic copy number of HeT-A served as an indicator of telomere length, where increased HeT-A indicated an increase in telomere length. While we observed a 1.4-fold increase in genomic HeT-A sequences in *dADD1* mutants in comparison to a Iso31 wild type background, this fold increase was deemed to be statistically insignificant.

dADD1 also significantly interacted with the protein Prod in our MS data set. Prod regulates telomeric HeT-A transcription and has been shown to interact with

Chro and Pzg at telomeres [66, 76]. Chro was enriched within the dADD1 interactome while Pzg was found in both the dADD1 and XNP data sets. While these interactions are detected by MS, co-immunoprecipitation as well as co-localization experiments need to be performed to verify these interactions. Elucidation of the telomere-associated complexes that dADD1 and XNP are members of would enable a better understanding of the function of these two proteins at telomeres.

4.2.3 Loss of dADD1 or XNP does not affect localization of HP1a, HP1b or H3.3 to chromatin

MS identified that both dADD1 and XNP interact with chromatin proteins HP1a and HP1b. HP1a and HP1b have distinct functions at chromatin where HP1a binds H3K9me3 marked histones and aids in the formation of densely packed, silenced heterochromatin, while HP1b is important for activation of target genes within euchromatin [6, 54]. Since HP1a is a component of heterochromatin, regions enriched for HP1a in nurse cells and follicle cells were considered heterochromatic regions in our image analyses. At nurse cell chromatin HP1b showed a relatively uniform staining, although in some instances HP1b was excluded from HP1a rich heterochromatic regions. In follicle cells HP1b localized to euchromatin and appeared to be excluded from heterochromatin.

In homozygous *dADD1*² and *XNP*⁴⁰³ mutant ovaries, HP1a and HP1b localized normally to nurse cell chromatin, demonstrating that neither dADD1 nor XNP is necessary for the recruitment of these proteins to chromatin. It is, however, possible that HP1a and HP1b recruit dADD1 and XNP to chromatin. Unfortunately, homozygous HP1a and HP1b mutants are lethal and only a few genetic tools exist to dissect HP1a and HP1b function. We were thus unable to perform reciprocal experiments to determine if HP1a or HP1b are necessary for chromatin recruitment of dADD1 and XNP.

Peptides corresponding to H3.3 were also identified in both the dADD1 and XNP MS samples, suggesting that dADD1 and XNP may interact with H3.3. To this end we tested the effect that loss of dADD1 and XNP had on the incorporation of H3.3 into chromatin. In control wild type egg chambers, H3.3 stainings showed a very similar pattern to that of dADD1 where H3.3 is enriched at heterochromatin but

is also present at euchromatin. The localization patterns of H3.3 was unchanged in homozygous *dADD1*² and *XNP*⁴⁰³ mutants, indicating that these proteins are not necessary for the incorporation of H3.3 into histones. This result is not surprising as previous work on XNP has shown HIRA, a second protein in *Drosophila* capable of replication independent H3.3 deposition, is able to compensate for loss of XNP [53].

4.2.4 **dADD1 increases levels of HP1a, H3.3, H3K9me3, HP1b and Bonus at heterochromatin**

While dADD1 was not necessary for the recruitment of HP1a, HP1b or H3.3 to chromatin, it was sufficient to recruit these factors to chromatin. Overexpression of dADD1 in egg chamber follicle cells resulted in increased dADD1 localization at heterochromatin and also increased heterochromatic localization of HP1a, HP1b and H3.3. Normally HP1b is excluded from follicle cells heterochromatin but overexpression of dADD1 resulted in HP1b localization to heterochromatin. The recruitment of HP1a, H3.3 and HP1b by dADD1 is specific to these factors since XNP was not recruited to dADD1 rich heterochromatin and overexpression of XNP did not result in increased recruitment of these proteins to XNP enriched domains.

We also tested H3K9me3 levels in cells overexpressing dADD1 as the ADD-domain of dADD1 binds to H3K9me3 and dADD1 interacts with the H3K9 methyltransferase Eggless. In cells overexpressing dADD1, H3K9me3 levels were increased at heterochromatin. This increase is potentially due to dADD1 recruiting Eggless to chromatin where it can then tri-methylate H3K9. Interestingly, *dADD1* homozygous mutant ovaries showed a slight decrease in cellular H3K9me3 levels in cell lysates. Decreased H3K9me3 in *dADD1* mutants further supports the notion that dADD1 is important for the implementation of H3K9me3 marks at chromatin. If the interaction with Eggless is required for the implementation of H3K9me3 at heterochromatin still needs to be tested.

Taken together this data presents the possibility for a self-sustaining loop where dADD1 is recruited to heterochromatin through ADD-domain binding to H3K9me3 and recruiting Eggless. In turn Eggless then tri-methylates H3K9me3, facilitating further binding of dADD1. This may be one mechanism that maintains dADD1-rich domains at heterochromatin. Unfortunately, we were unable to test if

Discussion

Eggless is recruited to heterochromatin in dADD1 overexpressing cells as Eggless antibodies generated by the lab of Dr. Elizabeth Kremmer did not detect Eggless at follicle cell or nurse cell chromatin (data not shown).

The increase in H3K9me3 at heterochromatin in cells overexpressing dADD1 may also contribute to the increased HP1a recruitment to heterochromatin, as the chromo-domain of HP1a binds to H3K9me3. This possibility needs to be tested, but first the dADD1-HP1a interaction motif needs to be identified. Once the dADD1-HP1a interaction domain is identified a fly line can be generated that contains an inducible dADD1 construct with a mutated HP1a binding site. Recruitment of HP1a to heterochromatin between the dADD1-GFP and dADD1-HP1a binding mutants could be compared and levels of H3K9me3 at heterochromatin also monitored. If HP1a is recruited to heterochromatin at similar levels in the dADD1-GFP and dADD1-HP1a binding mutant, and H3K9me3 levels are not effected in the mutants, then the increase in HP1a is likely the result of increased heterochromatic H3K9me3 recruiting HP1a and not the result of a direct interaction between dADD1 and HP1a.

To better understand if the observed increases in HP1a, H3.3 or H3K9me3 in dADD1-overexpressing cells represented a total cellular increase or simply over-recruitment of available proteins, we tested the total cellular level of these factors in S2 cells overexpressing dADD1 by western blot. Total cellular levels of HP1a remained unchanged in dADD1 overexpressing S2 cells, while levels of both H3.3 and H3K9me3 increased in comparison to control S2 cells. This indicated that the increased recruitment of HP1a to heterochromatin in follicle cells overexpressing dADD1 is the result of recruitment of available HP1a and not the result of increased HP1a expression. However, the increased protein levels of H3.3 indicate a transcriptional increase in H3.3 in cells overexpressing dADD1. An increase in cellular H3K9me3 would be expected if overexpression of dADD1 increased the recruitment of Eggless to heterochromatin, which would bring more H3K9 trimethylases in proximity of their target substrates.

As Bonus was able to recruit dADD1 to euchromatin in cells overexpressing Bonus, we also tested if dADD1 was able to recruit Bonus to heterochromatin in

dADD1 overexpressing cells. In wildtype follicle cells, Bonus is excluded from heterochromatin, but in follicle cells overexpressing dADD1 Bonus was enriched at dADD1-rich heterochromatin. This demonstrated that Bonus and dADD1 are somehow able to recruit one another to chromatin. However, we also observed HP1b recruitment to both euchromatic Bonus foci in Bonus-overexpressing cells and to dADD1-rich heterochromatin in dADD1-overexpressing cells, opening up the possibility that the reciprocal recruitment of dADD1 and Bonus may be facilitated through HP1b.

4.3 Model

Here we show that dADD1 and XNP are multifaceted chromatin-associated proteins that have many functions at chromatin. Both proteins interact with heterochromatin associated proteins such as HP1a, but also with euchromatic proteins such as HP1b. Common interaction partners implicate dADD1 and XNP in the regulation of telomeres and transposon sequences and suggest that dADD1 and XNP may be important for repair of DNA double-strand breaks.

Based on the knowledge garnered in this thesis, we suggest the following models for how dADD1 and XNP function at heterochromatin, euchromatin and in the repair of double strand DNA breaks (Figure 31).

At heterochromatin, both dADD1 and XNP associate with HP1a, and this interaction helps to recruit both proteins to heterochromatin. However, dADD1 is also recruited to heterochromatin through the ADD-domain binding to H3K9me3. Both proteins are likely required for the deposition of H3.3. Specifically, we show that dADD1 and XNP interact with H3.3 and that overexpression of dADD1 leads to increased H3.3 incorporation into heterochromatin. XNP has previously been shown to be important for incorporation of H3.3 into chromatin so it is possible that XNP aids in H3.3 deposition at both heterochromatin and euchromatin, but more work needs to be done to determine if XNP is generally necessary for H3.3 deposition [53].

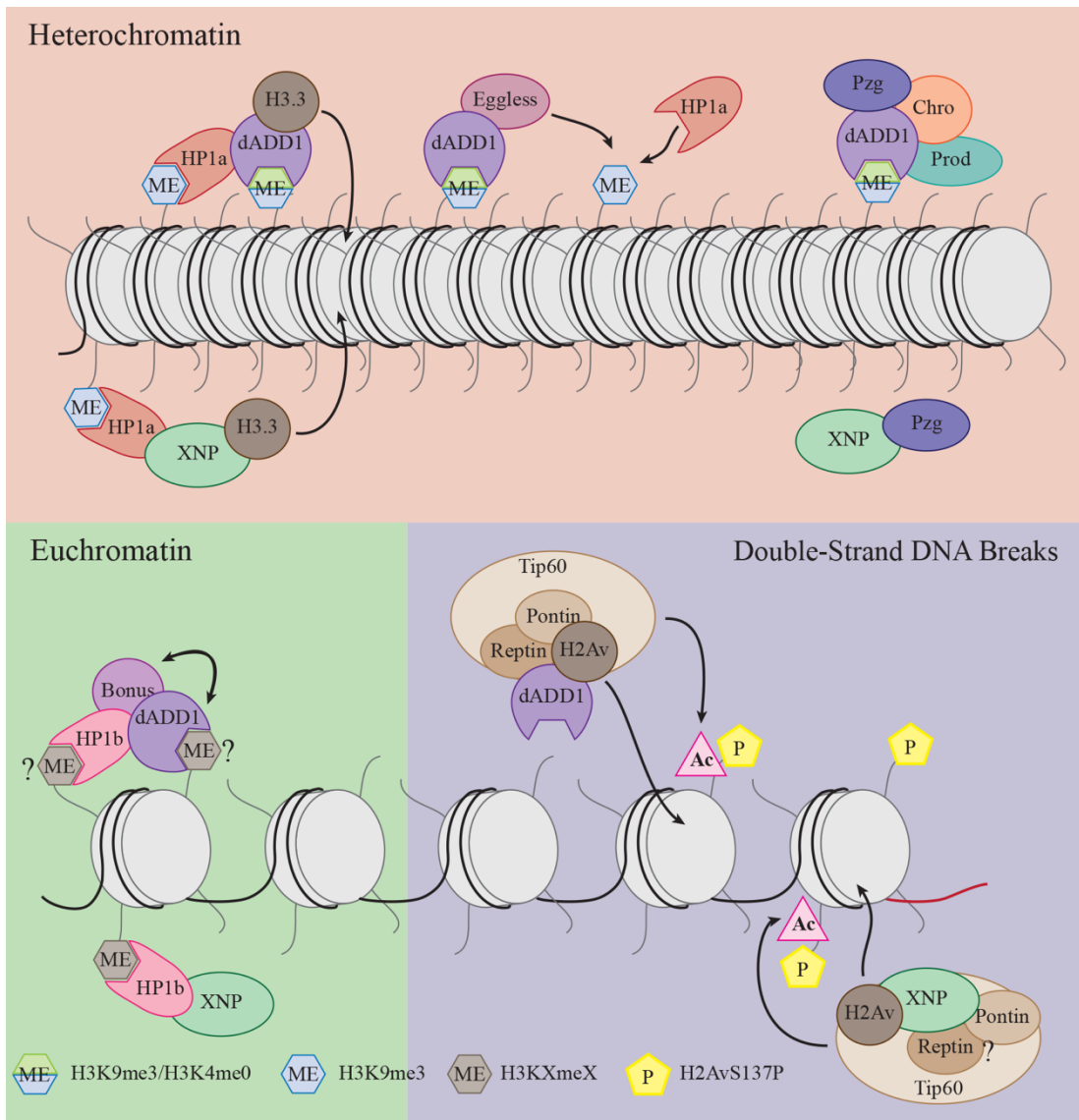


Figure 31: Model of dADD1 and XNP chromatin associated functions.

dADD1 and XNP are recruited to heterochromatin through interaction with HP1a, however, dADD1 is additionally recruited through ADD domain binding to H3K9me3. Both proteins interact with H3.3 and aid in deposition of this histone variant into chromatin. dADD1 recruits Eggless to heterochromatin where it tri-methylates H3K9, aiding in further recruitment of dADD1 and HP1a. dADD1 and XNP also play a role in regulation of telomeric heterochromatin where dADD1 interacts with Pzg, Chro and Prod, while XNP interacts with Pzg. At euchromatin dADD1 interacts with HP1b and Bonus and XNP interacts with HP1b. It is possible that HP1b and dADD1 bind specific histone methylation marks aiding in protein recruitment, however, if these marks are H3K9me3 needs to be shown. dADD1 and XNP are also involved in double strand DNA break repair where dADD1 and possibly XNP interact with members of the Tip60 DNA repair complex members Pontin, Reptin and H2Av. Here dADD1 and XNP may aid in the replacement of γ -H2Av with un-phosphorylated H2Av.

Based on dADD1 overexpression data and that dADD1 interacts with the H3K9 tri-methylase Eggless, it is likely that dADD1 recruits Eggless to heterochromatin and this results in tri-methylation of H3K9. This in turn can lead to

increased recruitment of HP1a and dADD1 to heterochromatin resulting in a self-sustaining recruitment loop.

dADD1 also significantly interacts with the telomeric associated proteins Prod, Chro and Pzg suggesting dADD1 may be important for regulation of telomeres. XNP interacts with the protein Pzg, which has been shown to be associated with telomeres, but is also important for general chromatin compaction at target DNA [77]. Although we identify here these new interaction partners, further work needs to be undertaken to validate these interactions and investigate the telomeric associated function of these proteins.

At euchromatin, both dADD1 and XNP likely interact with HP1b and this may be one of the ways in which these proteins are recruited to euchromatin. It is believed that the chromo-domain of HP1b binds to H3K9me3 similar to the chromo-domain of HP1a, although no work has been done to investigate HP1b-H3K9me3 binding. Since H3K9me3 very specifically localizes to heterochromatin and HP1b localizes to euchromatin we suggest the possibility that HP1b may bind a currently unknown combination of H3K9me histone tail modifications at euchromatin.

dADD1 also interacts with Bonus at euchromatin, where Bonus, dADD1 and HP1b associate at Bonus rich foci. Through overexpression experiments we showed that both dADD1 and Bonus are capable of recruiting one another, as well as HP1b, to dADD1 and Bonus enriched chromatin regions. The exact mechanism and order of recruitment is still unknown but further work should be undertaken to better understand the nature of this interaction and the function of this complex at euchromatin.

Repair of damaged DNA is an essential cellular process. Through our MS analysis, dADD1 was found to significantly interact with the Tip60 complex members Pontin, Reptin and H2Av, while XNP was shown to interact significantly with H2Av and possibly also with Pontin and Reptin. Experiments testing *dADD1* and *XNP* homozygous mutants for their ability to repair double-strand DNA breaks showed that both mutants had an impaired resolution of γ -H2Av, a marker of double-strand DNA breaks, at nurse cell chromatin of females treated with

Discussion

hydroxyurea. The Tip60 complex is involved in repair of double-strand DNA breaks, with part of the complex functioning to replace γ -H2Av with un-phosphorylated H2Av. Based on the interaction of dADD1 and XNP with H2Av it is possible that these proteins are involved in histone turnover at sites of DNA damage.

While dADD1 and XNP interact with similar proteins and have similar functions we do not observe an interaction between the two proteins. Therefore, our model does not include any direct protein interactions. The model presented here provides a foundation for further studies into the role that these two proteins play at specific chromatin regions and identifies many complexes that may mediate chromatin specific functions of dADD1 and XNP.

5 Conclusion

Maintenance of chromatin is very important for proper organism health and development. Misregulation or mutations within chromatin regulatory proteins underlie many human diseases such as cancer, neurological disorders, cardiovascular diseases and autoimmune diseases. ATRX syndrome, which causing learning and memory defects is one such disease that results from mutations within the protein ATRX with over 80% of mapped disease causing mutations falling within either the chromatin binding ADD domain or the chromatin remodeling SNF2 domain.

The ADD and SNF2 domain of ATRX map to two independent proteins in *Drosophila*, dADD1 and XNP. These domains show a high degree of sequence conservation to the human sequence and loss of these proteins in *Drosophila* results in similar phenotypes to ATRX mutants. These phenotypes include learning and memory defects, impaired DNA damage responses as well as defective transposon silencing, suggesting functional conservation of these proteins.

While the ADD and SNF2 domain of ATRX were split into two proteins in *Drosophila* we did not observe a direct interaction between dADD1 and XNP. We did however, identify a number of shared interaction partners, suggesting that while these proteins do not function together directly, they do function in shared pathways and have similar biological functions. This notion is further supported by the exacerbation of mutant phenotypes in combination.

Conclusion

There is still much to learn about the role that dADD1 and XNP play at chromatin and how these proteins function at both heterochromatin and euchromatin. Here we identified a number of new functions of dADD1 and XNP at chromatin, and have laid the foundation for the understanding of the role that these two proteins play in maintaining genomic stability and integrity.

6 Materials and Methods

6.1 General cell culture

6.1.1 Counting cells

Cells were counted using the Millipore Scepter Cell counter with 60 μm Sensors. Before counting cells were diluted 1/10 in TBS.

6.1.2 Freezing insect cell lines

Insect cell lines were frozen in Freezing Media containing 70% serum free media (Schneider's Medium for S2 cells and Sf-900™ II Medium for Sf21 cells), 20% FBS and 10% DMSO. When cells were growing optimally a culture of cells at approximately 5×10^6 cells/ml was spun down at $500 \times g$ for 5 minutes and the supernatant was discarded. The cells were then re-suspended in $\frac{1}{4}$ of the initial culture volume in Freezing Media and 500 μl of cells were aliquoted into cryovials. Initially the cells are frozen for 2-3 days at -80°C before being transferred to a liquid nitrogen freeze for long term storage.

6.2 S2 cell culture

6.2.1 Culturing conditions

All S2 derived cell lines were cultured in serum free Schneider's Medium supplemented with 10% Fetal Bovine Serum (FBS), 2 mM L-Glutamine (L-Glut) and 1% Penicillin-Streptomycin (P/S). For optimal growth, cells were split every 4-5 days

and for maintenance cells were split every 1.5-2 weeks. Cells were cultured in ventilated flasks at 25°C. For splitting cells were detached from the bottom of the flask using a rubber cell scraper. To break up cell clumps cells were pipet up and down 5-10 times against the bottom of the flask using a pipetman before being transferred to a new flask with fresh media. Normal splitting ratios were between 1/3 and 1/10 depending on the frequency of experiments and the density of cells.

Stable cells were cultured in supplemented Schneiders Medium containing hygromycin at a final concentration of 0.1 µg/µl.

6.2.2 Transfection

For transfections cells were split to 70-80% confluency a minimum of 2 hours before transfection. S2 cells were transfected using Roche X-tremeGENE transfection reagent. A master mix was incubated for 15-30 minutes at RT that contained serum free Schneiders Medium, 1/10th the volume of cell culture to be transfected (e.g. 3 ml of cells to be transfected = 300 µl serum free media), plasmid diluted to a concentration of 0.01 µg/µl in the master mix and 2 µl of transfection reagent per 100 µl of master mix volume. After incubation master mix was added to the cells and left overnight before inducing protein expression.

6.2.3 Stable cell line generation

Stable cells were generated by transfecting S2 DRSC cells with plasmids containing a hygromycin resistance marker. Cells were split to 70-90% confluency into 6 well plates in a total of 3 ml of media and allowed to settle for a minimum of 2 hours before transfection. After transfection cells sat for 2 days at 25°C before being split 1/10 into small ventilated flasks in 3 ml of media with added hygromycin to a final concentration of 0.1 µg/µl. Cells were monitored and split every 4-10 days, as necessary to maintain selection pressure.

6.2.4 RNAi

The number of cells was measured using the Scepter Cell Counter as described above (See 6.1.1 Counting cells). Remaining cell culture was collected in a falcon and spun at 700 x g for 10 minutes. Media was removed and cells were re-suspended in serum free Schneiders media to a concentration of 1-2 x 10⁶ cells/ml.

One ml of re-suspended cells were plated into a single well of a 6 well plate and allowed to settle for 30-60 minutes at 25°C before adding 10 µg of dsRNA. After addition of dsRNA cells were swirled very gently for 10 minutes at RT then placed back at 25°C for 50 minutes. After 50 minutes 2 ml of supplemented Schneiders Media was added to each well. The plates were sealed with parafilm to prevent evaporation and then left for 4-7 days at 25°C.

6.2.5 Whole cell lysis

S2 cells were collected and spun down at 700 x g for 5-10 minutes at RT. The media was discarded and cells were lysed in an appropriate volume of cell lysis buffer [20 mM Tris-HCl pH 7.5, 150 mM NaCl, 1 mM EDTA, 0.5% Triton X-100, 10 mM PMSF, Roche Mini Complete protease inhibitor cocktail]. After lysis cells were spun at 6 000 x g for 3 minutes at RT to remove cellular debris. The supernatant was transferred to a new tube and either prepared directly for western blot by adding 4 x Laemmli buffer to a final concentration of 1 x followed by boiling at 95°C for 5 minutes, or were used in immunoprecipitations (See 6.4.3 Immunoprecipitation). Proteins were either loaded directly onto an SDS gel or were stored at -20°C.

6.2.6 Salt nuclear extraction

Cells were collected by spinning 700 x g for 5 minutes at RT. The supernatant was discarded and the cells re-suspended in A+NP buffer [15 mM NaCl, 15 mM Tris-HCl pH 8.0, 13 mM EDTA, 60 mM KCl, 0.5% NP-40, 0.1% BME, 10 mM PMSF, Roche Mini Complete protease inhibitor cocktail, PhosSTOP phosphatase inhibitor]. Re-suspended cells were then drawn 10x through a 27 gage needle to destroy the outer cell membrane and then spun for 5 minutes at 300 x g at 4°C to remove cellular debris. After spinning the supernatant was transferred to a new tube and spun for 10 minutes at 6 000 x g at 4°C to pellet the nuclei. The remaining supernatant was transferred to a new tube and either discarded or prepared for loading onto an SDS gel, while the pellet containing the nuclei was lysed with RIPA buffer. Samples were then treated as was necessary for the following experiment.

6.2.7 Triton nuclear extraction

For Triton nuclear extraction cells were collected by spinning at 700 x g for 5 minutes at RT. The supernatant was discarded and cells were re-suspended in Triton

extraction buffer [1 x PBS, 0.3% Triton X-100, 10 mM PMSF, Roche Mini Complete protease inhibitor cocktail] and drawn 10 x through a 27 gage needed to disrupt the outer cellular membrane. Cells were then spun at 300 x g for 5 minutes at RT to remove cellular debris. The supernatant was then transferred to a new tube and spun for 10 minutes at 6 000 x g at 4°C to pellet the nuclei. After spinning the supernatant was transferred to a new tube and RIPA buffer was added to the nuclear pellet to disrupt the nuclear membrane. Laemmli buffer was added to both the supernatant and nuclear fractions to a final concentration of 1 x and the samples were boiled for 5 minutes at 95°C with vortexing and stored at -20°C before running on a western blot.

6.3 HELA Kyoto cell culture

6.3.1 Culturing conditions

HELA Kyoto cells were cultured at 37°C with CO₂ in serum free Dulbecco's Modified Eagle Medium (DMEM) supplemented with 10% FBS and 1% P/S. Cells were maintained in 10 cm plates in 10 ml of media and were split every 2-3 days. For splitting cells were rinsed twice with PBS, then trypsinized in 500 µl of trypsin to detach cells from the plate. Trypsinized cells were then re-suspended in 10 ml of fresh media and were pipet against the bottom of the plate until cells reached a single cell suspension. One ml of this single cells suspension was then transferred to 9 ml of fresh media in a new plate.

6.3.2 Transfection

For transfections HELA Kyoto cells were split to 70-90% confluency into 8 well IBIDI slides containing a final volume of 200 µl and allowed to settle for a minimum of 2 hours before transfection. Cells were transfected with Lipofectamine 3000. To begin two separate master mixes were prepared that contained per well 1) 12.5 µl OptiMEM, 0.25 µg Plasmid and 0.5 µl of P3000 or 2) 12.5 µl OptiMEM and 0.75 Lipofectamine 3000. These two master mixes were left for 10-15 minutes at RT before mixing together and waiting another 10-15 minutes. After the second

incubation the combined master mix was added to the cells before placing back in the incubator over night.

6.4 Protein expression, purification and detection

6.4.1 S2 cell protein expression

Proteins were expressed in S2 cells either by transiently transfecting cells with plasmids or by generating stable cells. Plasmids used in this thesis were under the control of the metallothionine promoter, which is a heavy metal inducible promoter. To this end we induced protein expression through the addition of copper sulphate (CuSO₄) to a final concentration of 0.2 mM for 24 hours. After protein expression cells were collected and lysed as above (See 6.2.5 Whole cell lysis).

6.4.2 Ovary, brain and imaginal disc protein extraction

Proteins were extracted from *Drosophila* tissue for western blot analysis. For ovaries females were fattened on yeast paste for 2 days with males before dissection. Brains were taken from both adult and 3rd instar larvae and imaginal discs were removed from 3rd instar larvae. All dissections took place in PBS. After dissection tissues were transferred to cell lysis buffer [20 mM Tris-HCl pH 7.5, 150 mM NaCl, 1 mM EDTA, 0.5% Triton X-100, 10 mM PMSF, Roche Mini Complete protease inhibitor cocktail] and pipetted vigorously for 30 seconds to lyse the tissues. Lysates were then spun at 6 000 x g for 3 minutes to remove cell debris. Supernatant was then transferred to a new tube and 4 x Laemmli was added to a final concentration of 1 x before boiling samples at 95°C for 5 minutes. Samples were either directly loaded onto an SDS gel or were stored at -20°C.

6.4.3 Immunoprecipitation

Cell lysates from S2 cells and Sf21 cells were used to further purify proteins of interest (See 6.2.5 Whole cell lysis and **Error! Reference source not found. Error! Reference source not found.**). For immunoprecipitations with Protein G beads from GE healthcare cell lysates were incubated overnight at 4°C with 1^o antibodies. Protein G beads or Flag M2 beads from Sigma were pre-blocked in 3% bovine serum

albumin (BSA)-TBS for 1 hour at 4°C before adding cell lysate to the beads and incubating 2 hours at RT. After incubation beads were washed quickly 3 x with TBS and proteins were eluted from the beads by boiling at 95°C for 5 minutes in 1 x Laemmli buffer with vortexing. Beads were then spun for 30 seconds at 6 000 x g and supernatants were transferred to a new tube and either loaded directly onto an SDS gel or were frozen at -20°C.

6.4.4 Measuring protein concentration

When necessary, protein concentration was measured using Pierce 660 nm Protein Assay Reagent. In a 96 well microplate 10 µl of cell lysate and 10 µl of proteins standards were mixed with 150 µl of Protein Assay Reagent. OD readings were taken with at 660nm. Protein concentration was calculated in excel by plotting OD of cell lysis sample on the graph generated using the protein standards.

6.4.5 Western blotting

SDS gels were prepared using the BioRad Mini-PROTEAN casting system. Cast gels were loaded into the Mini-PROTEAN Tetra Tank and run at 100-200V until desired separation was reached. Proteins were then wet blot transferred to a nitrocellulose membrane. Wet blotting was performed at 300mA either at 4°C or on ice until proteins were transferred to the membrane (1-3 hours). Membranes were blocked in 3% BSA-0.5%TBS-Tween (TBST) for 15 minutes before 1^o antibodies were added and incubated with the membrane overnight at 4°C. After 1^o incubation membranes were rinsed 3 x quickly in 0.5%TBST and then 3 x 15 minutes. Membranes were again blocked in 3% BSA-0.5%TBST and 2^o antibodies were added for 2 hours at RT. Following 2^o antibody incubation membranes were rinsed 3 x quickly in 0.5%TBST and then 3 x 10 minutes.

For horse radish peroxidase coupled 2^o antibodies, membranes were incubated for 1-2 minutes with ECL Western Blotting Substrate from pierce and then imaged with a BioRad Chemidoc. Blots were overlapped with the ladder and adjusted with Photoshop.

6.5 Fly Husbandry

All flies and crosses were kept on standard food and raised at room temperature. *dADD1*², *XNP*⁴⁰³ and *XNP*⁴⁰⁶ were isogenized to the Iso31 background over 10 generations to remove any possible background mutations. Alleles were followed by single fly PCR using the following primers received as a personal communication from Dr. Kami Ahmad:

dADD1-F 5'- AACTCGATATGTTTATACGGTCTC -3'

dADD1-R-5'-GATGTCACGGATGTAATCTTCA -3'

XNP-F-5'- TTCGAACTTAACTGAGTTGACG -3'

XNP-R-5'- AAATGTGGCGAGCCCCGTGA -3'.

For pupal survival, egg lays were performed for 6 hours at room temperature on grape plates with additional yeast paste. Eggs were kept at 25°C overnight and first instar larvae were transferred to new vials the following day. Pupae were counted before eclosion and eclosed adults were counted. For melanotic tumor incidence crosses were flipped daily onto new food and egg lays were kept at 25°C until eclosion. After eclosion remaining flies were anaesthetized with CO₂ and placed into isopropanol until they were scored. Pictures of females were taken using a Leica Z 6 Apo microscope with 1.25 x objective and processed using HeliconFocus.

6.6 Immunofluorescence

6.6.1 Imaginal discs

Wandering 3rd instar larvae were dissected in PBS leaving the imaginal discs attached to the cuticle. Discs were fixed for 5 minutes in 4% PFA in 0.01% PBS-Triton X-100 and were rinsed 3 x in 0.1% PBST before blocking for 20 minutes in 5% NGS-0.1% PSBT. Antibodies were added to the blocking solution and samples were incubated overnight at 4°C. Following 1^o antibody staining discs were rinsed 3 x quickly in 0.1% PBST and then for 3 x 10 minutes before being blocked in 5% NGS-

0.1% PSBT. DAPI, Phalloidin and appropriate secondary antibodies were added to the blocking solution and incubated for 2 hours at RT before 3 x quick rinse in 0.1% PBST followed by 3 x 10 minutes. Following the final wash cuticles were transferred to PBS in a dissection dish and the appropriate imaginal discs were fine dissected and then mounted on microscope slides with antifade.

6.6.2 Adult Brains

Adult flies were anaesthetized with CO₂ before being transferred to a dissection dish with PBS. Brains were fixed in 4% PFA-0.3% PBST for 20 minutes at RT, followed by blocking in 0.3% PBST with 5% Normal Goat Serum. Brains were left in blocking solution and rotated with primary (1^o) antibodies for two overnights at 4°C. Brains were washed 3 x 20 minutes at RT in 0.3% PBST. Secondary (2^o) antibodies were added to the samples and incubated for a total of 4 hours at RT in the blocking solution. During the final hour of secondary incubation DAPI and phalloidin were added. Samples were again washed 3 x 20 minutes in 0.3% PBST before mounting.

6.6.3 Larval Brains

Third instar larvae were transferred to a dissection dish with PBS. Brains were dissected and fixed in 2% PFA-PBL [1mM Lysine-HCl, 12mM Disodium Phosphate, PBS] for 15 minutes at RT. Samples were blocked in 0.5% PBST with 10% Normal Goat Serum for 15 minutes followed by primary antibody incubation overnight at 4°C. Samples were then washed 3 x 5 minutes in 0.5% PBST and incubated with secondary antibodies, phalloidin and DAPI for 2-3 hours at RT. Samples were then washed 2 x 15 minutes in 0.5% PBST and 2 x 15 minutes in PBS before mounting.

6.6.4 Ovaries

Young females and males were put together on yeast paste to fatten up for 2 days before dissection. Flies were anesthetized with CO₂ and females were dissected in a dissection dish containing PBS. Ovaries were removed from fattened females and fixed for 5 minutes in 4% PFA-PBS then rinsed twice in 0.5% PBS-Triton-X-100 (PBST). Primary antibodies were added to 0.5% PBST and samples were incubated overnight at 4°C. Samples were then quickly rinsed twice with 0.5% PBST and then

for 3 x 15 minutes. After washing samples were incubated with necessary fluorescent dyes and 2^o antibodies for 2 hours at RT. Samples were again rinsed quickly twice with 0.5% PBST and then for 3 x 10 minutes. When washing was complete ovaries were dissociated using a P200 pipet, allowed to settle and then mounted on slides in Antifade solution. Finally, to prevent evaporation the edges of the cover slip was sealed with nail polish. All incubation steps were performed on a nutator.

For dADD1 antibodies samples were blocked with 5% normal goat serum (NGS) in 0.5% PBST before and during 1^o and 2^o antibody stainings.

6.6.5 S2 Cells

8 well IBIDI plates were coated with Poly-L- Lysine for 30 minutes and then rinsed with sterile water. S2 cells were then plated into each well to a confluency of between 70-90% and the cells were allowed to adhere for a minimum of 2 hours before transfection. Transfections were performed as described in 6.2.2 Transfection and after an overnight incubation protein expression was induced by adding CuSO₄ to a final concentration of 0.2 mM for 24 hours. After induction cells were fixed for 15 minutes in 2% PFA by adding PFA directly to the cell culture media being careful not to dislodge the cells from the bottom of the well. The fixative was removed and cells were washed 3 x in 0.02% PBST and then incubated for 10 minutes at RT in 0.02% PBST to permeabilize the membranes. Samples were then blocked for 20 minutes in 5% NGS-0.02% PBST, 1^o antibodies were added to the blocking solution and incubated overnight at 4°C. Cells were rinsed 3 x quickly and then 3 x 10 minutes in 0.02% PBST before blocking again in 5% NGS-0.02% PBST. DAPI, Phalloidin and 2^o antibodies were added to the blocking solution and incubated at RT for 2 hours in the dark. 2^o antibodies were removed, cells were rinsed 3 x in 0.02% PBST and 3 x 10 minutes. Samples were stored in the fridge in PBS with 1/1000 sodium azide before imaging.

6.6.6 HELA Kyoto Cells

Cells were transfected with mammalian expression vectors containing a CMV promoter with a C-terminal GFP tag. Proteins were expressed for 16-24 hours before being rinsed quickly with PBS and then fixed for 10 minutes in 4% PFA-PBS. At the end of 10 minutes a drop of 0.02% PBST was added to the fixation solution

(recommendation from Dr. Irina Solovei to preserve chromatin structure). The PFA was then removed and the cells were rinsed twice with 0.02% PBST then for 20 minutes to permeabilize the cells. After permeabilization cells were blocked for 20 minutes in 5% NGS-0.02% PBST, antibodies were added and cells were incubated overnight at 4°C. Following 1^o antibody staining, cells were rinsed twice with 0.02% PBST and then 3 x 10 minutes at RT. Cells were again blocked in 5% NGS-0.02% PBST for 20 minutes before adding DAPI, phalloidin, α -GFP 488 Nano-Booster from ChromoTek and appropriate 2^o antibodies for 2 hours. After incubation cells were rinsed twice in 0.02% PBST and then 3 x 10 minutes. For storage cells were covered with a 0.25% Antifade-PBS solution containing a 1/1000 dilution of sodium azide (NaN₃) and kept in the dark at 4°C before imaging.

6.7 Nucleic acid techniques

6.7.1 Plasmid purification

Plasmids were purified from bacteria grown on LB agar plates with appropriate antibiotics for 24 hours at 37°C. Single colonies were then selected and grown overnight at 37°C with shaking in liquid LB media containing the appropriate antibiotics in 5 ml volume for mini preparations and 100 ml volume for midi preparations. Following amplification plasmids were extracted using the NucleoSpin Plasmid DNA purification kit from Machery-Nagel following the company instructions. Plasmids were verified through test digestions with restriction enzymes and then sent for sequencing.

6.7.2 Gateway cloning

cDNA was PCR amplified from plasmids or from cDNA with primers containing restriction enzyme recognition sites. PCR products were digested with restriction enzymes and then column purified using NucleoSpin Gel and PCR Clean-up kit from Machery-Nagel. The pENTR-AttR vector was digested, run out on an ethidium bromide gel and the backbone was gel purified. PCR products were ligated together with the pENTR-AttR backbone to generate pENTR-cDNA vectors. To generate AttR/L expression vectors recombination reactions were performed

containing the appropriate destination vectors and pENTR vectors. Recombination reactions were performed using the Gateway LR Clonase II Enzyme mix following the kit instructions, but using half of the reaction volume and components. Plasmids were then transformed into bacteria, selected on LB plates containing antibiotics and plasmids were purified as described in 6.7.1 Plasmid purification.

6.7.3 Rolling circle PCR

Rolling circle PCR was used to generate amino acid mutants and to insert short protein tags or other special features onto plasmids. Primers were designed so that the 5' ends bordered on one another but bound to complementary strands and amplified in opposite directions. Amino acid substitutions were induced by nucleotide substitutions that caused amino acid changes during translation, while the addition of tags (e.g. Flag) or other special features (e.g. TEV cleavage site) were inserted through overhangs on the primers. Target sequences were amplified as a linear fragment and the PCR reaction was digested with DpnI for 1 hour at 37°C to remove plasmid DNA. The PCR product was run on a gel to test for the correct size and then gel purified. Purified product was then treated with PNK kinase with added ATP to phosphorylate the 5' DNA ends and then column purified to remove the PNK before ligation to re-circularize the plasmid. Plasmids were then transformed into bacteria and the purified as described in 6.7.1 Plasmid purification and were then used for injections.

6.7.4 gDNA extraction

Genomic DNA was prepared from S2 cells, imaginal discs or whole larvae. Samples were lysed in 400 µl lysis buffer A [100 mM Tris-HCl pH 7.5, 100 mM EDTA, 100 mM NaCl, 0.5% SDS] and then incubated for 30 minutes at 65°C. After incubation 800 µl of 1 part 5 M potassium acetate (KAc) 2.5 parts 6 M lithium chloride (LiCl₂) were added and samples were precipitated on ice for 10 minutes then spun at 15 000 x g for 15 minutes at 4°C. Supernatant was separated into two new Eppendorf tubes and 700 µl of isopropanol was added per 1 000 µl of supernatant. The two tubes were spun 15 000 x g for 15 minutes at 4°C, the the supernatant was removed and the pellet was washed with 1 ml of cold ethanol before being again centrifuged at 15 000 x g for 5 minutes at 4°C. Following the final spin

the supernatant was removed and the pellet was allowed to briefly dry before being re-suspended in TE buffer.

6.7.5 RNA extraction

6.7.5.1 TRIzol RNA extraction

Ovaries from 10 females that had been fattened on yeast paste for at least 2 days were dissected before adding 1 ml of TRIzol. The tissue was then homogenized using a pipette and incubated at RT for 5 minutes. Following the incubation 200 μ l of chloroform and 10 μ g of glycogen were added to the samples. Samples were shaken by hand and incubated for 2-3 mins at RT then transferred to a gel-lock tube and then spun for 5 minutes at 12 000 x g at 4°C. The top aqueous phase was removed and precipitated with 500 μ l isopropanol for 5-10 minutes at RT and then again spun at 12 000 x g for 10 minutes at 4°C. The supernatant was removed and the pellet was washed with 75% ethanol and then spun again at 7 500 x g for 5 minutes. Following the final spin the ethanol was removed and the pellet was allowed to dry briefly before re-suspending in DEPC water.

6.7.5.2 Turbo DNase treatment

Contaminating DNA was removed from the RNA extractions with DNase treatment. 2 μ g total RNA was incubated with 1 μ l 10X Turbo DNA free reaction buffer and 1 μ l of TurboDNase for 30 minutes at 37°C. After incubation 2 μ l of milk was added to block the reaction and left at 25°C for 5 minutes. Samples were spun for 1.5 minutes at 10 000 x g and the supernatant was transferred to a cDNA reaction tube. The clean RNA was diluted in 4 μ l of water and analyzed on the Bioanalyzer for purity.

6.7.6 cDNA preparation

cDNA was prepared using the Superscript III reverse transcriptase kit. The following PCR reaction was set up on ice:

- 10 μ l 2X reaction mix
- 2 μ l RT enzyme mix
- 8 μ l RNA

These samples were then incubated in the PCR machine at 25°C for 10 minutes, 50°C for 30 minutes, 85°C for 5 minutes and the 4°C indefinitely. 1 µl of RNase H was then added to digest away the remaining RNA and the samples were incubated for 20 minutes at 37°C. Following RNase H treatment the cDNA was diluted in 200 µl of water.

6.7.7 RT-qPCR

For a single well the following reactions were prepared using the Power SYBR Green PCR Master Mix from AppliedBiosystems:

- 5 µl PCR Mix
- 4 µl cDNA template
- 0.5 µl Primer 1
- 0.5 µl Primer 2
- 0.6 µl water

Reactions were prepared in triplicate and ct values were averaged and then normalized to an average ct value from 4 different housekeeping genes using the $\Delta\Delta C_t$ method [78].

6.7.8 dsRNA

dsRNA was generated for cell culture RNAi knockdown. DNA was amplified from cDNA plasmids using primers containing T7 Polymerase promoters on the 5' end of each primer. PCR reactions were column purified and dsRNA was generated using the HiScribe T7 Quick High Yield RNA synthesis kit as per company instructions.

6.8 Materials

6.8.1 Fly stocks

Internal Reference Number	Description	Source
AC0806	CG8290 [2] / CG8290 [2]	Dr. Mitzi Kuroda
AC0816	CG8290-BioTAP #8	Dr. Mitzi Kuroda
AC0817	CG8290-BioTAP #9	Dr. Mitzi Kuroda
AC0812	CG8290 [2] iso31/CyO, ubi-GFP; XNP [403] iso31/TM6c	Isoginized this study
AC0813	CG8290 [2] iso31/CyO, ubi-GFP; XNP [406] iso31/TM6c	Isoginized this study
AC0808	CG8290 [2] iso31/CyO, ubi-GFP	Isoginized this study
AC0809	CG8290 [2] iso31/CG8290 [2] iso31	Isoginized this study
--	UAS dADD1-GFP/TM6c	This Study
--	dADD1 endoGFP	Bloomington Stock Center (BL 52172)
AC0825	w; xnp[403] / TM3-GFP	Dr. Kami Ahmad
AC0826	w; xnp[406] / TM3-GFP	Dr. Kami Ahmad
AC0827	XNP [403] iso31/TM6c	Isoginized this study
AC0829	Sp/ CyO, ubi-GFP; XNP [403]/TM6c iso31	Isoginized this study
--	XNP [403] iso31/XNP [403] iso31	Isoginized this study
AC0831	XNP [406] iso31/TM6c	Isoginized this study
AC0832	Sp/ CyO, ubi-GFP; XNP [406]/TM6c iso31	Isoginized this study
AC0834	UAS-XNP.HA / III	Bloomington Stock Center (BL26645)
AC0847	UAS-Bon-RFP [Hto-QYE]	Bloomington Stock Center (BL56534)
AC0002	iso 31	Dr. Annette Schenck
AC0046	hsflp [122]; FRT42D / CyO, ubi-GFP; Dr / TM6c	Dr. Anne Classen
AC0121	Act5c-Cas9, Lig4 [?]; Sco/CyO	Dr. Frank Schnorrer
AC0167	Pin[1]/CyO; nSyb-GAL4, UAS mCD8::GFP	Dr. Ilona Kadow
AC0190	TJ-GAL4, Mef20-GAL80/CyO	Dr. Sally Horne Badovinac
AC0366	DE Cad::dTomato/CyO	Bloomington Stock Center (BL 58789)
AC0403	Sp/ CyO; hp1:GFP-HP1/ TM6c	Bloomington Stock Center (BL30561)
AC0721	FRT42D Psc-Su(z)2[XL26]/ CTG	Dr. Anne Classen

6.8.2 Cell Lines

Cell Line	Derivative	Plasmid Integration	Source
Schneider 2 (S2)	<i>Drosophila melanogaster</i> embryo	--	Dr. Axel Imhof
S2 DRSC	S2 Cells	--	Dr. Axel Imhof
Sf21	<i>Spodoptera frugiperda</i> Ovaries	--	Dr. Catherine Regnard
HELA Kyoto	Human Cervical Cancer Cells	--	Dr. Heinrich Leonhardt
Cas9	S2 Cells	Act5c Cas9	Dr. Frank Schnorrer
dADD1-Flag/HA	S2 Cells	pMT-dADD1-RA-Flag/HA	Dr. Andreas Thomae
Psc 1-911 WT	S2 Cells	pMT-Psc 1-911 WT-Flag/HA	This study

6.8.3 Antibodies

6.8.3.1 Primary Antibodies

Primary Antibodies	Source	Animal	Western Blot	Immunofluorescence
Bonus	Dr. Hugo Bellen	Guinea Pig	1/500	1/100
dADD1	Dr. Andreas Thomae	Rat	1/20	1/20
Flag	Dr. Elizabeth Kremmer	Rat	1/200	--
Flag M2	Sigma	Mouse	1/1000	1/500
GFP	ImmunoKontakt	Rabbit	1/5000	1/1000
H3	abcam	Rabbit	1/5000	--
H3.3	abnova	Mouse	1/500	1/100
H3K9me3	abcam	Rabbit	1/500	1/200
HA	Dr. Elizabeth Kremmer	Rat	1/200	1/20
HA	Roche	Mouse	--	1/200
HP1a	DSHB	Mouse	1/200	1/200
HP1b	Dr. Axel Imhof	Rat	1/20	1/20
JNK	Santa-Cruz	Rabbit	1/5000	--
Myc	Roche	Mouse	1/1000	1/500
Myc	Dr. Elizabeth Kremmer	Rat	1/500	1/100
p-JNK	Promega	Rabbit	1/5000	--
Psc 39	Dr. Elizabeth Kremmer	Rat	1/20	1/10
Psc 77	Dr. Elizabeth Kremmer	Rat	1/50	1/10
Psc 78	Dr. Elizabeth Kremmer	Rat	1/20	1/10
Psc 79	Dr. Elizabeth Kremmer	Rat	1/20	1/10
Psc 8C8	Dr. Elizabeth Kremmer	Rat	1/20	1/10
Tubulin	Sigma	Mouse	1/5000	--
XNP	Dr. Kami Ahmad	Rabbit	--	1/8000
Protein-A	Sigma	Rabbit	1/500	1/1000

6.8.3.2 Secondary Antibodies

Secondary Antibodies	Conjugate	Source	Product Number	Western Blot	Immunofluorescence
a-GFP Nano-Booster	488	ChromoTek	ATTO 488	--	1/200
a-Guinea Pig	647	Life Technologies	A21450	1/500	1/400-1/500
a-Mouse	488	Life Technologies	A11001	--	1/400-1/500
a-Mouse	555	Life Technologies	A21422	--	1/400-1/500
a-Mouse	647	Life Technologies	A21235	--	1/400-1/500
a-Mouse	HRP	Promega	W4028	1/2500	--
a-Mouse Pre-cleared	488	abcam	ab150117	1/500	--
a-Mouse Trueblot Ultra	HRP	Rockland	18-8817-30	1/200	--
a-Rabbit	488	Life Technologies	A11008	--	1/400-1/500
a-Rabbit	555	Life Technologies	A21428	--	1/400-1/500
a-Rabbit	647	Life Technologies	A21244	--	1/400-1/500
a-Rabbit	HRP	Promega	W4018	1/2500	--
a-Rat	488	Life Technologies	A11006	--	1/400-1/500
a-Rat	555	Life Technologies	A21434	--	1/400-1/500
a-Rat	647	Life Technologies	A21247	--	1/400-1/500
a-Rat	HRP	Pierce	31471	1/5000	--

6.8.4 Plasmids**6.8.4.1 Backbone Plasmids**

Internal Reference Number	Plasmid Name	Source
P048	pENTR/D Bsa1	Dr. Thomas Ott
p279	pFastbac	Dr. Catherine Regnard
p433	pUASp-attB	This Project

6.8.4.2 cDNA Plasmids

Internal Reference Number	Plasmid Name	Source
P069	pFastBac1-Psc-FLAG	Addgene
p185	p-bsk	BDGC Gold Collection
p192	p-hep	BDGC Gold Collection
p215	p-Akt1-RA	BDGC Gold Collection
p218	p-CDK7-RA	BDGC Gold Collection
p261	p-cdc2 (CDK1)	BDGC Gold Collection
p263	p-cdc2c	BDGC Gold Collection
p364	pJet1 dXNP SNF2 Kinase Dead Mutant K495R	Dr. Andreas Thomae
p462	p-Polo- A	BDGC Gold Collection
p463	p-EGG- A	BDGC Gold Collection
p464	p-mod(MDG4)-W	BDGC Gold Collection
p465	p-mod(MDG4)-AA	BDGC Gold Collection
p466	p-mod(MDG4)-D	BDGC Gold Collection
p467	p-bon-B	BDGC Gold Collection

6.8.4.3 Gateway Destination Plasmids

Internal Reference Number	Plasmid Name	Source
P058	pAMW	Gateway Library
P079	pMT-W-FH	This Project
p389	pMT-W-Myc	This Project
p443	CMV-GW-GFP	Dr. Gunnar Schotta

6.8.4.4 Injection Plasmids

Internal Reference Number	Plasmid Name	Source
p434	pUASp attB CG8290 GFP	This Project
p534	p-attB hsp Psc FL WT Flag	This Project
p535	p-attB hsp Psc FL T726A S729A Flag	This Project
p536	p-attB hsp Psc FL T726E S729E Flag	This Project

6.8.4.5 Gateway Entry Plasmids

Internal Reference Number	Plasmid Name	Source
P077	pENTR/D- Psc-RA	This Project
P152	pENTR/D- Psc- RA- S729(727)A	This Project
P153	pENTR/D- Psc- RA- S729(727)E	This Project
P154	pENTR/D- Psc- RA- T726(724)A	This Project
P155	pENTR/D- Psc- RA- T726(724)E	This Project
P156	pENTR/D- Psc- RA- T726(724)A/S729(727)A	This Project
P157	pENTR/D- Psc- RA- T726(724)E/S729(727)E	This Project
p168	pENTR/D- Psc 456-911 T726A S729A	This Project
p169	PENTR/D- Psc 456-911 T726E S729E	This Project
p176	pENTR/D- Psc 456-911 WT	This Project
p197	pENTR/D- Psc WT 1-911	This Project
p198	PENTR/D- Psc 1-911 T726A/S729A	This Project
p199	PENTR/D- Psc 1-911 T726E/S729E	This Project
p222	pENTR/D- CDK7	This Project
p224	pENTR/D- Jil-1 FL Ohne CTC	Dr. Catherine Regnard
p228	pENTR/D- Jil-1 FL dead mutant	Dr. Catherine Regnard
p237	pENTR/D- Psc 674-783 WT	This Project
p244	pENTR/D- Psc 647-783 T726E/S729E	This Project
p246	pENTR/D- bsk	This Project
p248	pENTR/D- hep	This Project
p266	pENTR/D- Psc 1-1220	This Project
p267	pENTR/D- Psc 1-1438	This Project
p268	pENTR/D- Psc 1-1487	This Project
p288	pENTR/D- bsk T181A (dom.-neg.)	This Project
p289	pENTR/D- bsk K53R (kinase-dead)	This Project
p290	pENTR/D- cdc2-RA (CDK1)	This Project
p291	pENTR/D- cdc2c-RA (CDK2)	This Project
p298	pENTR/D- Psc Full Length T1213A/S1217A	This Project
p299	pENTR/D- Psc Full Length T1213E/S1217E	This Project
p310	pENTR/D- XNP	This Project
p321	pENTR/D- Psc 1154-1263 Wild type	This Project
p322	pENTR/D- Psc 1154-1263 T1213E/S1217E	This Project
p337	pENTR/D- GFP	This Project
p353	pENTR/D- Psc 1-911 C287A RING dead Mutant	This Project
p354	pENTR/D- CG8290 (xPHD) Isoform A	This Project
p365	pENTR/D- AKT1 F327I	This Project
p460	pENTR/D- Psc 674-783 T726A/S729A	This Project
p468	pENTR/D- Polo- A	This Project
p469	pENTR/D- EGG- A	This Project
p470	pENTR/D- mod(MDG4)-W	This Project
p471	pENTR/D- mod(MDG4)-AA	This Project
p472	pENTR/D- mod(MDG4)-D	This Project
p473	pENTR/D- bon-B	This Project
p498	pENTR/D- XNP	This Project
p500	pENTR/D- XNP SNF2 Kinase Dead Mutant K495R	This Project

6.8.4.6 *Expression Plasmids*

Internal Reference Number	Plasmid Name	Source
P117	p-MT-Psc[GW-attB]-FH	This Project
p180	p-MT- Psc- T726A/S729A-[GW attB]-F-hy	This Project
p181	p-MT- Psc- T726E/S729E-[GW attB]-F-hy	This Project
p182	p-MT- Psc 456-911 T726A/S729A-[GW attB]-F-hy	This Project
p183	p-MT- Psc 456-911 T726E/S729E-[GW attB]-F-hy	This Project
p184	p-MT- Psc 456-911-[GW attB]-F-hy	This Project
p200	p-MT- Psc WT 1-911-[GW attB]-F-hy	This Project
p201	p-MT- Psc 1-911 T726A/S729A-[GW attB]-F-hy	This Project
p202	p-MT- Psc 1-911 T726E/S729E-[GW attB]-F-hy	This Project
p270	p-MT-Psc 1-1220 [GW attB] F HA-hy	This Project
p271	p-MT-Psc 1-1438 [GW attB] F HA-hy	This Project
p272	p-MT-Psc 1-1487 [GW attB] F HA-hy	This Project
p284	pFastbac-Psc-456-911-FLAG	This Project
p285	pFastbac-Psc-456-911-T726A S729A-FLAG	This Project
p286	pFastbac-Psc-456-911-T726E_S729E-FLAG	This Project
p287	pFastbac-Cdk7-FLAG	This Project
p300	pMT- Psc 674-783 WT- F-HA-Hy	This Project
p301	pMT-Psc 674-783 T726E/S729E - F-HA-Hy	This Project
p302	pMT-Flag-HA CG8290 (xPHD) - Hy	Dr. Andreas Thoma
p305	pMT- Flag-HA dXNP (ATRX) -Hy	Dr. Andreas Thoma
p311	pMT-Psc Full Length T1213A/S1217A-F-HA-Hy	This Project
p312	pMT- Psc Full Length T1213E/S1217E-F-HA-Hy	This Project
p316	pAct5C Myc- XNP GW	This Project
p323	pMT-Psc 1154-1263 Wild type-F-HA	This Project
p324	pMT Psc 1154-1263 T1213E/S1217E- F-HA	This Project
p338	p-MT - GFP [GW attB] hy	This Project
p366	pFastbac- AKT1- FLAG	This Project
p367	pFastbac- AKT1 F327I -FLAG	This Project
p372	pFastbac- bsk- FLAG	This Project
p374	pFastbac-bsk K53R - FLAG	This Project
p375	pMT-Psc 1-911 Ring Dead- FLAG/HA Hygromycin	This Project
p461	pMT Psc 674-783 T726A/S729A	This Project
p474	pMT Polo- A- Myc	This Project
p475	pMT EGG- A- Myc	This Project
p476	pMT mod(MDG4)-W - Myc	This Project
p477	pMT mod(MDG4)-AA - Myc	This Project
p478	pMT mod(MDG4)-D - Myc	This Project
p479	pMT bon-B - Myc	This Project
p480	pCMV CG8290 GFP	This Project
p481	pFastbac-Psc-456-911-TEV-FLAG	This Project
p482	pFastbac-Psc-456-911-T726A S729A-TEV-FLAG	This Project
p483	pFastbac-Psc-456-911-T726E_S729E-TEV-FLAG	This Project
p485	pCMV XNP GFP	This Project
p505	pMT- Psc 456-911 WT- Myc	This Project
P507	pFastBac- Bsk 2x TEV Flag	This Project
P508	pFastBac Bsk K53R 2x TEV Flag	This Project
P509	pFastBac Akt1 2xTEV Flag	This Project

Expression Plasmids Continued

Internal Reference Number	Plasmid Name	Source
P510	pFastBac Akt1 F327I 2xTEV Flag	This Project
P511	pFastBac CDK7 2xTEV Flag	This Project
P512	pFastBac Polo 2x TEV Flag	This Project
P513	pFastBac CDK9 2xTEV Flag	This Project
P514	pFastBac CDK1 (cdc2) 2xTEV Flag	This Project
P515	pFastBac CKA 2xTEV Flag	This Project
P516	pFastBac Jil-1 FL without CTC 2xTEV Flag	This Project
P517	pFastBac Jil-1 FL Dead mutant without CTC 2x TEV Flag	This Project
p519	pCMV XNP GW FLAG	This Project
p521	pFastBac XNP 2x TEV Flag	This Project
p522	pFastBac XNP Kinase Dead 2x TEV Flag	This Project
p529	pMT Bsk Myc	This Project
p530	pMT Jil-1 FL Ohne CTC Myc	This Project
p531	pMT CDC2 (CDK1) Myc	This Project
p532	pMT CDK7 Myc	This Project
p533	pMT AKT1 Myc	This Project

6.8.5 Primers

6.8.5.1 Cloning Primers

Internal Reference Number	Sequence 5'-3'	Description
CP11	accgggtatgacgacgcccagaatcgaaag	5' Psc-RA with ATG for Gateway
CP12	accggggcttggcttttgggcccgg	3' Psc-RA without STOP for Gateway C-term & N-term fusion
CP015	agatactcagacaagtttgacaaaaaaagctgaaccgaga	5' Gateway cassette insert
CP016	agatactcagctacgctatcgaccacactttgacaaagaaagctgaaccga	3' Gateway cassette insert with TRIPLE STOP option
CP035	ctcagaccgggtatgacacgcccagaatcgaaag	5' Psc-RA with ATG for Gateway
CP036	aggcgcccccttggcttttgggcccgg	3' Psc-RA without STOP for Gateway C-term & N-term fusion
CP048	gaaagcgiccgctggcttgcattc	Addie cloning, Hygromycin cassette into pMT
CP049	agcaagcgatgacagacatgataagatacattg	Addie cloning, Hygromycin cassette into pMT
CP051	agcgcgctatgacgacagctcagcac	5' bsk for cloning into GW pENTR_BSA1 vector
CP052	aggcgcgctcccgcttctatatttgaatgigt	3' bsk for cloning into GW pENTR_BSA1 Vector No Stop Codon
CP053	agcgcgctatgtccaccattgagttcgaa	5' hep for cloning into GW pENTR_BSA1 vector
CP054	aggcgcgctttgatctatcgtacggtagatgc	3' hep for cloning into GW pENTR_BSA1 Vector No Stop Codon
CP055	cttggcttcagtgcaacagtc	Psc mutagenesis: Forward Serine Primers No Mutation
CP056	cttggcttcagtgcaacagtc	Psc mutagenesis: Forward Serine Primer Alanine Mutation (No P)
CP057	cttggcttcagtgcaacagtc	Psc mutagenesis: Forward Serine Primer Alanine Mutation (P Mimic)
CP058	cgsggtagtgctctggtttaaag	Psc mutagenesis: Reverse Threonine Primer No Mutation
CP059	cgsggtagtgctctggtttaaag	Psc mutagenesis: Reverse Threonine Primer Alanine Mutation (No P)
CP060	cgsggtagtgctctggtttaaag	Psc mutagenesis: Reverse Threonine Primer Alanine Mutation (P Mimic)
CP063	aggcgcgcttggaaacgggatgcaccc	Psc AA 456 Fwd Primer
CP064	aggcgcgcttggaaacgggatgcaccc	Psc AA 911 Rev Primer
CP067	aggcgcgcttggaaacgggatgcaccc	Akt1 Fwd with ATG for cloning into GW pENTR_BSA1 Vector
CP068	aggcgcgcttggaaacgggatgcaccc	Akt1 Rev without stop for Cloning into GW pENTR_BSA1 Vector N and C term fusions
CP071	aggcgcgcttggaaacgggatgcaccc	CDK7 Fwd with ATG for cloning into GW pENTR_BSA1 Vector
CP072	aggcgcgcttggaaacgggatgcaccc	CDK7 Rev without stop for Cloning into GW pENTR_BSA1 Vector N and C term fusions
CP075	aggcgcgcttggaaacgggatgcaccc	Psc Fwd Primer AA 674 for cloning into GW pENTR_BSA1 Vector
CP076	aggcgcgcttggaaacgggatgcaccc	Psc Rev Primer AA 783 for Cloning into GW pENTR_BSA1 Vector
CP103	aggcgccccgaagttgctcaggctccaattg	3' Psc-RA 1-1438 without STOP for Gateway C-term & N-term fusion
CP104	aggcgccccgaagttgctcaggctccaattg	3' Psc-RA with ATG for Gateway
CP113	atctgtcagatgatgacgccagaaatcgaaag	3' Psc-RA with FLAG tag and STOP for pFastbac
CP114	atctgtcagatgatgacgccagaaatcgaaag	3' Akt1 with FLAG tag and STOP for pFastbac
CP115	atctgtcagatgatgacgccagaaatcgaaag	3' CDK7 with FLAG tag and STOP for pFastbac
CP116	atctgtcagatgatgacgccagaaatcgaaag	cdt2-RA (CDK1) fwd primer for cloning into GW pENTR_BSA1 Vector
CP117	atctgtcagatgatgacgccagaaatcgaaag	cdt2-RA (CDK1) rev primer for cloning into GW pENTR_BSA1 Vector without stop
CP123	atctgtcagatgatgacgccagaaatcgaaag	cdt2c-RA (CDK2) fwd primer for cloning into GW pENTR_BSA1 Vector
CP124	atctgtcagatgatgacgccagaaatcgaaag	cdt2c-RA (CDK2) rev primer for cloning into GW pENTR_BSA1 Vector without stop
CP125	atctgtcagatgatgacgccagaaatcgaaag	3' bsk for cloning into GW pENTR_BSA1 Vector No Stop Codon
CP126	atctgtcagatgatgacgccagaaatcgaaag	Psc Mutagenesis: Forward Serine 1217 NO MUTATION (Kingston clone)
CP129	atctgtcagatgatgacgccagaaatcgaaag	Psc Mutagenesis: Forward Serine 1217 Alanine Primer (Kingston Clone)
CP130	atctgtcagatgatgacgccagaaatcgaaag	Psc Mutagenesis: Forward Serine 1217 Glutamate Primer (Kingston Clone)
CP131	atctgtcagatgatgacgccagaaatcgaaag	Psc Mutagenesis: Reverse Threonine 1213 NO MUTATION (Kingston Clone)
CP132	atctgtcagatgatgacgccagaaatcgaaag	
CP133	atctgtcagatgatgacgccagaaatcgaaag	

Cloning primers Continued

Internal Reference Number	Sequence 5'-3'	Description
CP134	cggtggagcggccacatttg	Psc Mutagenesis: Reverse Threonine 1213 Alanine Primer (Kingston Clone)
CP135	cggtggjtcggccactttg	Psc Mutagenesis: Reverse Threonine 1213 Glutamate Primer (Kingston Clone)
CP138	agcggccatgggaaagaaaaccccaacggcc	dXNP (ATRX) fwd primer for cloning into GW_pENTR_BSA1 Vector - Added ATG site
CP139	aggggacctatcccggttcaaaagccgg	dXNP (ATRX) rev primer for cloning into GW_pENTR_BSA1 Vector- Without STOP
CP168	agcggccgcatgagataacagtgctccgggtag	Fwd Primer for cloning CG8290 into GW ENTR vector
CP 169	aggggacctagcccaacaattctcagccgtg	Reverse Primer with stop codon for Cloning CG8290 into GW ENTR vector
CP174	GCAGACATCGGTCTGTGCAAG	Forward Primer AKT1 kinase dead mutagenesis F3271
CP175	GACCTTATGTGACCATCTTTGTCC	Reverse Primer AKT1 kinase dead mutagenesis F3271
CP176	gcaictcgagttactttgtcattcgccttcttctgagcttgcacatcgacacttctg	Reverse Primer AKT1 into FastBac vector with FLAG tag and STOP
CP178	gcaictcgagttactttgtcattcgccttcttctgagcttgcacatcgacacttctg	Reverse Primer bsk into FastBac vector with flag tag and stop
CP225	atctcgacataactagaaattggccgctctagc	Forward Primer for UASp for cloning into attB transgenic vector
CP226	tactgagtcgatcaatgaacaggacctaacg	Reverse Primer for UASp for cloning into attB transgenic vector
CP243	agcggccgatggccggcaagcccgag	Fwd Primer Polo into pENTR vector
CP244	aggggacctgtgaaacatcttctcagcaatttc	REV primer Polo into ENTR Vector NO STOP CODON!
CP245	aggggacctgtgaaacatcttctcagcaatttc	Fwd Primer EGG into pENTR vector
CP246	aggggacctgtgaaacatcttctcagcaatttc	REV primer EGG into ENTR Vector NO STOP CODON!
CP247	aggggacctgtgaaacatcttctcagcaatttc	Fwd Primer mod(mdg4)-RW/RAA/RD into pENTR vector
CP248	aggggacctgtgaaacatcttctcagcaatttc	REV primer mod(mdg4)-RW into ENTR Vector NO STOP CODON!
CP249	aggggacctgtgaaacatcttctcagcaatttc	REV primer mod(mdg4)-RD into ENTR Vector NO STOP CODON!
CP250	aggggacctgtgaaacatcttctcagcaatttc	REV primer mod(mdg4)-RAA into ENTR Vector NO STOP CODON!
CP251	aggggacctgtgaaacatcttctcagcaatttc	Fwd Primer bon into pENTR vector
CP252	aggggacctgtgaaacatcttctcagcaatttc	REV primer bon into ENTR Vector NO STOP CODON!
CP253	actccaaggcactacaaaggaccagatgac	Fwd Primer for adding TEV cleavage to any Flag Tagged pFastBac Vector
CP254	acaggcttctcttttggggcagattactgtgt	Rev Primer for Adding TEV to any Psc 456-911 pFastBac Vector
CP257	aggggacctgtgaaacatcttctcagcaatttc	Rev Primer XNP in frame for cloning into C-term CMV-GW-GFP vector without STOP
CP264	Ggagaacctgttctcaaggcgagaaaccttctcaagggacta	Fwd Primer pFASTBac TEV and FLAG overlap
CP265	acgggacctgttctcaaggcgagaaaccttctcaagggacta	Reverse Primer pFASTBac with added restriction sites
CP266	gacgagctatgacgacagctcagcagc	Fwd Primer bsk for pFastBac MCS 2xTEV Flag 2 use CP052 as reverse primer
CP267	tcadagatgtcaataaaacacactttcgacc	Fwd Primer akt1 for pFastBac MCS 2xTEV Flag 2 use CP068 as reverse primer
CP268	gacgagctatgacgacagctcagcagc	Fwd Primer cdk7 for pFastBac MCS 2xTEV Flag 2 use CP072 as reverse primer
CP269	gacgagctatgacgacagctcagcagc	Fwd Primer polo for pFastBac MCS 2xTEV Flag 2 use CP244 as reverse primer
CP270	tcadagatgtcaataaaacacactttcgacc	Fwd Primer cdk9 for pFastBac MCS 2xTEV Flag 2 use CP128 as reverse primer
CP271	tcadagatgtcaataaaacacactttcgacc	Fwd Primer cdk2 for pFastBac MCS 2xTEV Flag 2 use CP124 as Reverse primer
CP272	gacgagctatgacgacagctcagcagc	Fwd Primer cka for pFastBac MCS 2xTEV Flag 2 use CP144 as Reverse primer
CP273	tcadagatgtcaataaaacacactttcgacc	Fwd Primer jil for pFastBac MCS 2xTEV Flag 2
CP274	aggggacctgtgaaacatcttctcagcaatttc	Fwd Primer jil for pFastBac MCS 2xTEV Flag 2 without stop Codon
CP275	aggggacctgtgaaacatcttctcagcaatttc	Fwd Primer hep for pFastBac 6xHis-TEV without start ATG for Nlenn fusion
CP276	aggggacctgtgaaacatcttctcagcaatttc	Rev Primer hep for pFastBac 6xHis-TEV with STOP
CP277	GACGACGATGACAAAGaaaggcggactcta	Fwd Primer addition of Flag tag into pCMV XNP by rolling circle
CP278	ctttgacttcctcgaacctttgttcaagaagg	Rev Primer addition of Flag tag into pCMV XNP by rolling circle
CP279	ctaggctatgggaaagaaaaccccaacggcc	Fwd Primer cloning of XNP into pFastBac 2x TEV- Flag
CP280	aggggacctatcccggttcaaaagcccgcc	Rev Primer cloning of XNP into pFastBac 2x TEV- Flag

6.8.5.2 CRISPR Primers

Internal Reference Number	Sequence 5'-3'	Description
PscR01	agtctcgtgagGCCAGAAAGATGAGAAACAGCACG	Psc fwd 1.5kb Upstream of exon 3 for cloning genomic fragment into pENTR Vector
PscR02	aggfegccttaGATGATGTTCACAGCGGAGCTCAG	Psc Rev 1.8kb downstream of 3' UTR for cloning genomic fragment into pENTR Vector
PscR03	agctctcgtgagCTCACCGGTGAGATAIAGTGTGGA	Psc fwd 2kb Upstream of exon 3 for cloning genomic fragment into pENTR Vector
PscR04	aggfegccttaCACCATGTCCGCGAGTCACG	Psc Rev 1.9kb downstream of 3' UTR for cloning genomic fragment into pENTR Vector
PscR05	CATGAAGGTACCCCGGACG	Psc Rev Primer start of exon 4 for amplification of HR Intron US of Exon 3 and Exon 3-Exon 4
PscR06	CTGAGTTGGTGGACACACTGG	Psc Fwd Primer Start of Exon 4 into 3' UTR and HR
PscR07	TCCGGCATTCCGGTCACTTCT	Psc Rev Primer Middle of Exon 4
PscR08	CAAGAAGTGGCCGCCACG	Rev Primer Sequencing 5' HR
PscR09	GCACGAGCTTGATACACTATCG	Fwd Primer Sequencing 3' HR
PscR10	GTAGTGAGCCAAACGGCTCTGT	Fwd Primer Sequencing 3' HR
PscR11	CATAGCCGTAAGCGGATGATAATC	Rev Primer Sequencing of 3' HR
PscR12	gattctataattttccagcataat	Rev Primer Sequencing of 3' HR
PscR13	gcatgccacataccgcatgt	Scarfolding primer for generation of sgRNAs
PscR14	AAAAGCACGACTCGGTGCCACTTTTCAAGTGTGATAACGGACTAGCCCTTATTTTACTTCTTACTTAAAC	Antisense primer for amplifying sgRNAs (reverse primer matching scaffold)
PscR15	AAAAGCACGACTCGGTGCC	Fwd Primer Psc 5HR genomic PCR for testing sgRNA efficiency
PscR16	CTTGGCCCTTATGTAATG	Rev Primer Psc 5HR genomic PCR for testing sgRNA efficiency
PscR17	AAAAGACGGGAACAGACA	Rev Forward Primer for gibson to pENTR vector
PscR18	cactgagaccggtccctcTCGAGGCCAGAAAGATGAG	Psc Rev Primer for gibson to pENTR vector
PscR19	ctttgacaagaagctgggtggCGCGCTTAGATGATGTC	sgRNA 5HR #1 Complementary to (+) Strand with 17 promoter and scaffold annealing sequence
PscR20	TAATACGACTCACTATAG GGACAGTACTATGTTCTTGG GTTTTAGACTAGAAAATAGC	sgRNA 5HR #2 Complementary to (+) Strand with 17 promoter and scaffold annealing sequence
PscR21	TAATACGACTCACTATAG GATGGTCGATGATGATAGTGG GTTTTAGAGCTAGAAAATAGC	sgRNA 3HR #3 Complementary to (-) Strand with 17 promoter and scaffold annealing sequence
PscR22	TAATACGACTCACTATAG ATGGCGTAAACCATGGTTCGAAAG GTTTTAGAGCTAGAAAATAGC	sgRNA 3HR #4 Complementary to (-) Strand with 17 promoter and scaffold annealing sequence
PscR23	TAATACGACTCACTATAG CCCGAAAGGGAAAGCTATCTGGG GTTTTAGAGCTAGAAAATAGC	Fwd Primer Psc 3HR genomic PCR for testing sgRNA efficiency
PscR24	catcaggatgaaggatgaac	Rev Primer Psc 3HR genomic PCR for testing sgRNA efficiency
PscR25	cgagctcggatggccc	FWD Primer pENTR vector with Psc 3 Overlap
PscR26	gctcgtgacaatcaitcaaggCGCCGCCGCCAGCCACTTT	Rev Primer Psc Overlap with pENTR vector
PscR27	AAAGCTGGTCCGCCGCCCTcttgatgattgtaagcggagc	FWD Primer Psc for complete fusion to pENTR vector
PscR28	ggccaagaagatgagaacagcaag	Rev Primer pENTR vector for complete fusion with Psc
PscR29	TGCCATAATGCCACCCTCCAG	Fwd Primer Psc 5HR genomic PCR for testing sgRNA efficiency
PscR30	TCCCCTCCTCCCTCCATAGT	Rev Primer Psc 5HR genomic PCR for testing sgRNA efficiency
PscR31	AAATCACCCTGGATGAGGAC	Fwd Primer Psc 3HR genomic PCR for testing sgRNA efficiency
PscR32	tggtgctttgtgtgctcg	Rev Primer Psc 3HR genomic PCR for testing sgRNA efficiency
PscR33	gctgtagaahggaggcctc	sgRNA 5HR #5 Complementary to (+) Strand with 17 promoter and scaffold annealing sequence
PscR34	TAATACGACTCACTATAG ACACAGCAGCAACTFAGACAGG GTTTTAGAGCTAGAAAATAGC	sgRNA 5HR #6 Complementary to (+) Strand with 17 promoter and scaffold annealing sequence
PscR35	TAATACGACTCACTATAG AATAAGGGAAAGTGAAGGGACGGG GTTTTAGAGCTAGAAAATAGC	Fwd Primer for 3HR with BsmBI site complementary to pBS-dsRed cassette from sgRNA #3 cut site
PscR36	ACGTCTCATGTTaggggactcaattgcta	Rev primer for 3HR with BsmBI site complementary to pBS GCAC-ATGC donor Plasmid
PscR37	CGGTCTCTGCAIgalgattgtaangggagctc	Fwd Primer for 5HR with BsmBI site complementary to pBS GGAC-ATGC donor Plasmid
PscR38	CGGTCTCAGGACgactggtagagctgatac	Rev primer for 5HR with BsmBI site complementary to pBS dsRed cassette from sgRNA #6 cut site
PscR39	GCGTCTCTCTGGgggcggggaagtaactatg	Rolling circle Rev primer for AttB1-2 Psc Genomic Cloning Pairs with PscR 42
PscR44	ctccgctccaccggaac	Rolling circle Fwd primer for AttB1-2 Psc Genomic Cloning Pairs with PscR 43
PscR45	ggagggttccggaggtaagta	

6.8.5.3 RNAi Primers

Target	Strand	Sequence	Features	Source
Bonus	F	TAATACGACTCACTATAG CCATCCTCTCGAGCAAAAAG	T7 Promoter	This Study
Bonus	R	TAATACGACTCACTATAG CATATTCTGCGGATGTGTGG	T7 Promoter	This Study
Bonus	F	TAATACGACTCACTATAG GTCATTGAGCTCCTCTTCGC	T7 Promoter	This Study
Bonus	R	TAATACGACTCACTATAG GGCTTGATCGTGTGATCCTT	T7 Promoter	This Study

6.8.5.4 RT-qPCR Primers

Target	Strand	Sequence 5'-3'	Source
297	F	AGGCACCTGGTACCCGATAA	This Study
297	R	GGAGATATCCGTGGTTGGTGTGTC	This Study
Roo	F	AGCCTCTACCAGCAGCAGAA	This Study
Roo	R	AGCTGATGTCGTTGTTGTTGC	This Study
mdg3	F	GAGCCACCTGTACAGCCAAC	This Study
mdg3	R	CCTGGTTCACGTTTGGGCTT	This Study
HeT-A	F	CGCGCGGAACCCATCTTCAGA	Chengjian Li et al. Cell 2009
HeT-A	R	CGCCGAGTCGTTTGGTGAGT	Chengjian Li et al. Cell 2009
412	F	CACCGGTTTGGTCGAAAG	Chengjian Li et al. Cell 2009
412	R	GGACATGCCTGGTATTTTGG	Chengjian Li et al. Cell 2009
Act5c	F	GGCGCAGAGCAAGCGTGGTA	Marco La Fortezza
Act5c	R	GGGTGCCACACGCAGTCCAT	Marco La Fortezza
Tubulin	F	TGGGCCCGTCTGGACCACAA	Marco La Fortezza
Tubulin	R	TCGCCGTCACCGGAGTCCAT	Marco La Fortezza
RpL32	F	AAGCGGCGACGCACTCTGTT	Marco La Fortezza
RpL32	R	GCCCAGCATACAGGCCAAAG	Marco La Fortezza
RpL13	F	AGCTGAACCTCTCGGGACAC	Marco La Fortezza
RpL13	R	TGCCTCGGACTGCCTTGTAG	Marco La Fortezza

6.8.6 Reagents and buffers

6.8.6.1 Kits

Kit Name	Company	Product Number
NucleoSpin Gel and PCR Clean-up Kit	Macherey-Nagel	740609.25
NucleoSpin Plasmid DNA Purification Kit	Macherey-Nagel	740588.25
NucleoBond Xtra Plasmid DNA Purification Kit	Macherey-Nagel	740414.1
SuperScript III Reverse Transcriptase	Invitrogen	11752-050
Colloidal Blue Staining Kit	Invitrogen	LC6025
MEGAclear Kit	ambion	AM1908
Gibson Assembly Master Mix	BioLabs	E2611S
QuantiTect Reverse Transcription Kit	Qiagen	205310
Fast SYBR Green Master Mix	appliedbiosystems	4385612
CloneJET PCR Cloning Kit	Thermo-Scientific	K1231
Gateway LR Clonase II Enzyme Mix	Invitrogen	11791-020
HiScribe T7 Quick High Yield RNA Synthesis Kit	New England Biolabs	E2050S
Advantage cDNA Polymerase Mix	Clontech	639105

6.8.6.2 Reagents

Reagent	Company	Product Number
2-Mercaptoethanol (BME)	Sigma-Aldrich	M3148
2-Propanol	Roth	6752.1
4',6-Diamidino-2-phenylindole dihydrochloride (DAPI)	Sigma-Aldrich	32670
660 nm Protein Assay Reagent	Pierce	22660
Agar	Roth	5210.2
Agarose	Sigma-Aldrich	A9539
Albumin Fraction V (BSA)	Roth	8076.4
Antarcitic Phosphatase	New England Biolabs	M0289S
Antarcitic Phosphatase 10x Buffer	New England Biolabs	B0289S
Bad Stabil	neoLab	1-6095
Bromophenol Blue	AppliChem	A3640
BSA Standards	Pierce	23208
cOmplete Mini Protease Inhibitor Cocktail Tablets	Roche	11836153001
Copper (II) sulphate pentahydrate	Sigma-Aldrich	C8027
di-Sodium Phosphate	Roth	T877.1
Dimethyl sulfoxide (DMSO)	AppliChem	A3006
Dithiothreitol (DTT)	Sigma-Aldrich	D0632
Dulbecco's Modified Eagle Medium (DMEM) Serum Free	Sigma-Aldrich	D6429
ECL Western Blotting Substrate	Pierce	32209
Ethanol	Roth	P075.1
Ethidium bromide	Serva	21238.01
Ethylenediamine tetraacetic acid disodium salt dihydrate (EDTA)	Roth	8043.2
Fetal Bovine Serum	PAA	A15-151
Flag M2 Sepharose Beads	Sigma-Aldrich	A2220
Glycine	Roth	3187.4
HEPES	Roth	HN77.5
Hydrochloric Acid	Sigma-Aldrich	H1758
Hydrogen Peroxide	Sigma-Aldrich	216763
Hydroxyurea	Sigma-Aldrich	H8627
Hygromycin	Sigma-Aldrich	H3274-50MG
L-Glutamine	PromoCell	Discontinued
LB Broth	Roth	X968.3
Lipofectamine 3000	Thermo Fischer Scientific	L3000001
Lithium chloride	Sigma-Aldrich	L9650
Lysine	Sigma-Aldrich	L5501
Meliseptol	B Braun	18890
Methanol	Roth	CP43.4
Nitrocellulose Membrane	BIO-RAD	162-0115
Normal Goat Serum (NGS)	BIOZOL	VEC-S-1000-CE
NP-40 (Tergitol solution)	Sigma-Aldrich	NP40S
OptiMEM	Thermo Fischer Scientific	31985070
PageRuler Plus Prestained Protein Ladder	Thermo Fischer Scientific	26619
Paraformaldehyde (PFA) 16%	Electron Microscopy Sciences	15710
Paraformaldehyde (PFA) 32%	Electron Microscopy Sciences	15714
PBS tablets	Sigma-Aldrich	P4417
Penicillin-Streptomycin	Sigma-Aldrich	P4333
Phalloidin-Tetramethylrhodamine B isothiocyanate	Sigma-Aldrich	P1951
Phenol/Chloroform	Roth	A156.1
Phenylmethanesulfonyl fluoride (PMSF)	Sigma-Aldrich	P7626
PhosSTOP Phosphatase Inhibitor Cocktail Tablets	Roche	04906837001
Potassium Chloride	Roth	6781.1
Powdered Milk	Roth	T145.2
Protein G Sepharose Beads	GE Healthcare	17-0618-01
RNAlater RNA Stabilization Reagent	Qiagen	1017980
Rotiphorese Gel 30 (37.5:1) Acrylamide	Roth	3029.1
Schneiders Drosophila Medium Serum Free Media	AMIMED	1-43F00-I

Reagent	Company	Product Number
SDS Pellets	Roth	CN30.3
Sf900™ II Serum Free Media	Thermo Fischer Scientific	10902-088
Silver Nitrate	Sigma-Aldrich	S6506
SlowFade Gold Antifade reagent	Life Technologies	S36936
Smart Ladder Short Fragment	Eurogentec	MW-1800-04
Sodium Azide	Sigma-Aldrich	S8032
Sodium bicarbonate	Sigma-Aldrich	S-6014
Sodium Chloride	AppliChem	4I017481
Sodium Orthovanadate	Sigma-Aldrich	450243
T7 endonuclease	New England Biolabs	M0302
Tetramethylethylenediamin (TEMED)	Roth	2367.3
TRIS	Roth	2449.3
Triton X-100	Sigma-Aldrich	T8787
TRIzol	ambion	15596026
Trypsin	Sigma-Aldrich	T4174
TURBO DNA-free	ambion	1406057
Tween 20	Roth	9127.1
Urea	Roth	2317.1
X-tremeGENE HP DNA Transfection Reagent	Roche	06366236001

Materials and Methods

6.8.6.3 Buffers

Buffer	Component
S2 Cell Lysis Buffer	20 mM Tris-HCl pH 7.5 150 mM NaCl 1 mM EDTA 0.5% Triton X-100 10 mM PMSF -Added Fresh cOmplete mini protease inhibitor cocktail - Added Fresh PhosSTOP phosphatase inhibitor - Added Fresh * XX mM Sodium Orthovanadate - Added Fresh *
Sf21 Cell Lysis Buffer	25 mM HEPES pH 7.6 5% Glycerol 0.5 mM EDTA 300 mM KCl 3 mM MgCl ₂ 0.1% NP-40 1 mM DTT - Added Fresh cOmplete mini protease inhibitor cocktail - Added Fresh PhosSTOP phosphatase inhibitor - Added Fresh * XX mM Sodium Orthovanadate - Added Fresh *
TBS (10 x)	200 mM Tris-HCl 1.5 M NaCl Distilled water Adjust pH to 7.5 with HCl
Wet Blot Transfer Buffer	10% 10 x Wet Blot Buffer 20% Methanol Water
Wet Blot Buffer (10 x)	1.92 M Glycine 250 mM Tris-HCl Water
TBST	1 x TBS 0.05% Tween-20
Laemmli Buffer (4 x)	2% SDS 10% Glycerol 60 mM Tris-HCl 0.02% Bromophenolblue-sodium-salt 1.25% BME 200 mM DTT
Bead Blocking Solution	2 g BSA 100 ml TBS (1 x)

Buffer	Component
Membrane Blocking Solution	3 g BSA 100 ml TBST
Tissue Blocking Solution	500 ul NGS 9.5 ml 0.1-0.5% PBST
PBST	1 PBS Tablet 200 ml Water Triton X-100 to final concentration
SDS Buffer (10 x)	3.5 mM SDS 25 mM Tris-HCl 1.92 M Glycine Water
PBL	1 mM Lysine-HCl 12 mM Disodium Phosphate PBS (1 x)
A+NP Nuclear Extraction Buffer	15 mM NaCl 15 mM Tris-HCl pH 8.0 13 mM EDTA 60 mM KCl 0.5% NP-40 0.1% BME 10 mM PMSF -Added Fresh cComplete mini protease inhibitor cocktail - Added Fresh PhosSTOP phosphatase inhibitor - Added Fresh *

6.8.7 Equipment

6.8.7.1 Microscope Equipment

Microscope Equipment	Company
Confocal Laser Scanning Microscope TCS Sp5	Leica
Diode Laser 405 nm, 25 mV	Leica
Argon Laser 458, 476, 488 and 514 nm	Leica
DPSS Laser 561 nm, 10 mV	Leica
HeNe Laser 633 nm, 10 mV	Leica
HCX PL APO Lambda Blue 20x 0.7 imm	Leica
HCX PL APO Lambda Blue 63x 1.4 oil	Leica
Immersion oil 518F	Carl Zeiss
Software: Leica Application Suite	Leica
Stereoscopic Zoom Microscope SMZ745	Nikon
KL 1500 LCD with flexible light guides	Schott AG
Halogen lamp 15V/150W, Type 6423FO	Phillips
Fluorescence Stereomicroscope StereoLumar v12	Carl Zeiss
Neolumar S 0.8x FWD 80mm, PI 10x/23 eyepieces	Carl Zeiss
Filters: 38 HeGFP BP470/40, BP525/50	Carl Zeiss
43 Cy3 BP545/25, BP605/70	Carl Zeiss
Lightsources: HXP 120 C	Carl Zeiss

6.8.7.2 Consumables

General Equipment and Consumables	Company
Scepter™ 2.0 Cell Counter	Millipore
Scepter™ 2.0 Cell Counter Sensors	Millipore
Typhoon Scanner	GE Healthcare
ChemiDoc	BioRad
CryoPure Tubes	Starstedt
TC Flask T75, Cell+	Starstedt
TC Flask T25, Cell+	Starstedt
TC Plate, 6 well, Cell+, F	Starstedt
5 ml Pipetman tips	Starstedt
10 ml Pipetman tips	Starstedt
25 ml Pipetman tips	Starstedt
Parafilm	Parafilm
Cell Scraper 25 cm	Starstedt
Erlenmyer Flask with vented cap (100 ml)	Corning
Erlenmyer Flask with vented cap (1000 ml)	Corning
Tube (15 ml)	Starstedt
Tube (50 ml)	Starstedt
Microplate, 96 Well, PS, F-Bottom	Bio-one
Mini-PROTEAN Western Blot System	BioRad
Tissue Culture dish 100 x 20 mm	Falcon
ibidi 8 well slides	ibidi
Cover Slips 18 x 18	Menzel-Gläser
Microscope Slides SuperFrost White	Roth
Omnifix-F 1ml syringe	B Braun
Sterican 27 G Needle	B Braun
Sterican 21 G Needle	B Braun
S2 Cell Culture Incubator	Binder
Sf21 Cell Culture Incubator	Infors HT Multitron
HELA Cell Incubator	Binder
Filtropur S 0.45 um	Starstedt
Filtropur S 0.2 um	Starstedt
Äkta purifier	Amersham Biosciences
96 Well qPCR plates	Starstedt
SafeSeal Tube 1.5 ml	Starstedt
SafeSeal Tube 0.5 ml	Starstedt
SafeSeal Tube 2.0 ml	Starstedt
Chromotography Paper, type MN260	Roth
Biosphere Fil.Tip 20 ul	Starstedt
Biosphere Fil.Tip 200 ul	Starstedt
Biosphere Fil.Tip 1000 ul	Starstedt
Pipette Tip 200 ul	Starstedt
Pipette Tip 1000 ul	Starstedt
Pipette Tip 20 ul	Starstedt
Nitrile Lite Examination Gloves (M)	VWR
Filtropur V25 0.2 um, 250 ml	Starstedt
Fine forceps	Fine Science Tool
Immersion oil 518F	Carl Zeiss
Agilent 2100 Bioanalyzer	Agilent Technologies
CFX96 Real-Time PCR Detection System	Bio-Rad
Incubator (18 °C), Percival	CLF Plant Climatics
Incubator (25°C), Mir-154	Panasonic Biomedical
Nutating Mixer	VWR
Vortex mixer	Scientific Industries
Water bath	Julabo
Power Scanner	TECAN
Superdex 200 10/300 GL	GE Healthcare

6.8.7.3 Software

Software	Company
Adobe Illustrator CS5.1	Adobe Systems
Adobe Photoshop CS5.1	Adobe Systems
Image J1.48 b	Wayne Rasband, National Institutes of Health
Office 2008, 2016	Microsoft

Abbreviations

Abreviation	Long form
ADD	ATRX-DNMT3-DNMT3L domain
ATRX	Alpha-thalasemia mental retardation X-linked
BLAST	Basic local alignment search tool
Bon	Bonus
BSA	Bovine serum albumin
cDNA	complementary DNA
ChIP	Chromatin immunoprecipitation
chro	chromator
CuSQ	Copper sulphate
DAPI	4', 6-diamidino-2-phenylindole
El.	Elution
FL	Full length
gDNA	genomic DNA
GFP/RFP	Green/red fluorescent protein
Gnf1	Germ line transcription factor 1
GW	Gateway
H2Av	Histone 2A variant
H3K4	Histone 3 Lysine 4
H3K4me3	Histone 3 Lysine 4 tri-methylation
H3K9	Histone 3 Lysine 9
H3K9me3	Histone 3 Lysine 9 tri-methylation
HA	Hemagglutinin
HP1	Heterochromatin protein 1
HP1a	Heterochromatin protein 1 a
HP1b	Heterochromatin protein 1 b
In.	Input
IP	Immuno-precipitation

Abbreviations

Abreviation	Long form
kD	Kilo-dalton
LC-MS/MS	Liquid Crystal- Mass Spectroscopy /Mass Spectroscopy
LMG	Lemming
MAPK	Mitogen activated protein kinase
MS	Mass Spectroscopy
NGS	Normal goat serum
O-GlcNAc	O-linked N-acetylglucosamine
PAR	Poly-(ADP Ribose)
pMT	Metallothionine Promoter
Prod	Protein proliferation disrupter
PTM	Post translational modification
Pzg	putzig
RT-qPCR	Real time- quantitative PCR
SDS	Sodium dodecyl sulfate
TTC	Trials to criterion
upd	Unpaired ligand
UTR	Untranslated region
WT	Wild type
γ -H2Av	Phosphorylated Histone 2A variant

References

1. Hutchison, C.A., 3rd, et al., *Design and synthesis of a minimal bacterial genome*. *Science*, 2016. **351**(6280): p. aad6253.
2. Technologies, I.D. *Molecular Facts and Figures*. 2011 [cited 2016 June 3]; Available from: <https://www.idtdna.com/pages/docs/educational-resources/molecular-facts-and-figures.pdf?sfvrsn=4>.
3. Pruitt, K.D., et al., *RefSeq: an update on mammalian reference sequences*. *Nucleic Acids Res*, 2014. **42**(Database issue): p. D756-63.
4. Marino-Ramirez, L., et al., *Histone structure and nucleosome stability*. *Expert Rev Proteomics*, 2005. **2**(5): p. 719-29.
5. Luger, K., et al., *Crystal structure of the nucleosome core particle at 2.8 Å resolution*. *Nature*, 1997. **389**(6648): p. 251-60.
6. Eissenberg, J.C. and S.C. Elgin, *HP1a: a structural chromosomal protein regulating transcription*. *Trends Genet*, 2014. **30**(3): p. 103-10.
7. Bannister, A.J. and T. Kouzarides, *Regulation of chromatin by histone modifications*. *Cell Res*, 2011. **21**(3): p. 381-95.
8. Gillette, T.G. and J.A. Hill, *Readers, writers, and erasers: chromatin as the whiteboard of heart disease*. *Circ Res*, 2015. **116**(7): p. 1245-53.
9. Torres, I.O. and D.G. Fujimori, *Functional coupling between writers, erasers and readers of histone and DNA methylation*. *Curr Opin Struct Biol*, 2015. **35**: p. 68-75.
10. Virani, S., et al., *Cancer epigenetics: a brief review*. *ILAR J*, 2012. **53**(3-4): p. 359-69.
11. Dawson, M.A. and T. Kouzarides, *Cancer epigenetics: from mechanism to therapy*. *Cell*, 2012. **150**(1): p. 12-27.

References

12. Haluskova, J., *Epigenetic studies in human diseases*. Folia Biol (Praha), 2010. **56**(3): p. 83-96.
13. Gibbons, R.J., et al., *Mutations in the chromatin-associated protein ATRX*. Hum Mutat, 2008. **29**(6): p. 796-802.
14. Garrick, D., et al., *Loss of Atrx affects trophoblast development and the pattern of X-inactivation in extraembryonic tissues*. PLoS Genet, 2006. **2**(4): p. e58.
15. Jiao, Y., et al., *DAXX/ATRX, MEN1, and mTOR pathway genes are frequently altered in pancreatic neuroendocrine tumors*. Science, 2011. **331**(6021): p. 1199-203.
16. Jiao, Y., et al., *Frequent ATRX, CIC, FUBP1 and IDH1 mutations refine the classification of malignant gliomas*. Oncotarget, 2012. **3**(7): p. 709-22.
17. Liu, X.Y., et al., *Frequent ATRX mutations and loss of expression in adult diffuse astrocytic tumors carrying IDH1/IDH2 and TP53 mutations*. Acta Neuropathol, 2012. **124**(5): p. 615-25.
18. Schwartzenuber, J., et al., *Driver mutations in histone H3.3 and chromatin remodelling genes in paediatric glioblastoma*. Nature, 2012. **482**(7384): p. 226-31.
19. Yang, S.H., A.D. Sharrocks, and A.J. Whitmarsh, *MAP kinase signalling cascades and transcriptional regulation*. Gene, 2013. **513**(1): p. 1-13.
20. Liao, J.Y., et al., *Alternative lengthening of telomeres phenotype in malignant vascular tumors is highly associated with loss of ATRX expression and is frequently observed in hepatic angiosarcomas*. Hum Pathol, 2015. **46**(9): p. 1360-6.
21. Nakazato, H., et al., *Early-Stage Induction of SWI/SNF Mutations during Esophageal Squamous Cell Carcinogenesis*. PLoS One, 2016. **11**(1): p. e0147372.
22. Heaphy, C.M., et al., *Altered telomeres in tumors with ATRX and DAXX mutations*. Science, 2011. **333**(6041): p. 425.
23. Ritchie, K., et al., *Loss of ATRX leads to chromosome cohesion and congression defects*. J Cell Biol, 2008. **180**(2): p. 315-24.
24. De La Fuente, R., et al., *ATRX, a member of the SNF2 family of helicase/ATPases, is required for chromosome alignment and meiotic spindle organization in metaphase II stage mouse oocytes*. Dev Biol, 2004. **272**(1): p. 1-14.
25. Iwase, S., et al., *ATRX ADD domain links an atypical histone methylation recognition mechanism to human mental-retardation syndrome*. Nat Struct Mol Biol, 2011. **18**(7): p. 769-76.

26. Eustermann, S., et al., *Combinatorial readout of histone H3 modifications specifies localization of ATRX to heterochromatin*. Nat Struct Mol Biol, 2011. **18**(7): p. 777-82.
27. Dhayalan, A., et al., *The ATRX-ADD domain binds to H3 tail peptides and reads the combined methylation state of K4 and K9*. Hum Mol Genet, 2011. **20**(11): p. 2195-203.
28. Wong, L.H., et al., *ATRX interacts with H3.3 in maintaining telomere structural integrity in pluripotent embryonic stem cells*. Genome Res, 2010. **20**(3): p. 351-60.
29. Sadic, D., et al., *Atrx promotes heterochromatin formation at retrotransposons*. EMBO Rep, 2015. **16**(7): p. 836-50.
30. Goldberg, A.D., et al., *Distinct factors control histone variant H3.3 localization at specific genomic regions*. Cell, 2010. **140**(5): p. 678-91.
31. Drane, P., et al., *The death-associated protein DAXX is a novel histone chaperone involved in the replication-independent deposition of H3.3*. Genes Dev, 2010. **24**(12): p. 1253-65.
32. Voon, H.P. and L.H. Wong, *New players in heterochromatin silencing: histone variant H3.3 and the ATRX/DAXX chaperone*. Nucleic Acids Res, 2016. **44**(4): p. 1496-501.
33. Leung, J.W., et al., *Alpha thalassemia/mental retardation syndrome X-linked gene product ATRX is required for proper replication restart and cellular resistance to replication stress*. J Biol Chem, 2013. **288**(9): p. 6342-50.
34. EMBL-EBI, *ADD domain*, in *InterPro Protein sequence analysis & classification*. 2016, EMBL-EBI: <https://www.ebi.ac.uk/interpro/entry/IPR025766>.
35. Otani, J., et al., *Structural basis for recognition of H3K4 methylation status by the DNA methyltransferase 3A ATRX-DNMT3-DNMT3L domain*. EMBO Rep, 2009. **10**(11): p. 1235-41.
36. Ooi, S.K., et al., *DNMT3L connects unmethylated lysine 4 of histone H3 to de novo methylation of DNA*. Nature, 2007. **448**(7154): p. 714-7.
37. Clapier, C.R. and B.R. Cairns, *The biology of chromatin remodeling complexes*. Annu Rev Biochem, 2009. **78**: p. 273-304.
38. Flaus, A., et al., *Identification of multiple distinct Snf2 subfamilies with conserved structural motifs*. Nucleic Acids Res, 2006. **34**(10): p. 2887-905.
39. Eisen, J.A., K.S. Sweder, and P.C. Hanawalt, *Evolution of the SNF2 family of proteins: subfamilies with distinct sequences and functions*. Nucleic Acids Res, 1995. **23**(14): p. 2715-23.

References

40. Xue, Y., et al., *The ATRX syndrome protein forms a chromatin-remodeling complex with Daxx and localizes in promyelocytic leukemia nuclear bodies.* Proc Natl Acad Sci U S A, 2003. **100**(19): p. 10635-40.
41. Mitson, M., et al., *Functional significance of mutations in the Snf2 domain of ATRX.* Hum Mol Genet, 2011. **20**(13): p. 2603-10.
42. Lopez-Falcon, B., et al., *Characterization of the Drosophila group ortholog to the amino-terminus of the alpha-thalassemia and mental retardation X-Linked (ATRX) vertebrate protein.* PLoS One, 2014. **9**(12): p. e113182.
43. Komander, D. and M. Rape, *The ubiquitin code.* Annu Rev Biochem, 2012. **81**: p. 203-29.
44. Bond, M.R. and J.A. Hanover, *A little sugar goes a long way: the cell biology of O-GlcNAc.* J Cell Biol, 2015. **208**(7): p. 869-80.
45. Lu, P., et al., *Poly(ADP-ribose) polymerase-1 causes mitochondrial damage and neuron death mediated by Bnip3.* J Neurosci, 2014. **34**(48): p. 15975-87.
46. Schneiderman, J.I., et al., *The XNP remodeler targets dynamic chromatin in Drosophila.* Proc Natl Acad Sci U S A, 2009. **106**(34): p. 14472-7.
47. Graveley, B.R., et al., *The D. melanogaster transcriptome: modENCODE RNA-Seq data for dissected tissues.* 2011.
48. Berkley Drosophila Genome Project
49. van der Voet, M., et al., *Drosophila models of early onset cognitive disorders and their clinical applications.* Neurosci Biobehav Rev, 2014. **46 Pt 2**: p. 326-42.
50. Darbo, E., et al., *Transcriptional and epigenetic signatures of zygotic genome activation during early Drosophila embryogenesis.* BMC Genomics, 2013. **14**: p. 226.
51. Ahmad, K. and S. Henikoff, *The histone variant H3.3 marks active chromatin by replication-independent nucleosome assembly.* Mol Cell, 2002. **9**(6): p. 1191-200.
52. Chow, C.M., et al., *Variant histone H3.3 marks promoters of transcriptionally active genes during mammalian cell division.* EMBO Rep, 2005. **6**(4): p. 354-60.
53. Schneiderman, J.I., et al., *Nucleosome-depleted chromatin gaps recruit assembly factors for the H3.3 histone variant.* Proc Natl Acad Sci U S A, 2012. **109**(48): p. 19721-6.
54. Zhang, D., D. Wang, and F. Sun, *Drosophila melanogaster heterochromatin protein HP1b plays important roles in transcriptional activation and development.* Chromosoma, 2011. **120**(1): p. 97-108.

55. Greil, F., et al., *Distinct HP1 and Su(var)3-9 complexes bind to sets of developmentally coexpressed genes depending on chromosomal location*. *Genes Dev*, 2003. **17**(22): p. 2825-38.
56. Alekseyenko, A.A., et al., *Heterochromatin-associated interactions of Drosophila HP1a with dADD1, HIPPI1, and repetitive RNAs*. *Genes Dev*, 2014. **28**(13): p. 1445-60.
57. Minakhina, S. and R. Steward, *Melanotic mutants in Drosophila: pathways and phenotypes*. *Genetics*, 2006. **174**(1): p. 253-63.
58. Bidla, G., M.S. Dushay, and U. Theopold, *Crystal cell rupture after injury in Drosophila requires the JNK pathway, small GTPases and the TNF homolog Eiger*. *J Cell Sci*, 2007. **120**(Pt 7): p. 1209-15.
59. Figueiredo, M.L., et al., *HP1a recruitment to promoters is independent of H3K9 methylation in Drosophila melanogaster*. *PLoS Genet*, 2012. **8**(11): p. e1003061.
60. Beckstead, R.B., et al., *Bonus, a Drosophila TIF1 homolog, is a chromatin-associated protein that acts as a modifier of position-effect variegation*. *Genetics*, 2005. **169**(2): p. 783-94.
61. Ito, H., et al., *Fruitless recruits two antagonistic chromatin factors to establish single-neuron sexual dimorphism*. *Cell*, 2012. **149**(6): p. 1327-38.
62. Savitsky, M., et al., *Distinct Roles of Chromatin Insulator Proteins in Control of the Drosophila Bithorax Complex*. *Genetics*, 2016. **202**(2): p. 601-17.
63. Nielsen, A.L., et al., *Interaction with members of the heterochromatin protein 1 (HP1) family and histone deacetylation are differentially involved in transcriptional silencing by members of the TIF1 family*. *EMBO J*, 1999. **18**(22): p. 6385-95.
64. Ryan, R.F., et al., *KAP-1 corepressor protein interacts and colocalizes with heterochromatic and euchromatic HP1 proteins: a potential role for Kruppel-associated box-zinc finger proteins in heterochromatin-mediated gene silencing*. *Mol Cell Biol*, 1999. **19**(6): p. 4366-78.
65. Torok, T., et al., *The product of proliferation disrupter is concentrated at centromeres and required for mitotic chromosome condensation and cell proliferation in Drosophila*. *Genes Dev*, 1997. **11**(2): p. 213-25.
66. Torok, T., et al., *The protein encoded by the gene proliferation disrupter (prod) is associated with the telomeric retrotransposon array in Drosophila melanogaster*. *Chromosoma*, 2007. **116**(2): p. 185-95.
67. Antao, J.M., et al., *Protein landscape at Drosophila melanogaster telomere-associated sequence repeats*. *Mol Cell Biol*, 2012. **32**(12): p. 2170-82.

References

68. Sawarkar, R., C. Sievers, and R. Paro, *Hsp90 globally targets paused RNA polymerase to regulate gene expression in response to environmental stimuli*. Cell, 2012. **149**(4): p. 807-18.
69. Madigan, J.P., H.L. Chotkowski, and R.L. Glaser, *DNA double-strand break-induced phosphorylation of Drosophila histone variant H2Av helps prevent radiation-induced apoptosis*. Nucleic Acids Res, 2002. **30**(17): p. 3698-705.
70. Swaminathan, J., E.M. Baxter, and V.G. Corces, *The role of histone H2Av variant replacement and histone H4 acetylation in the establishment of Drosophila heterochromatin*. Genes Dev, 2005. **19**(1): p. 65-76.
71. Zhang, Z. and B.F. Pugh, *Genomic organization of H2Av containing nucleosomes in Drosophila heterochromatin*. PLoS One, 2011. **6**(6): p. e20511.
72. Lake, C.M., et al., *The development of a monoclonal antibody recognizing the Drosophila melanogaster phosphorylated histone H2A variant (gamma-H2AV)*. G3 (Bethesda), 2013. **3**(9): p. 1539-43.
73. Kusch, T., et al., *Acetylation by Tip60 is required for selective histone variant exchange at DNA lesions*. Science, 2004. **306**(5704): p. 2084-7.
74. Petermann, E., et al., *Hydroxyurea-stalled replication forks become progressively inactivated and require two different RAD51-mediated pathways for restart and repair*. Mol Cell, 2010. **37**(4): p. 492-502.
75. Lovejoy, C.A., et al., *Loss of ATRX, genome instability, and an altered DNA damage response are hallmarks of the alternative lengthening of telomeres pathway*. PLoS Genet, 2012. **8**(7): p. e1002772.
76. Takacs, S., et al., *Protein interactions on telomeric retrotransposons in Drosophila*. Int J Biol Sci, 2012. **8**(7): p. 1055-61.
77. Eggert, H., A. Gortchakov, and H. Saumweber, *Identification of the Drosophila interband-specific protein Z4 as a DNA-binding zinc-finger protein determining chromosomal structure*. J Cell Sci, 2004. **117**(Pt 18): p. 4253-64.
78. Livak, K.J. and T.D. Schmittgen, *Analysis of relative gene expression data using real-time quantitative PCR and the 2(-Delta Delta C(T)) Method*. Methods, 2001. **25**(4): p. 402-8.

7 Supplementary Materials

Table 4: *dADD1* specific interactors with \log_2 iBAQ (*dADD1/S2* control) greater than 3 and P-Value less than 0.06.

Gene Name	FB ID	ID Volcano Plot	Log ₂ dADD1/Control	P-Value
prod	FBgn0014269	270	12.02	1.53E-03
Hsp60	FBgn0015245	8	11.37	6.06E-11
Eb1	FBgn0027066	230	11.19	1.07E-07
Chro	FBgn0044324	294	10.74	6.74E-04
Vps29	FBgn0031310	398	10.33	6.91E-10
CG15107	FBgn0041702	220	9.59	4.88E-04
RpL21	FBgn0032987	336	9.32	2.75E-11
Hsc70-5	FBgn0001220	76	8.80	5.51E-07
ncd	FBgn0002924	60	8.52	5.40E-03
deltaCOP	FBgn0028969	456	8.09	2.15E-03
Jra	FBgn0001291	58	8.03	6.22E-03
beta'COP	FBgn0025724	19	7.85	1.21E-03
Sep2	FBgn0014029	106	7.76	3.67E-09
gammaCOP	FBgn0028968	143	7.57	7.62E-11
AnxB9	FBgn0000083	63	7.34	3.43E-09
cg	FBgn0000289	244	7.25	1.90E-02
26-29-p	FBgn0250848	326	7.21	8.91E-03
CG4552	FBgn0031304	397	7.16	6.66E-10
RpII33	FBgn0026373	263	6.86	2.57E-03
Rpt1	FBgn0028687	288	6.33	2.24E-02
Dap160	FBgn0023388	253	6.31	1.09E-04
Ranbp9	FBgn0037894	358	6.27	1.14E-07
RpS5a	FBgn0002590	124	6.26	9.25E-08
Cdc5	FBgn0265574	439	5.95	2.55E-03
epsilonCOP	FBgn0027496	459	5.86	5.00E-02
Sep1	FBgn0011710	90	5.86	4.22E-09
woc	FBgn0010328	248	5.56	9.24E-08
thoc5	FBgn0034939	204	5.56	3.90E-09

Supplementary Materials

Table 4 Continued

Gene Name	FB ID	ID Volcano Plot	Log2 dADD1/Control	P-Value
pod1	FBgn0029903	250	5.51	3.19E-07
CG4038	FBgn0011824	140	5.49	5.03E-02
Nsf2	FBgn0266464	105	5.47	1.25E-02
kz	FBgn0001330	16	5.25	1.99E-06
Prp31	FBgn0036487	412	5.03	4.99E-02
HIPP1	FBgn0037027	392	5.00	6.57E-04
Deaf1	FBgn0013799	123	4.94	5.11E-02
E(bx)	FBgn0000541	203	4.88	3.95E-09
CG32549	FBgn0052549	420	4.72	5.87E-09
Dhx15	FBgn0033160	281	4.64	2.73E-02
SelD	FBgn0261270	12	4.53	4.98E-02
Usp7	FBgn0030366	201	4.33	1.72E-09
betaCop	FBgn0008635	91	4.12	5.00E-02
Act5C	FBgn0000042	45	4.11	1.17E-03
Zasp52	FBgn0265991	3	4.11	3.40E-07
CG9246	FBgn0032925	184	4.11	3.04E-07
fl(2)d	FBgn0000662	215	4.09	4.98E-02
bon	FBgn0023097	223	4.06	5.05E-02
Klp10A	FBgn0030268	157	3.99	4.98E-02
mip130	FBgn0023509	455	3.98	5.00E-02
Hsc70-3	FBgn0001218	75	3.75	1.51E-03
Pen	FBgn0267727	103	3.66	5.10E-02
Nup358	FBgn0039302	217	3.38	2.50E-02
Mat89Ba	FBgn0261286	144	3.22	5.00E-02
MBD-R2	FBgn0038016	357	3.09	5.10E-02
Spt6	FBgn0028982	209	3.01	5.81E-02

Table 5: XNP specific interactors with \log_2 iBAQ (XNP/S2 control) greater than 3 and P-Value less than 0.06.

Gene Name	FB ID	ID Volcano Plot	Log2 XNP/Control	P-Value
clu	FBgn0034087	5	14.70	8.95E-12
RpL11	FBgn0013325	94	12.29	2.63E-03
Su(var)2-10	FBgn0003612	232	11.95	4.97E-12
CG43736	FBgn0263993	260	11.91	7.06E-12
CG9253-RA	FBgn0032919	369	11.39	1.10E-08
tsr	FBgn0011726	92	10.86	3.49E-03
CHIP	FBgn0027052	457	10.64	5.67E-08
NHP2	FBgn0029148	169	10.26	8.31E-09
CG8036	FBgn0037607	365	9.93	4.92E-04
Nop60B	FBgn0259937	14	9.66	3.94E-03
Bin1	FBgn0024491	177	9.66	2.27E-06
SmD3	FBgn0023167	15	9.62	5.89E-12
Cct5	FBgn0010621	285	9.38	5.63E-03
RpL7A	FBgn0014026	95	9.32	8.82E-08
CG4164	FBgn0031256	396	9.30	6.08E-07
Rbm13	FBgn0030067	450	9.12	1.44E-03
msn	FBgn0010909	435	9.07	4.31E-09
CG7637	FBgn0033548	171	9.02	2.45E-06
Aldh	FBgn0012036	382	8.94	5.47E-03
RpL13	FBgn0011272	88	8.87	4.17E-11
RpS15Aa	FBgn0010198	96	8.57	9.34E-03
Sry-delta	FBgn0003512	36	8.57	5.92E-06
REG	FBgn0029133	324	8.46	9.12E-03
Tcp-1eta	FBgn0037632	364	8.44	1.47E-07
CkIIbeta	FBgn0000259	39	8.32	5.66E-02
PCNA	FBgn0005655	56	8.15	2.32E-10
nudC	FBgn0021768	413	7.89	5.59E-03
CG2063	FBgn0033400	278	7.86	1.12E-14
CG17078-RA	FBgn0086855	395	7.83	4.56E-03
RfC3	FBgn0032244	381	7.83	9.53E-03
U3-55K	FBgn0053505	304	7.76	1.12E-07
eIF-2alpha	FBgn0261609	89	7.73	2.98E-02
abs	FBgn0015331	165	7.60	7.43E-03
TER94	FBgn0261014	137	7.58	1.34E-02
Art1	FBgn0037834	359	7.52	5.01E-07
mbf1	FBgn0262732	257	7.51	9.44E-09
CG5641	FBgn0038046	179	7.14	4.60E-10
Hsp70Bbb	FBgn0051354	145	7.14	3.65E-02
mbm	FBgn0086912	394	7.04	1.04E-07
Arpc4	FBgn0031781	384	6.99	3.91E-09
mod	FBgn0002780	51	6.94	3.29E-07
Saf-B	FBgn0039229	297	6.86	2.83E-05
Nopp140	FBgn0037137	258	6.85	1.42E-06
CG3817	FBgn0038275	178	6.80	1.67E-08

Table 7 Continued

Gene Name	FB ID	ID Volcano Plot	Log2 XNP/Control	P-Value
Ubqn	FBgn0031057	417	6.49	1.35E-02
MEP-1	FBgn0035357	264	6.42	3.14E-03
Su(fu)	FBgn0005355	355	6.41	5.48E-08
PIP4K	FBgn0039924	306	6.20	5.08E-02
gfzf	FBgn0250732	269	6.16	1.03E-02
CG3163	FBgn0034961	442	6.14	1.73E-07
Zn72D	FBgn0263603	292	5.99	3.51E-10
Rad23	FBgn0026777	328	5.98	1.29E-02
Mi-2	FBgn0262519	23	5.82	6.19E-03
simj	FBgn0010762	256	5.69	5.89E-11
CG5787	FBgn0032454	377	5.66	1.31E-02
Aats-asn	FBgn0086443	332	5.62	1.01E-02
Dbp73D	FBgn0004556	70	5.45	3.37E-04
MTA1-like	FBgn0027951	221	5.44	1.10E-06
Tep4	FBgn0041180	255	5.34	6.62E-11
Past1	FBgn0016693	312	5.32	5.90E-07
Uba1	FBgn0023143	310	5.26	2.01E-02
l(2)34Fd	FBgn0261535	323	5.24	1.99E-06
Akap200	FBgn0027932	293	5.20	5.04E-02
CG18592	FBgn0031678	385	5.10	1.21E-06
RpI135	FBgn0003278	59	5.09	5.22E-05
CG1440	FBgn0030038	462	5.04	2.48E-07
RpS19a	FBgn0010412	84	5.02	5.59E-02
grsm	FBgn0040493	227	5.00	5.12E-02
Mlf	FBgn0034051	163	4.95	4.99E-02
CG6316	FBgn0052075	308	4.86	5.00E-02
CG12909	FBgn0033507	276	4.86	5.17E-02
CG40045	FBgn0058045	307	4.81	5.00E-02
Rpt4	FBgn0028685	410	4.75	5.13E-02
CG9281	FBgn0030672	427	4.66	5.01E-02
Dpit47	FBgn0266518	229	4.57	5.11E-02
jim	FBgn0027339	259	4.54	4.99E-02
CG1677-RB	FBgn0029941	453	4.54	6.31E-10
RpI1	FBgn0019938	114	4.53	2.47E-03
Pdi	FBgn0014002	108	4.46	4.40E-02
Prosalph4	FBgn0004066	65	4.41	5.00E-02
RpS18	FBgn0010411	87	4.35	5.00E-02
Rpb5	FBgn0033571	273	4.34	5.65E-02
RpL18	FBgn0035753	193	4.30	5.09E-02
Mtap	FBgn0034215	173	4.29	5.00E-02
hng1	FBgn0034599	447	3.98	4.99E-02
Irbp	FBgn0011774	121	3.89	4.98E-02
Vps4	FBgn0027605	460	3.85	4.99E-02
CG1091	FBgn0037470	224	3.84	5.07E-02

Table 7 Continued

Gene Name	FB ID	ID Volcano Plot	Log2 XNP/Control	P-Value
CG32409	FBgn0052409	296	3.79	5.03E-02
AnxB10	FBgn0000084	64	3.74	5.06E-02
Syp	FBgn0038826	225	3.71	5.42E-02
Aatf	FBgn0031851	189	3.70	5.32E-02
CG12007	FBgn0037293	388	3.40	5.12E-02
CG8545-RA	FBgn0033741	239	3.40	5.33E-02
Dlic	FBgn0030276	432	3.24	4.99E-02
CG3909	FBgn0027524	458	3.22	5.43E-02
Chd3	FBgn0023395	9	3.15	5.06E-02
nito	FBgn0027548	287	3.12	5.00E-02
Top1	FBgn0004924	77	3.03	4.99E-02

Supplementary Materials

Table 6: Shared interactors of dADD1 and XNP with log₂ greater than 3 and P-Value less than 0.06 listed in alphabetical order.

Gene Name	Log2 dADD1/Control	P-Value dADD1	Log2 XNP/Control	P-Value XNP
14-3-3epsilon	6.51	2.06E-05	6.80	1.60E-05
14-3-3zeta	7.88	1.79E-02	7.72	1.95E-02
alphaCOP	8.34	2.19E-03	3.89	5.45E-02
alphaTub84D	5.51	1.76E-04	4.65	4.50E-04
betaTub56D	6.36	1.96E-03	6.26	2.13E-03
betaTub60D	7.20	4.33E-03	7.08	4.70E-03
betaTub97EF	7.79	4.52E-03	6.74	8.84E-03
blanks	9.92	3.93E-04	9.88	4.02E-04
blw	7.75	6.42E-07	7.13	1.06E-06
CaBP1	5.89	4.15E-02	5.31	5.86E-02
Caf1	5.33	5.14E-02	10.36	3.29E-03
capt	10.93	2.98E-10	10.85	3.11E-10
Cctgamma	6.67	2.72E-07	8.33	7.20E-08
CG10139	10.17	1.52E-05	8.29	4.91E-05
CG11999	6.52	7.97E-03	7.39	4.46E-03
CG1316	9.60	1.00E-07	7.96	3.08E-07
CG15784	5.19	5.05E-02	9.27	4.77E-03
CG2199	7.74	1.83E-04	8.72	9.35E-05
CG2691	4.34	1.46E-05	4.31	1.54E-05
CG2982	7.78	1.55E-08	8.05	1.26E-08
CG3335	7.58	1.64E-06	7.74	1.45E-06
CG4747	10.62	7.65E-08	10.53	8.07E-08
CG5168	8.39	4.10E-08	7.00	1.21E-07
CG5525	6.67	1.33E-07	7.51	6.53E-08
CG6937	7.83	9.09E-06	7.01	1.74E-05
CG7033	6.44	3.60E-05	8.85	5.68E-06
CG7946	7.65	9.13E-07	7.36	1.15E-06
CG8258	4.90	5.11E-02	8.65	5.16E-03
CG8414	4.30	4.42E-05	5.58	9.71E-06
cher	8.49	1.63E-04	5.58	1.56E-03
chic	13.32	3.21E-03	6.89	4.99E-02
Ckl1alpha	6.27	1.49E-04	14.49	1.16E-06
Dp1	11.08	3.07E-04	3.65	4.99E-02
dre4	7.95	2.27E-03	7.11	3.92E-03
Droj2	11.80	6.12E-08	12.06	5.38E-08
Ef1alpha48D	8.41	1.22E-02	7.88	1.60E-02
Ef1gamma	5.03	5.23E-02	7.62	1.06E-02
EF2	9.28	2.02E-05	11.18	6.86E-06
eIF-4a	7.65	1.19E-03	7.88	1.03E-03
eIF4G	7.45	2.97E-09	5.86	1.25E-08
Fib	10.29	4.57E-04	8.64	1.16E-03
FK506-bp1	11.99	6.44E-10	13.96	2.58E-10
Fmr1	6.59	1.11E-03	7.01	8.03E-04
Gfat2	8.74	2.11E-05	7.36	5.65E-05
Gnf1	7.19	3.52E-06	8.32	1.48E-06
Got1	5.60	5.68E-02	6.48	3.44E-02
Hel25E	4.42	5.06E-02	6.71	1.01E-02

Curriculum Vitae

Addie Kolybaba-Stewart

Born 21/01/1988 Calgary Canada

Current

Graduate School Life Science Munich and Integrated Research Training Group:
Chromatin Dynamics Graduate Program, Munich, Germany

Ph.D. Student Biology

Direct entry from Bachelors into Ph.D. Enrolled since October 4th, 2011, in the Ph.D. programs from the Graduate School Life Science Munich and the IRTG Chromatin Dynamics in coordination with Ludwig Maximilian University (LMU) Munich. Doctoral research is currently being conducted in the laboratory of Dr. Anne-Kathrin Classen.

Education

September 2006 - May 2011, Simon Fraser University, Burnaby, Canada

Bachelor of Science

B.Sc. with First Class Honours in Health Sciences

Focus on Virology and Immunology

Cumulative GPA of 3.89 (A - 4.0, A⁻ - 3.67)

Ranked within the top 5% of students pursuing a B.Sc. in Health Science

September 2002 - June 2006, Hunting Hills High School, Red Deer, Canada

High School Diploma

Honours with Distinction average of 90%

Graduated as 3rd overall academic in a class of over 350

Publications

La Fortezza, M., Schenck, M., Cosolo, A., **Kolybaba, A.**, Grass, I., Classen, A.K. (Accepted). *JAK/STAT signalling mediates cell survival in response to tissue stress.*

Massah, S., Hollebakken, R., Labrecque, M.P., **Kolybaba, A.**, Beischlag, T.V. and Prefontaine, G.G. (2014). *Epigenetic characterization of the growth hormone gene identifies SmcHD1 as a regulator of autosomal gene clusters.* PLOS One. Vol. 9(5): e97535

Kolybaba, A.M. and Classen, A.K. (2014). *Sensing cellular states - signaling to chromatin pathways targeting Polycomb and Trithorax group function.* Cell and Tissue Research. Vol. 356(3): 477-93

Tam, K.J., Watson, C.T., Massah, S., **Kolybaba, A.M.**, Breden, F., Prefontaine, G.G., Beischlag, T.V. (2011). *Regulatory function of conserved sequences upstream of the long-wave sensitive opsin genes in teleost fishes.* Vision Research. Vol. 51(21-22): 2295-303.